การสังเคราะห์อนุพันธ์ 1,4-ไดไฮโครพิริดีนิลกลูโคซามีนเพื่อใช้เป็นฟลูออเรสเซนต์เซ็นเซอร์ที่ละลายน้ำได้

นายโอฬาร ปิ่นรัตน์

วิทยานิพนธ์นี้เป็นส่วนหนึ่งของการศึกษาตามหลักสูตรปริญญาวิทยาศาสตรมหาบัณฑิต
สาขาวิชาปิโตรเคมีและวิทยาศาสตร์พอลิเมอร์
คณะวิทยาศาสตร์ จุฬาลงกรณ์มหาวิทยาลัย
ปีการศึกษา 2555
ลิขสิทธิ์ของจุฬาลงกรณ์มหาวิทยาลัย

SYNTHESIS OF 1,4-DIHYDROPYRIDINYL GLUCOSAMINE DERIVATIVE AS
WATER SOLUBLE FLUORESCENT SENSOR

Mr. Oran Pinrat

A Thesis Submitted in Partial Fulfillment of the Requirements

for the Degree of Master of Science Program in Petrochemistry and Polymer Science

Faculty of Science

Chulalongkorn University

Academic Year 2012

Thesis Title   SYNTHESIS OF 1,4-DIHYDROPYRIDINYL GLUCOSAMINE DERIVATIVE AS WATER SOLUBLE FLUORESCENT SENSOR

By   Mr. Oran Pinrat

Field of Study   Petrochemistry and Polymer Science

Thesis Advisor   Anawat Ajavakom, Ph.D.

Thesis Co-advisor   Mongkol Sukwattanasinitt, Ph.D.

          Accepted by the Faculty of Science, Chulalongkorn University in Partial Fulfillment of the Requirements for the Master's Degree

…………………………………..Dean of the Faculty of Science

(Professor Supot Hannongbua, Dr.rer.nat)

THESIS COMMITTEE

……………………………………Chairman

(Assistant Professor Warinthron Chavasiri, Ph.D.)

……………………………………Thesis Advisor

(Anawat Ajavakom, Ph.D.)

……………………………………Thesis Co-advisor

(Associate Professor Mongkol Sukwattanasinitt, Ph.D.)

……………………………………Examiner

(Associate Professor Nuanphun Chantarasiri, Ph.D.)

……………………………………External Examiner

(Nakorn Niamnont, Ph.D.)

โอฬาร ปิ่นรัตน์ :   การสังเคราะห์อนุพันธ์ 1,4-ไดไฮโดรพิริดินิลกลูโคซามีนเพื่อใช้เป็น ฟลูออเรสเซนต์เซ็นเซอร์ที่ละลายน้ำได้ (SYNTHESIS OF 1,4-DIHYDROPYRIDINYL GLUCOSAMINE DERIVATIVE AS WATER SOLUBLE FLUORESCENT SENSOR) อ.ที่ปรึกษาวิทยานิพนธ์หลัก : ดร. อนวัช อาชวาคม, อ. ที่ปรึกษาวิทยานิพนธ์ร่วม : รศ. ดร. มงคล สุขวัฒนาสินิทธิ์, 71 หน้า.

กลูโคซามีนเป็นน้ำตาลที่มีหมู่อะมิโนสังเคราะห์ได้จากไคตินและไคโตซานของสัตว์ทะเล เปลือกแข็ง 2 ชนิด คือ กุ้งและปู ซึ่งเป็นวัตถุดิบที่มีมากมายในประเทศไทย แนวทางใหม่ในการนำ กลูโคซามีนมาใช้ประโยชน์ได้ถูกคิดค้นขึ้น มิฉะนั้นวัตถุดิบนี้จะถูกทิ้งเป็นขยะมากกว่า 500,000 ตันต่อปี 1,4-ไดไฮโดรพิริดินิลกลูโคซามีน (Glc-DHP **1**) ได้ถูกสังเคราะห์ขึ้นเพื่อใช้เป็นฟลูออเรส เซนต์เซ็นเซอร์ชนิดใหม่ที่ละลายน้ำได้ เอมีนปฐมภูมิได้มาจากการนำกลูโคซามีนไฮโดรคลอไรด์มา ใช้เป็นวัตถุดิบตั้งต้นโดยใช้วิธีการสังเคราะห์ตามกระบวนการที่ได้มีการรายงานก่อนหน้านี้ จาก ปฏิกิริยาการเติมของเอมีนปฐมภูมิและเอทิลโพรพิโอเลตโดยใช้ไดคลอโรมีเทนเป็นตัวทำละลาย ภายใต้อุณหภูมิการควบแน่นเป็นเวลา 3 วัน จะให้สารผลิตภัณฑ์ที่เป็นเบต้า-อะมิโน อะครีเลต การทำปฏิกิริยาปิดวงของเบต้า-อะมิโน อะครีเลต เกิดเป็นผลิตภัณฑ์ Glc-DHP **1** ได้โดยการเติม ไทเทเนียมเททระคลอไรด์ลงไปเพียงเล็กน้อย อนุพันธ์ DHP นี้สามารถละลายน้ำได้และเมื่ออยู่ใน สารละลายจะให้สัญญาณฟลูออเรสเซนซ์สีน้ำเงินด้วยประสิทธิภาพการเรืองที่ 0.29 เนื่องจากมี สมบัติในการให้สัญญาณฟลูออเรสเซนซ์ได้, Glc-DHP **1** จึงถูกใช้เป็นฟลูออเรสเซนต์เซ็นเซอร์ที่ ละลายน้ำได้ในการตรวจวัดสารประกอบวัตถุระเบิดไนโตรอะโรมาติก Glc-DHP **1** แสดงการระงับ สัญญาณการเรืองแสงได้อย่างจำเพาะเจาะจงกับสารประกอบ 2,4,6,-ไนโตรฟีนอลโดยปราศจาก การรบกวนจากสารไนโตรอะโรมาติกชนิดอื่น โดยมีค่าคงที่ของการระงับสัญญาณการเรืองแสง (K_{sv}) เท่ากับ 44,700 M^{-1} และค่าต่ำสุดที่สามารถตรวจวัดได้ (LOD) คือ 0.94 μM การตรวจวัด สารมารถเห็นด้วยตาเปล่าภายใต้แสงยูวีคลื่นสั้น นอกจากนั้น Glc-DHP **1** ยังสามารถใช้ในการ ตรวจวัดโปรตีน เช่น BSA, papain และ ฮีโมโกลบิน การเรืองแสงของ Glc-DHP **1** ลดลงเมื่อเติม ฮีโมโกลบิน ไซโทโครม ซี และ ไมโอโกลบิน ให้ค่าคงที่ของการระงับสัญญาณการเรืองแสง (K_{sv}) เท่ากับ 424,000 M^{-1} 53,400 M^{-1} และ 52,200 M^{-1} ตามลำดับ

สาขาวิชา ปิโตรเคมีและวิทยาศาสตร์พอลิเมอร์   ลายมือชื่อนิสิต...

ปีการศึกษา   2555   ลายมือชื่อ อ.ที่ปรึกษาวิทยานิพนธ์หลัก....................

ลายมือชื่อ อ.ที่ปรึกษาวิทยานิพนธ์ร่วม.....................

5372398323 : MAJOR PETROCHEMISTRY AND POLYMER SCIENCE
KEYWORDS : 1, 4-DIHYDROPYRIDINE/ FLUORESCENCE SENSOR/ 2,4,6-TRINITROPHENOL/HEMOGLOBIN

ORAN PINRAT: SYNTHESIS OF 1,4-DIHYDROPYRIDINYL GLUCOSAMINE DERIVATIVE AS WATER SOLUBLE FLUORESCENT SENSOR ADVISOR : ANAWAT AJAVAKOM, Ph.D., CO-ADVISOR: MONGKOL SUKWATTANASINITT, Ph.D., 71 pp.

Glucosamine (GlcNH) is an amino sugar synthesizable from chitin and chitosan of two marine crustaceans: shrimp and crab, abundant resource in Thailand. The new way to utilize GlcNH has to be developed; otherwise this resource will be wasted more than 500,000 tons a year. 1,4-Dihydropyridinyl Glucosamine (Glc-DHP **1**) has been synthesized as a new fluorescent sensor. Primary amine was obtained from D-glucosamine hydrochloride (GlcNHCl) as the starting material by using the reported synthetic procedure [55]. Subsequent addition reaction of the primary amine and ethyl propiolate in CH_2Cl_2 under refluxing temperature for 3 days was carried out to produce β-amino acrylate. The cyclotrimerization (3 eq.) of the β-amino acrylate to Glc-DHP **1** was observed smoothly in the presence of $TiCl_4$. This DHP derivative is soluble in aqueous media and the solution gives blue fluorescent signal with quantum yield of 0.29. By possessing fluorescence property, this Glc-DHP **1** was used as fluorescent chemosensor for the detection of explosive compounds. The fluorescence signal of Glc-DHP **1** was selectively quenched by 2,4,6-trinitrophenol without the interference of other nitroaromatics with high quenching efficiency (K_{sv} = 44,700 M^{-1}) and a detection limit of 0.94 µM. Also the detection could be observed by naked eye under black light. Moreover, Glc-DHP **1** was also tested as fluorescent biosensor for the detection of protiens; e.g. BSA, hemoglobin, papain, etc. The fluorescence signal of Glc-DHP **1** was selectively quenched by hemoglobin, cytochrome c and myoglobin with K_{sv} = 424,000 M^{-1}, 53,400 M^{-1} and 52,200 M^{-1}, respectively.

Field of Study : Petrochemistry and Polymer Science   Student's Signature ....

Academic Year : ....2012..............................   Advisor's Signature ....

Co-advisor's Signature ....

ACKNOWLEDGEMENTS

First of all, I would like to express my sincere gratitude to my thesis advisor, Dr. Anawat Ajavakom, for valuable advice, guidance and encouragement throughout the course of this research. Sincere thanks are also extended to Assistant Professor Dr. Warinthron Chavasiri, Associate Professor Dr. Nuanphun Chantarasiri, and Dr. Nakorn Niamnont, attending as the committee members, for their valuable comments and suggestions.

I would like to especially thank my co-advisor, Associate Professor Dr. Mongkol Sukwattanasinitt for his generous assistance, invaluable guidance and kindness throughout this research. I also would like to thank Assistant Professor Dr. Paitoon Rashatasakhon and Assistant Professor Dr. Sumrit Wacharasindhu for his attention and suggestion during our group meeting.

My appreciation is also given to many people in our research group; Ms. Sasiyada Homraruen for training; Mr. Thirawat Sirijindalert, Dr. Nakorn Niamnont, Ms. Warathip Siripornnoppakhun, Mr. Watcharin Ngampueng and Ms. Kanoktorn Boonkitpatarakul for their helpful suggestion, Ms. Nattaporn Kimpitak, Ms. Wannapa Yuanboonlim, Mr. Akachai Khumsri, Mr. Pharkphoom Auttapornpitak, Ms. Wanwisa Thongmalai, and everyone in MAPS group for a greatest friendships and encouragement.

In particular, I am thankful to the National Nanotechnology Center for supporting my thesis.

Finally, I would like to specially thank my family and friends for their encouragement and understanding throughout. I would not be able to reach this success without them.

CONTENTS

Page

LIST OF TABLES

Page

LIST OF FIGURES

LIST OF SCHEMES

Scheme   **Page**

LIST OF ABBREVIATIONS

Ar	aryl group
calcd	calculated
^{13}C NMR	carbon-13 nuclear magnetic resonance
$CDCl_3$	deuterated chloroform
CH_2Cl_2	methylene chloride
DMSO-d_6	deuterated dimethyl sulfoxide
DMSO	dimethylsulfoxide
d	doublet (NMR)
dd	doublet of doublet (NMR)
ESIMS	electrospray ionization mass spectrometry
EtOAc	ethyl acetate
equiv	equivalent (s)
g	gram (s)
^{1}H NMR	proton nuclear magnetic resonance
Hz	Hertz
HRMS	high resolution mass spectrum
h	hour (s)
J	coupling constant
mg	milligram (s)
mL	milliliter (s)
mmol	millimole (s)
m.p.	melting point
nm	nanometer (s)
m/z	mass per charge
m	multiplet (NMR)
M.W.	molecular weight
M	molar
MHz	megahertz
q	quartet (NMR)

rt	room temperature
s	singlet (NMR)
t	triplet (NMR)
THF	tetrahydrofuran
TLC	thin layer chromatography
UV	ultraviolet
δ	chemical shift
°C	degree Celsius
µL	microliter (s)
µM	micromolar (s)
ε	molar absorptivity
λ	wavelength
Φ	quantum yield
% yield	percentage yield

CHAPTER I

INTRODUCTION

1.1   Introduction of glucosamine

Chitin, a naturally abundant mucopolysaccharide, and the supporting material of crustaceans, insects, etc., is known to consist of 2-acetamodo-2-deoxy-β-D-glucose through a β (1→4) linkage. Chitosan is the *N*-deacetylated derivative of chitin, although this *N*-deacetylation is almost never complete. A shape nomenclature with respect to the degree of *N*-deacetylation has not been defined between chitin and chito san [1-2]. *N*-acetyl-D-glucosamine and D-glucosamine are monomers of chitin and chitosan, respectively **Figure 1.1**. There are two hydrolytic methods, chemical hydrolysis and enzymatic hydrolysis, which can be normally used for the preparation of the monomers and chitooligosaccharides from chitin and chitosan [3-4].
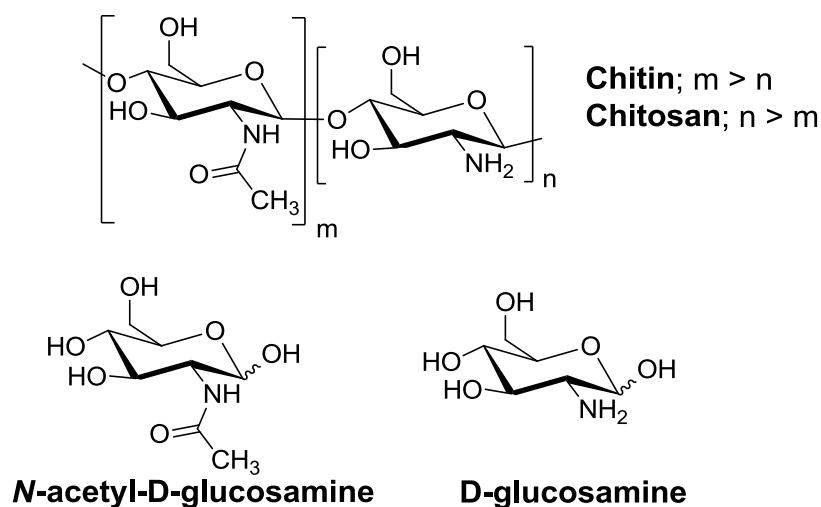
Figure 1.1 Structures of chitin, chitosan, *N*-acetyl-D-glucosamine and D-glucosamine

The use of chitin-chitosan in Thailand has advantage over other countries, due to the availability of raw materials (squid skeleton, shrimp and crab shell). Shrimp is regarded as economic ocean creature which is widely fed, and most of all, is one of the major export products of Thailand. The demand of fresh shrimp in frozen shrimp industry is about 600,000 tons per year while leftover shrimp heads and shells being thrown away or partly supplied to the industry as raw material in the production of chitin-chitosan about 200,000 tons per year. Other raw materials to produce chitin-

chitosan production are derived from other seafood industries about 300,000 tons per year [5].

Glucosamine hydrochloride (GlcNHCl) is a well-known neutrapharmaceutical agent prescribed for osteoarthritis patients. Hydrolysis of shrimp shell α-chitin in concentrated hydrochloric acid under evaluated temperature is a general method for production of GlcNHCl [6]. In 2012, Sulaleewan and coworkers [7] have developed the method to speed up the hydrolysis process, microwave assisted hydrolysis. With microwave irradiation, the hydrolysis rate is faster comparing to that of the conventional heating. Only 12 minutes of reaction time is required to complete the hydrolysis when the microwave is utilized, while 90-120 minutes is generally required for the conventional heating. The reaction typically gave 55% isolated yield with 99-100% pure of GlcNHCl.

1.2 Introduction of 1,4-dihydropyridines (DHPs).

The 1,4-dihydropyridine (DHP) is a heterocyclic molecule, in which the parent molecule pyridine, is semi-saturated with two hydrogens replacing one double bond at the position of 1 and 4 of the pyridine ring, as shown in **Figure 1.2**.
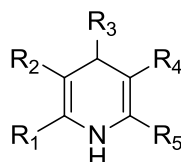
Figure 1.2 Basic structure of 1,4-dihydropyridine (DHP).

The first DHP was successfully prepared by Hantzsch reaction in the year of 1882 [8]. Since then their derivatives have been used for a variety of applications [9-15]; e.g. modeling NADH in biochemistry [9], photosensitive polymers [10] and pharmaceutical medicines [11-15]. Some DHPs are drugs belonging to the class of pharmacological agents known as calcium channel blockers [11-12]. For instance, the inhibition of calcium ion cell penetration by DHP derivatives was reported to weaken the contractility of the cardiac muscle [13]. These compounds were also shown to be very effective vasodilators and useful in the treatment of hypertension, ischemic heart disease and other cardiovascular disorders [14-15].

In the past, numerous methods to synthesize DHP derivatives were reported [16-19]. Though these methods could provide DHPs with substituent at positions adjacent to the nitrogen atom in high yield, they have difficulties to perform in the same manner to obtain the DHP product with hydrogen atom at the same position. Accordingly, Kikuchi and team [16] synthesized DHPs **3** bearing a carboethoxy methyl group at 4-position **(Figure 1.3)** from the reaction of aniline with ethyl propiolate catalyzed by scandium(III) triflate in toluene under reflux conditions. This method gave DHP product **3** in a GC yield of 42%.
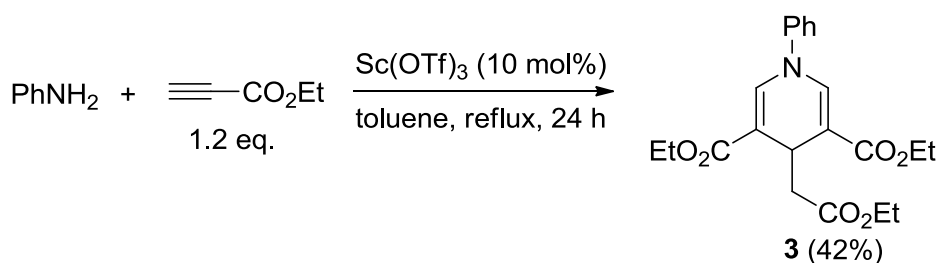
Figure 1.3 The synthetic scheme of DHP derivative **3**.

In 2006, Vohra and coworkers [17] reported the synthetic route of DHPs **4** without the separation of such enamine intermediate by using two Lewis acids **(Figure 1.4)**. The coupling reaction between β-ketoester and primary aliphatic amine, followed by addition of α,β-unsaturated aldehyde was successfully performed in one pot, leading to the asymmetric DHPs **4** in high yields under mild reaction conditions.

Lewis acid	R_1	R_2	%yield
FeCl$_3$.6H$_2$O	OEt	Bn	98
Sc(OTf)$_3$	OEt	Bn	75
	OEt	n-Bu	80
	Me	n-Bu	80
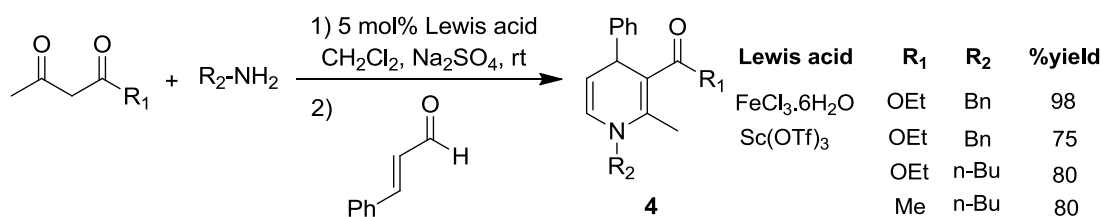
Figure 1.4 The synthetic scheme of compound **4**.

In 2010, Sirijindalert and coworkers [18] reported the synthesis of DHPs **6** from the corresponding β-amino acrylates **5** by using titanium(IV) chloride under facile conditions (**Figure 1.5**). The cyclotrimerization of β-amino acrylates to *N*-substituted DHP was achieved by three addition/elimination steps in high to excellent yields (70–83%). This synthetic method has been developed among our group and will be utilized to make fluorescence chemosensor molecules.
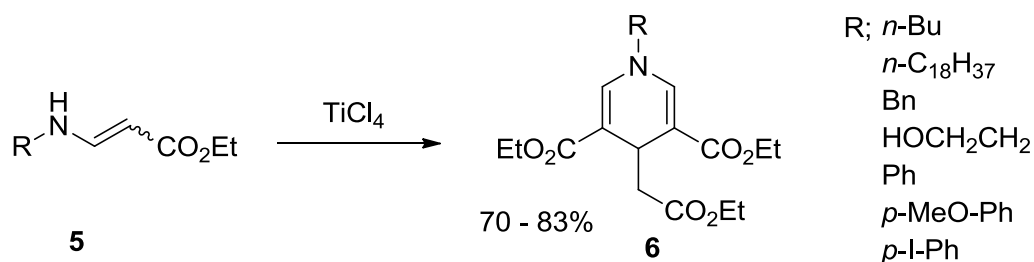
Figure 1.5 The synthetic scheme of DHP derivatives **6**.

In 2011, Sueki and coworkers [19] synthesized DHP derivatives **7** by using Tb(OTf)$_3$ as a catalyst (**Figure 1.6**). In their work, several Lewis acids were attempted for the condensation reaction of aniline, aldehyde and acetal protected β-ketoester. The series of DHP were synthesized by using 2.5 mol% Yb(OTf)$_3$ in 1,4-dioxane at 90 °C for 16 hours in poor to good yields.
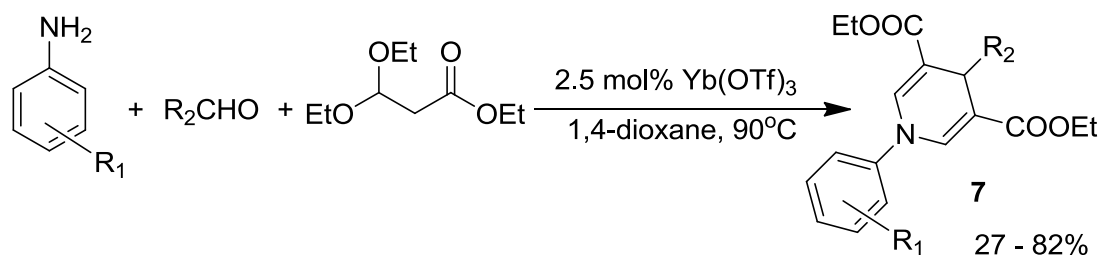
Figure 1.6 The synthetic scheme of DHP derivatives **7**.

The structure of DHP consisted of the π-conjugated chromophores is endowed by a strong absorption with the maximum around 350 nm and maximum emission around 450 nm [20-21]. Due to their optical properties, the photophysical characteristics of DHP have been continuously reported [22-26].

1.3 Introduction of fluorometry

Fluorometry is a class of techniques that assay the state of a biological chemical system by studying its interaction with fluorescent probe molecules. This interaction is monitored by measuring the changes in the/of the optical properties fluorescent probe. The fluorescence characterizes the relationship between absorbed and emitted photons at specified wavelength. It is a precise quantitative and qualitative analytical technique that is not only highly sensitive and highly specific but with even greater advantages of rapid testing, inexpensive and easy to use.

Fluorescence is a photon emission process that occurs when a molecule absorbs light photons from the UV visible light, known as excitation, and then rapidly emits light photons when return to their ground state. The phenomenon is usually described by the Jablonski diagram [27], which offers a convenient representation of the excited state structure and the relevant transitions, to illustrate possible various molecular processes. A simplified Jablonski diagram shown in **Figure 1.7**, demonstrates that a photon is excited to singlet excited electronic states (S1 or S2) and form an excited photon. The fluorescence signal is observed when an excited electron relaxes to a ground singlet electronic state (S0) via photon emission. The time required to complete this whole process takes only around nano-second.
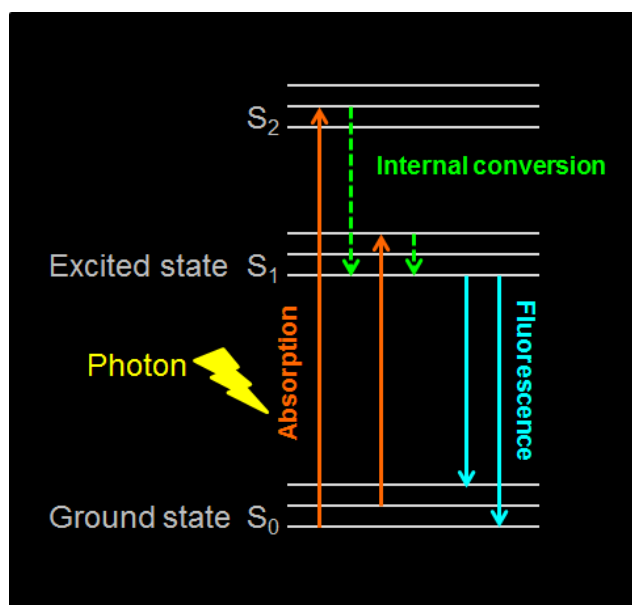
Figure 1.7 Jablonski diagram illustrating the fluorescent processes [27].

1.4 Fluorescent sensor

A fluorescence signal change normally resulted from the interaction between fluorophore and analyst (target compound), which can be a metal ion, an anion or an organic molecule. Fluorescence sensor will then exhibit a new fluorescence behavior, detectable by the fluorometry.

Fluorescent sensors are usually composed of three components: a receptor, a fluorophore and a spacer or linker. These three parts do exactly correspond to the three components shown in **Figure 1.8**. When a fluorescent sensor specifically

interacts with analyte, the read-out is usually measured as a change in fluorescence intensity, intensity decay lifetime, or a shift of the emission wavelength. The mechanism which controls the quenching response of a fluoroionophore to substrate binding includes photo-induced electron transfer (PET), photo-induced charge transfer (PCT), fluorescence (Förster) resonance energy transfer (FRET), and excimer/exciplex formation or extinction. An important feature of the fluorescent sensors is that signal transduction of the analytes leading to the readout can happen in a very short time (less than nanoseconds) and without any other assistances. This makes real-time and real-space detection of the analyte possible as well as the imaging associated with analyte distribution [28].
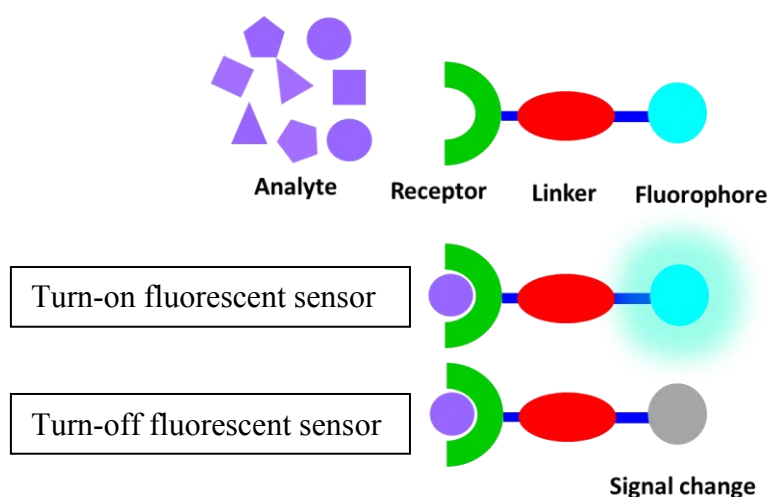
Figure 1.8 Schematic illustration of a sensor device.

1.5 Fluorescence Resonance Energy Transfer (FRET)

Fluorescence (or Förster) Resonance Energy Transfer (FRET) has been widely used in all applications of fluorescence, including medical diagnostic, optical imaging and DNA analysis. FRET occurs between a donor molecule in the excited state and an acceptor molecule in the ground state. If the emission spectrum of donor molecules overlaps with the absorption spectrum of the acceptor, the energy transfer will occur as the result of long-range dipole-dipole interactions between the donor and acceptor. The emission signal of the acceptor (solid yellow arrow, **Figure 1.9**) occurs through the excitation of the donor molecule (solid purple arrow), while the emission of the

donor molecule is reduced (dashed blue arrow). The donor fluorescence (solid blue arrow) is diminished during the transition to a lower quantum state. The efficiency of the transferred energy depends on the molecular distance between 1-10 nm, the extent of spectral overlap of the emission spectrum of the donor with the absorption spectrum of the acceptor, the quantum yield of the donor, the relative orientation of the donor and acceptor transition dipoles, and the distance between the donor and acceptor molecules [29].
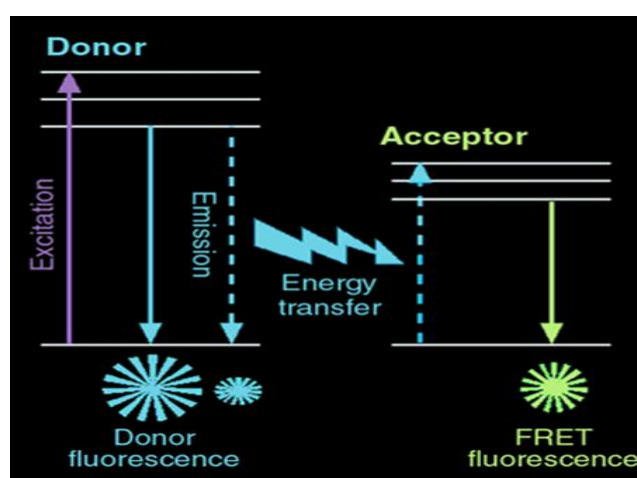
Figure 1.9 Jablonski diagram showing the energy levels of the fluorescent dyes and the rates and states involved in FRET [29].

1.6   Application of fluorescent sensors

Fluorescent small molecule sensors have become an important class of materials in a wide variety of applications, including small ions [30] or biomolecules i.e. proteins and nucleic acids [31]. Useful responsive small-molecule ligands that provide immediate optical feedback can overcome such limitations because their use does not require sophisticated instrumentation or sample preparation. The most important consideration influences the design of small molecule ligands for sensing metal ion. The probe should be highly selective for the metal over all other components in the environmental or biological sample. Some examples reported herein show the focus on the design and synthesis of such small-molecule-based metal ion sensors.

1.6.1 Metal ion fluorescent sensors

In 2008, Mitra and coworkers [32] designed the new glucose-based C2-derivatized colorimetric chemo-sensor **8** by a one-step condensation of glucosamine and 2-hydroxy-1-naphthaldehyde (**Figure 1.10**). The recognition of transition metal ions resulted in visual color change only in the presence of Fe^{2+}, Fe^{3+} and Cu^{2+} in MeOH. Moreover, in an aqueous HEPES buffer (pH 7.2) it is only the Fe^{3+} that gave a distinct visual color change even, up to a concentration of 280 ppb without any interferences from other metal ions.
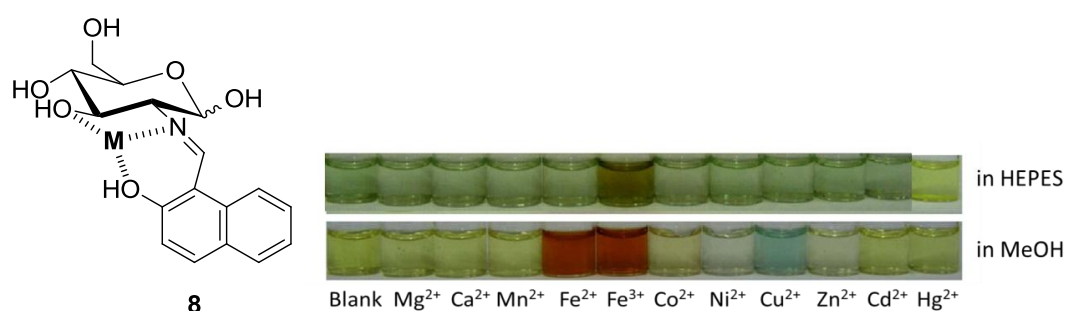
Figure 1.10 Structure of glucose-based derivative **8** and its fluorogenic response in MeOH (bottom row), HEPES buffer solutions (top row) [32].

In 2011, Sirilaksanapong and coworkers [33] synthesized water-soluble fluorophores from 1,3,5-tris-(4'-iodophenyl)benzene **9** (**Figure 1.11**). These compounds containing three phenylene-ethynylene units and three salicylic acid peripheral groups exhibited a highly selective fluorescence quenching by Cu^{2+} ions. The detection limit for Cu^{2+} improved from 6.49 to 0.19 ppb in aqueous media in the presence of Triton X-100 surfactant as well as the quantum efficiency.
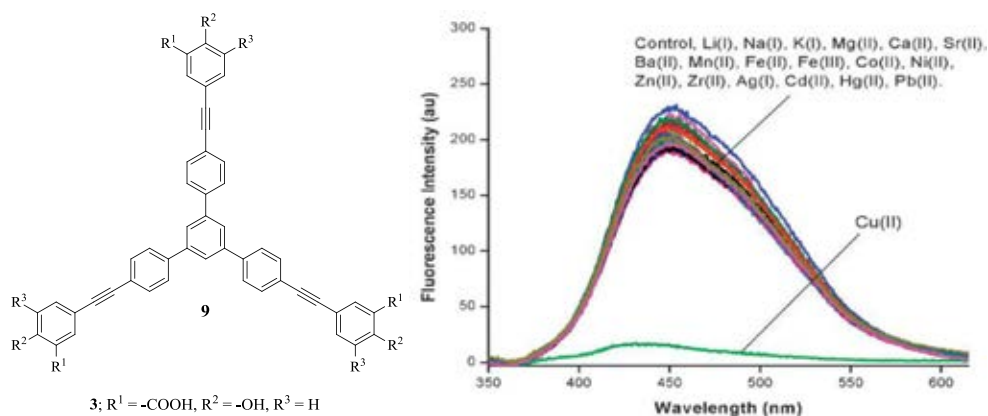
Figure 1.11 Water-soluble fluorophore **9** and its selectivity toward Cu^{2+} ion [33].

In 2009, Niamnont and coworkers [34] reported the synthesis and sensing properties of water soluble fluorescent dendritic compound **10** (**Figure 1.12**). This dendritic compound composed of phenylene-ethynylene repeating units and anionic carboxylate peripheries. Without a surfactant, compound **10** exhibited a low fluorescent quantum yield, but a good selectivity toward Hg^{2+}. After adding Triton X-100, the quantum yield was drastically increased and the sensitivity for the detection of Hg^{2+} was also improved. The increase in fluorescence quantum yields (Φ_F) strongly agrees with the assumption that Triton X-100 facilitates the intermolecular dissociation of these compounds.
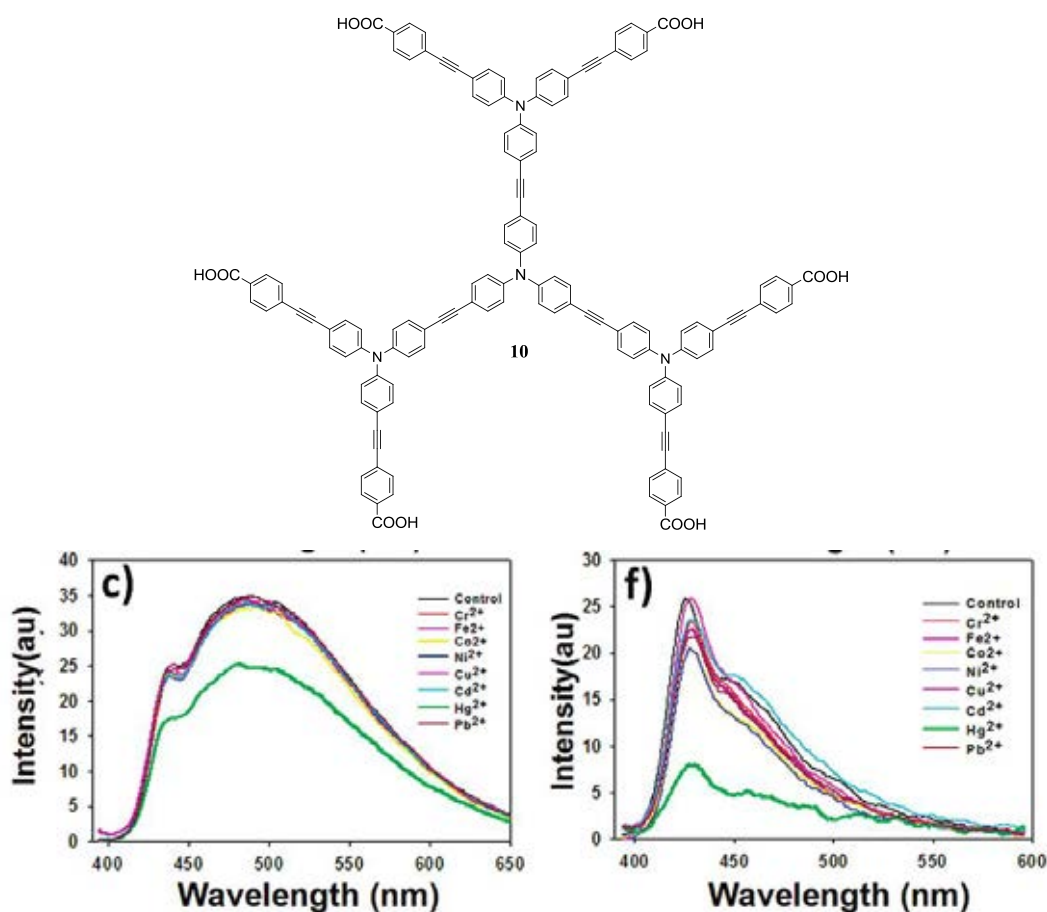
Figure 1.12 Dendritic fluorophore **10** and its selectivity toward Hg^{2+} ion before (c) and after (f) the addition of surfactant [34].

In 2013, Homraruen and coworkers [35] reported a new fluorescent 1,4-dihydropyridine (DHP) tricaboxylic acid **11 (Figure 1.13)**, which can be used as a selective chemodosimeter for Hg^{2+} in aqueous solution. The decrease of fluorescence signal was proportional to Hg^{2+} concentration with high quenching efficiency (K_{sv}=78,300) providing a detection limit of 0.2 mM. The quenching process involves an oxidation of the DHP into a pyridinium ring **12** specifically induced by Hg^{2+} that brought about its remarkable selectivity over other metal ions.
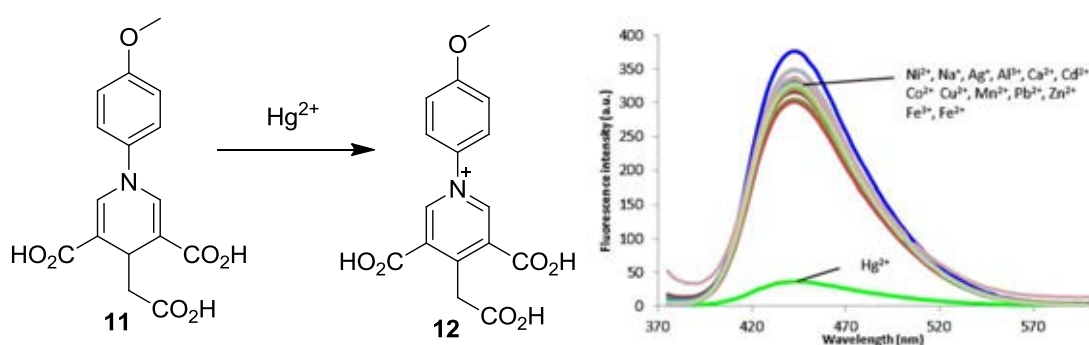
Figure 1.13 Structure of DHP fluorescent sensor **11** and its selectivity toward Hg^{2+} ion [35].

1.6.2 Nitroaromatic explosive fluorescent sensors

Selective and sensitive sensor for detection of nitroaromatic explosives, in particular 2,4,6-trinitrotoluene (TNT), 2,4,6-trinitrophenol or picric acid (TNP or PA) and 3,5-dinitro-2,6-bispicrylamino pyridine (PYX), are of great current interest in both national security and environmental protection, because they are not only explosives but also recognized as toxic pollutants [36-37]. TNP is a common chemical used frequently in several organic transformations and in leather/dye industries as a pigment. Due to its high rate of thermal expansion upon initiation with external stimuli, TNP has long been used as important component in manufacturing of explosives and rocket fuels. It was proved that the long time exposure to the vapor of TNP can cause headaches, anemia, and toxic to living organisms [38]. Furthermore, among various techniques used for the detection of nitroaromatics, fluorescence-based

detection offers several advantages; high sensitivity, specificity, and real-time monitoring with short response time [39-40].

2,4,6-trinitrotoluene (TNT)   2,4,6-trinitrophenol (TNP)   3,5-dinitro-2,6-bispicrylamino pyridine (PYX)
Picric acid
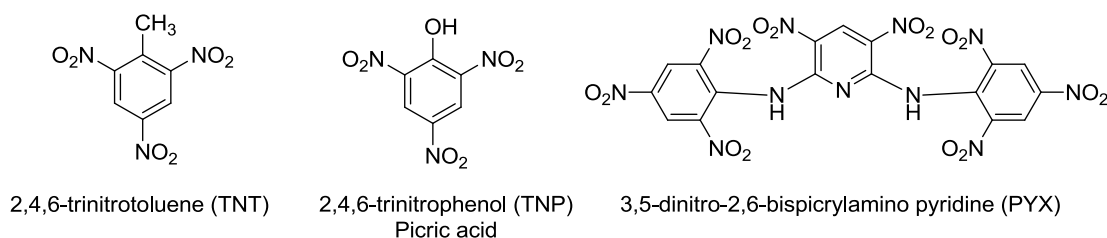
Figure 1.14 Structures of TNT, TNP and PYX

In 2012, Ma and coworkers [41] synthesized 8-hydroxyquinoline aluminum (Alq_3)-based bluish green fluorescent composite nanospheres via self-assembly under vigorous stirring and ultrasonic treatment **(Figure 1.14)**. The nanocomposite was selectively quenched by TNP in an aqueous solution, independent of the interference of other nitroaromatic explosives. In addition, a convenient paper sensor for TNP-selective detection was fabricated.
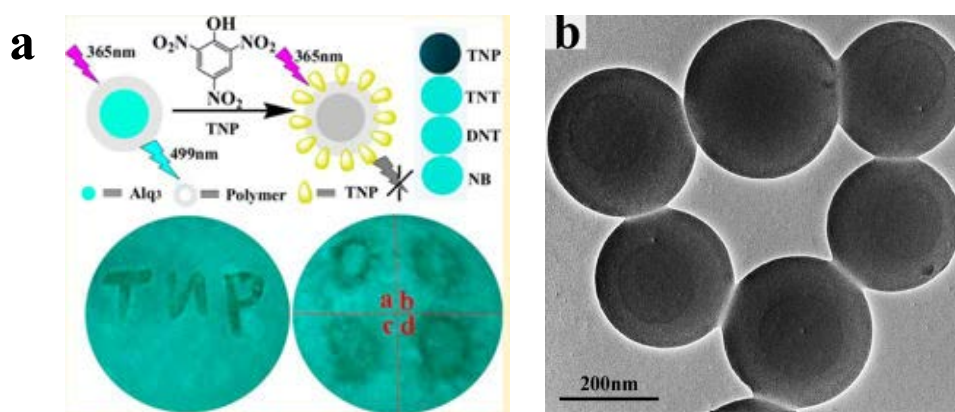
Figure 1.14 (a) The selective fluorescence quenching for TNP of nanocomposite and (b) TEM image of Alq_3 based nanocomposite [41].

In 2012, Bhalla and coworkers [42] reported novel pentacenequinone derivative **13 (Figure 1.15)** using the Suzuki-Miyaura coupling protocol which forms fluorescent nanoaggregates in aqueous media due to its aggregation-induced emission enhancement attributes. The nanoaggregates selectively quenched TNP with a detection limit of 500 ppb probably due to energy transfer.
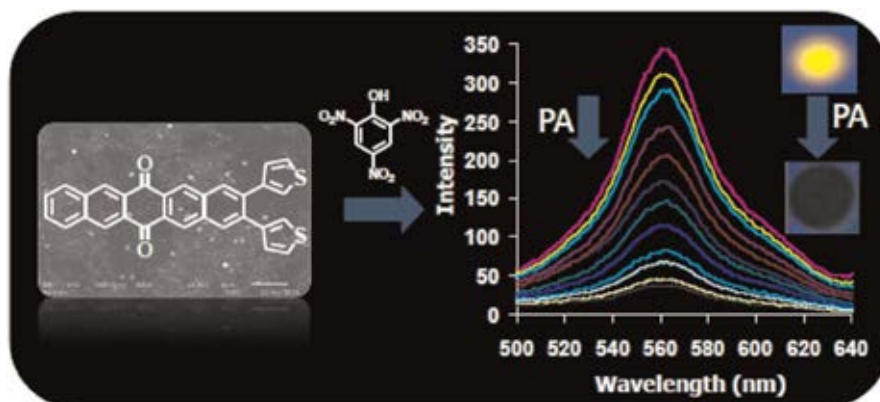
Figure 1.15 Structure of fluorescent **13** nanoaggregate and its selectivity toward TNP [42].

In 2013, Liu and coworkers [43] synthesized four novel terthiophene (3T) derivatives by employing Grignard coupling reaction **(Figure 1.16)**. The structural modification of **4** has furnished highly selective and sensitive fluorescent chemosensors for the nitro-containing explosives. Among them, TNP and PYX are much more effective quenchers than others, and furthermore, common organic solvents and interferents show little effect to the sensing process.
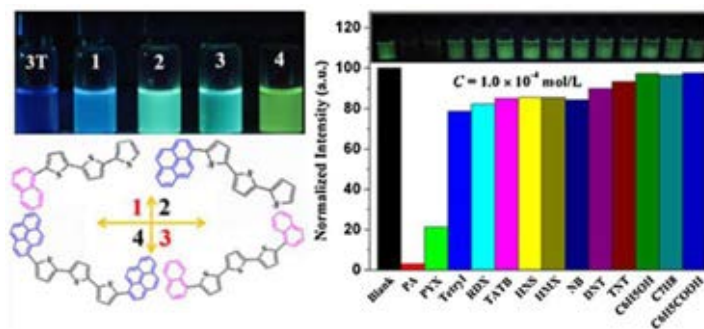
Figure 1.16 Structures of terthiophene derivatives and the selective fluorescence quenching for TNP and PYX of compound **4** [43].

In 2011, Zhao and coworkers [44] designed and synthesized a starburst luminogen (THPSTPA) **(Figure 1.17)**. Whereas it is weakly luminescent when molecularly dissolved in THF, it becomes highly emissive when aggregated in water, less dissoluble solvent, exhibiting a novel phenomenon of aggregation-induced emission. The emission of its aggregates can be quenched exponentially by TNP due

to the energy transfer from the excited state of THPSTPA to the ground state of TNP via the spectral overlap of the absorption of TNP and emission of the THPSTPA.
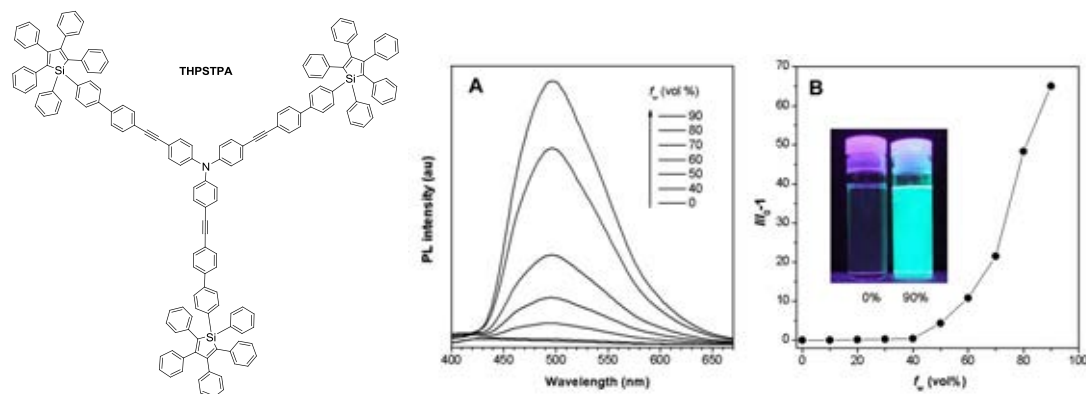
Figure 1.17 Structure of THPSTPA and its novel phenomenon of aggregation-induced emission [44].

In 2011, He and coworkers [45] synthesized two poly(pyrene-co-phenylene-ethynylene)s of different composition (PyPE-**14**) **(Figure 1.18)**. Then PyPE-**14** was casted onto glass plate surfaces to fabricate films for sensing of 2,4,6-trinitrotoluene (TNT) in aqueous phase. Moreover, the quenching efficiencies of TNT to the fluorescence emission of film **14** in pure water and in seawater were proved to be the same level, as the two Stern-Volmer plots ware nearly overlapped. Thus, the smart performances of the film guarantee that the films can be developed into sensor devices for the supersensitive detection of TNT in groundwater or seawater.
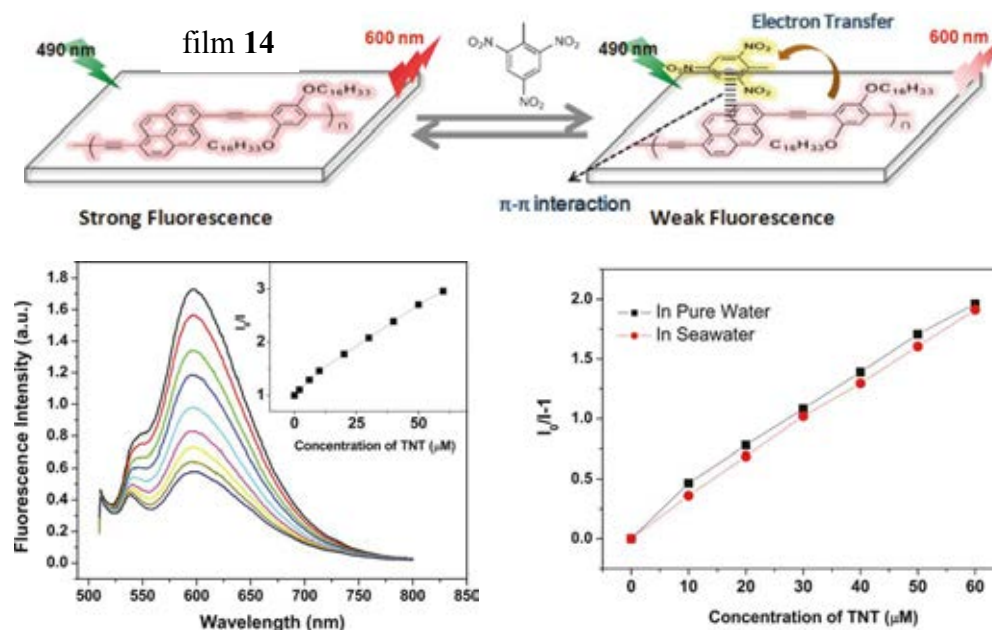
Figure 1.18 Structure of PyPE-**14** (top) casted film. Fluorescence emission spectra of film **14** in the presence of different concentrations of TNT in an aqueous medium (bottom left)and Stern-Volmer plots of film **14** against the concentrations of TNT in pure water and in seawater (bottom right) [45].

In 2013, Roy and coworkers [46] reported the synthesis of new anthracene-functionalized fluorescent tris-imidazolium salt **15 (Figure 1.19)**, which proven to be selective sensor for TNP at the ppb level in both organic and aqueous media. The quenching mechanism is probably due electron transfer from TNP to the sensor molecule **15**.
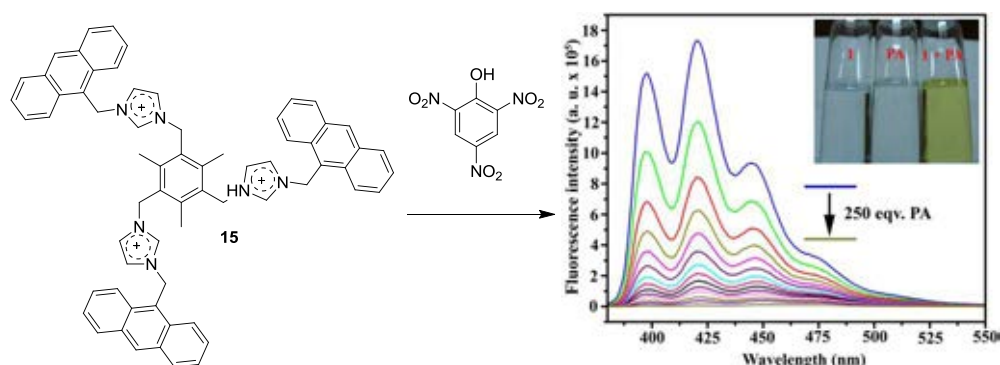
Figure 1.19 Structure of anthracene-functionalized fluorescent sensor **15** and its fluorescence quenching containing different amount of TNP in aqueous media [46].

1.6.3 Protein fluorescent sensor

To keep pace with growing demands on proteomics, medical diagnosis and pathogenic detections, the development of new protein sensors is of great importance [47]. For the last 2-3 decades, heme proteins, metalloproteins containing the heme prosthetic group, either covalently or non-covalently bound to the protein, have been extensively studied, due to their capacities to undergo reduction and oxidation at the iron heme (**Figure 1.20**). Some of these proteins are electron carriers (cytochrome c, catalase), others are involved in catalysis (e.g. peroxidase, cytochrome coxidase) and in active membrane transport or in oxygen transport (e.g. hemoglobin, myoglobin, cytoglobin) [48]. Among the current methods for proteins detection, fluorescence-based biosensors have received considerable attention due to their sensitivity and detection simplicity.
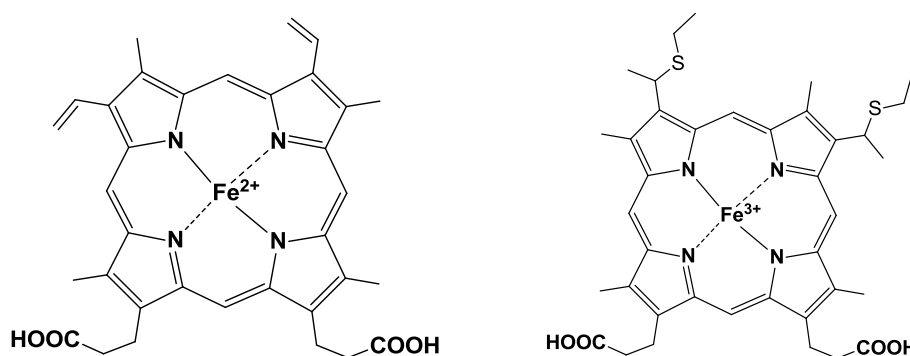
Figure 1.20 Structures of heme protein in hemoglobin, myoglobin (left) and heme protein in cytochrome c (right).

In 2012, Earmrattana and coworkers [49] have accomplished the synthesis of two new anionic fluorophores from truxene core decorated by 2-(2'-methoxy)ethoxyethyl groups to enhance the hydrophilicity of these fluorophores **16, 17** (**Figure 1.21**). Preliminary screening on sensing application shows that their fluorescent signals can be selectively quenched by porphyrin-containing metalloproteins e.g. cytochrome c (Cyt C) and myoglobin (Myo).
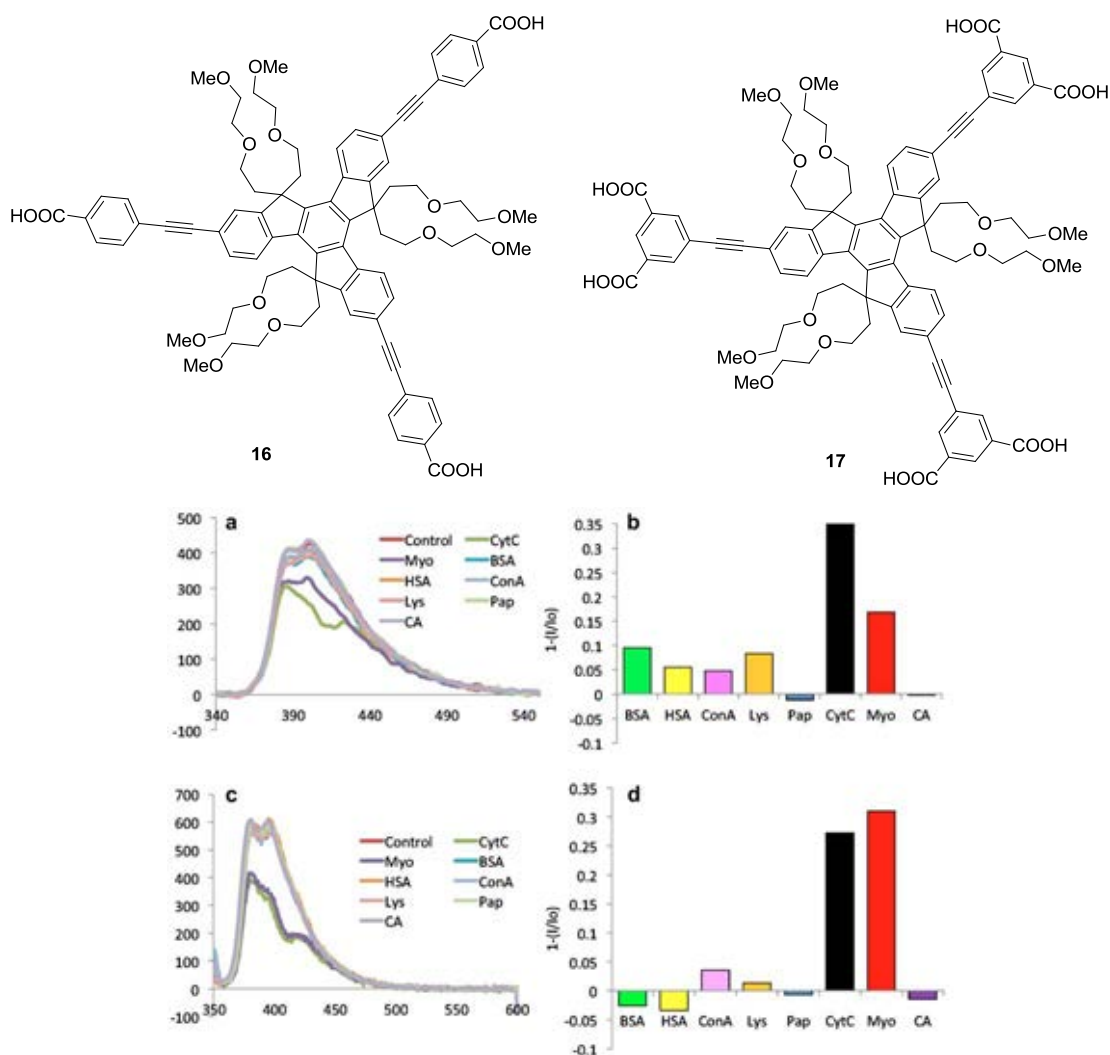
Figure 1.21 Structures of anionic fluorophores from truxene core **16**, **17** and their fluorescence responses to various protein solution in PBS pH 7.4 (compounds **16** and **17** are shown in graph **a**, **b** and **c**, **d** respectively) [49].

In 2010, Niamnont and coworkers [50] synthesized a protein fluorescent sensor array based on variously charged dendritic fluorophores **(Figure 1.22)**. The data set of fluorescent intensities was obtained from 5 repleted or duplicated the experiments by using 9 fluorophores and 8 proteins. The data was statistically sorted for the easy discrimination into eight clusters corresponding to each protein by principal component analysis (PCA).
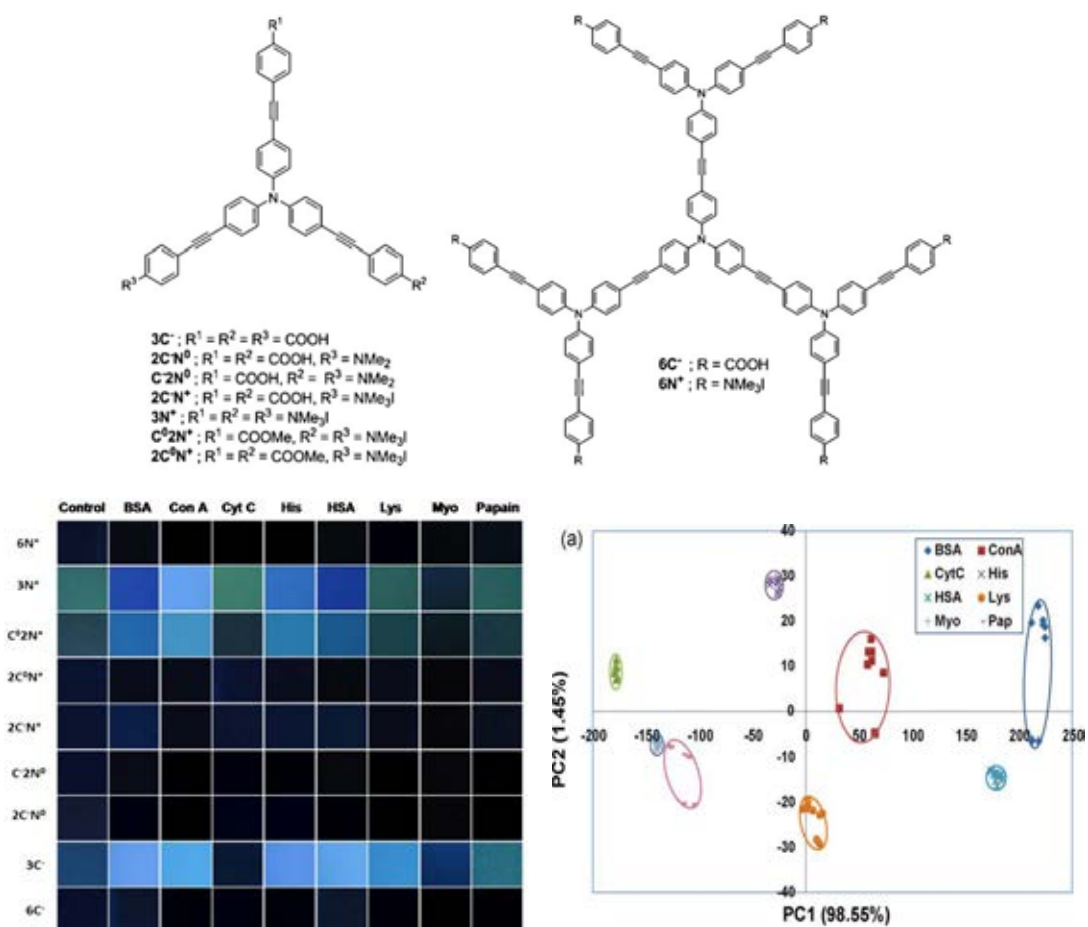
Figure 1.22 Structures of variously charged dendritic fluorophores (top). Photographic image of all fluorophore solutions upon addition of each protein (bottom left). And PCA score plot of ΔI data set obtained from 9 replicates of 8 proteins inducing fluorescence responses of fluorophores (bottom right) [50].

In 2010, Chen and coworkers [51] studied the interaction between salvianolic acid B (Sal B) and human hemoglobin (HHb) under physiological conditions by UV–vis absorption, fluorescence and synchronous fluorescence techniques **(Figure 1.23)**. The experimental results indicated that the quenching mechanism of fluorescence is a static quenching procedure due to K_{sv} values decrease with an increase in temperature. Based on Förster's theory of non-radiative energy transfer, the overlap of the UV–vis absorption of Sal B with the fluorescence emission spectrum of HHb also indicated that the energy transfer from HHb to Sal B occurs with high probability.
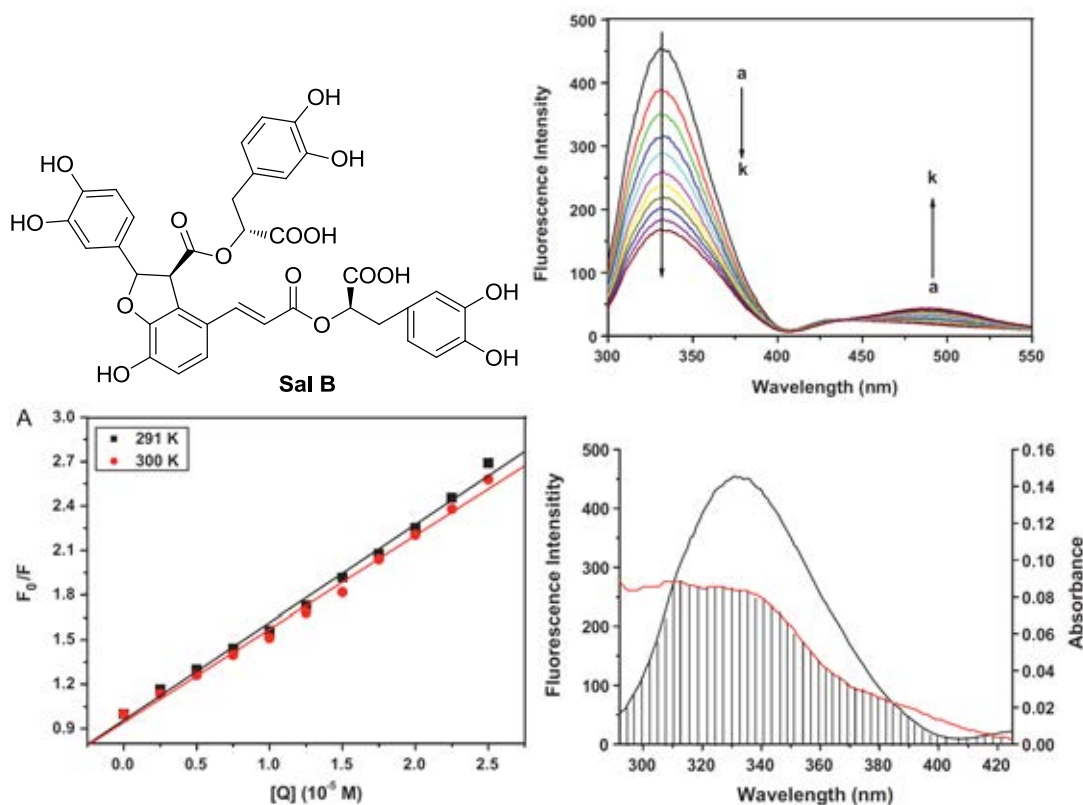
Figure 1.23 Structure of Sal B (top left) and effect of Sal B on fluorescence spectra of HHb (top right). Stern–Volmer curves for the quenching of HHb fluorescence by Sal B at different temperatures (291 K and 310 K) (bottom left) and the overlap of the UV–vis absorption of Sal B to fluorescence emission spectrum of HHb (bottom right) [51].

1.7 Statement of problem

Glucosamine (GlcN) is an abundant compound in Thailand, particularly from two marine crustaceans: shrimp and crab. The new way to utilize GlcN is to develop it as a new fluorescent sensor; otherwise this resource will be wasted around 500,000 tons a year. Due to the small molecule fluorescent sensors nowadays showed incompetence of good water solubility. Only a few systems can be used in aqueous media. In 2010, Fang and coworkers [52] studied the formation of an enamine **18** and DHP **19** (**Figure 1.24**) from reaction between malondialdehyde (MDA) and glucosamine (GlcN). The results indicated that GlcN reacted readily with MDA at supraphysiological conditions to form different products, particularly a nonfluorescent

enamine **18** and a lipofuscin-like fluorescent DHP **19** (Ex. 392 nm/Em. 454 nm). Consequently, GlcN also greatly inhibited the formation of lipofuscin-like fluorescence induced by MDA reacted with BSA protein. As a result, the reaction of GlcN with MDA suggested a novel anticarbonylation function of GlcN in pathophysiological situations related to aging-related diseases and provided insight into the reaction mechanism of GlcN in protecting proteins against carbonyl stress.
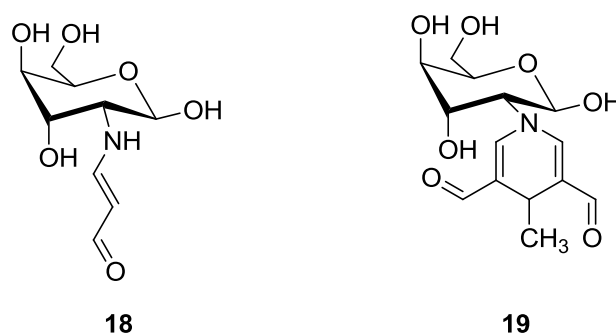
Figure 1.24 Structures of compound **18** and **19**

      Thus, our target molecule was designed to possess the structure that consists of hydroxyl groups. As a background, the hydrolysis of triester DHP to tricarboxylic acid decreased fluorescent efficiency of this DHP in aqueous system [35]. As water soluble moiety, glucosamine unit with four hydroxyl groups are then used in the synthesis of this DHP derivative. Therefore, Glc-DHP **2** can be expected to readily soluble in aqueous media for the test with metal ions, biomolecules and nitroaromatic explosives. The Glc-DHP **1** is considered as an easy and facile synthesis via cyclotrimerization of *N*-Glucopyranosyl β-aminoacrylates under mild conditions. Though high yield is not expected due to the bulkiness of glucosamine, this Glc-DHP **2** has potential to be applied as a fluorescent sensor.
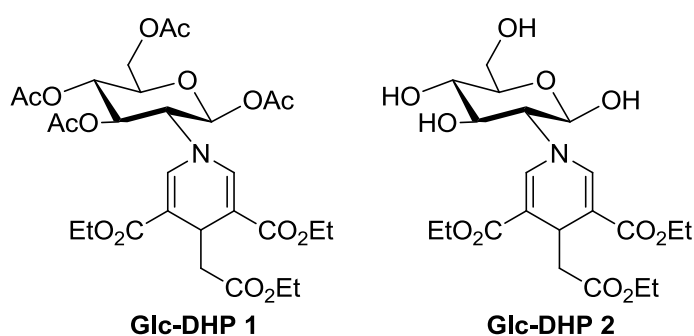
Figure 1.25 Target molecules Glc-DHP **1** and Glc-DHP **2**.

Therefore, concept of this work is to use hydroxy groups of glucosamine unit as water soluble moiety without hydrolysis of triester DHP to tricarboxylic acid for maintaining high fluorescent efficiency.

1.8   Objectives of this research

This research involved the synthetic preparation of a series of 1,4-dihydropyridine (DHP) **1** and **2** (**Figure 1.25**). The photophysical properties of these DHP will be investigated in sodium phosphate buffer solution (PBS) pH 7.4 and milliQ water. The applications of these DHP for nitroaromatic explosive sensor will also be investigated in pure water, seawater and industrial water. Furthermore, this project also focused on the fluorescent sensing of biomolecules and metal ions by using triester DHP.

CHAPTER II

EXPERIMENTAL

2.1   Chemicals and materials

Ethyl propiolate and TiCl$_4$ were purchased from Sigma-Aldrich and Merck. Dichloromethane (CH$_2$Cl$_2$) was dried over CaH$_2$ and distilled prior to use. Thin layer chromatography (TLC) was carried out using Merck 60 F254 plates with a thickness of 0.25 mm. Column chromatography was performed on Merck silica gel 60 (70-230 mesh). All other reagents were analytically pure. All other reagents were non-selectively purchased from Sigma-Aldrich, Fluka or Merck (Germany). For most reactions, solvents such as ethanol and acetone were reagent grade stored over molecular sieves. In anhydrous reactions, solvents such as THF was dried and distilled before use according to the standard procedure. Solvents used for extraction and chromatography such as dichloromethane, hexane, ethyl acetate and methanol were commercial grade and distilled before use while diethyl ether was reagent grade. MilliQ water was used in all experiments unless specified otherwise. The most reactions were carried out under positive pressure of N$_2$ filled in rubber balloons.

2.2   Analytes and real samples

Nitro-containing explosive compounds, including TNP (2,4,6-trinitrophenol), TNT (2,4,6-trinitritoluene), DNT (2,4-Dinitrotoluene), NB (Nitrobenzene), NBA (2-Nitrobenzoic acid), BA (Benzoic acid) and CBA (4-Chlorobenzoic acid) were of analytical grade and used directly without purification. These highly explosive nitro-containing compounds used in the present study were handled only in small quantities. Bovine serum albumin (BSA) was purchased from Fluka (Switzerland). Concanavalin A (ConA, from Jack bean), cytochrome c (Cyt C, from equine heart), histone (His, from calf thymus, typeIII-S), lysozyme (Lys, from chicken egg white), myoglobin (Myo, from equine heart) and papain (Pap, from papaya latex) were purchased from Sigma and used without further purification. The seawater and industrial water were collected from the gulf of Thailand, Jom tien beach located in

Pattaya, and from Ban Khai industrial estate, Rayong, respectively. Both were used without any purification.

2.3 Analytical instruments

^{1}H-NMR and ^{13}C-NMR spectra were acquired from sample solutions in CDCl$_3$, acetone-d[6], CD$_3$CN, CD$_3$OD and DMSO-*d6* on Varian Mercury NMR spectrometer (Varian, USA) at 400 MHz and NMR spectrometer (Bruker) at 100 MHz, respectively. Absorption spectra were measured by a Varian Cary 50 UV-Vis spectrophotometer. Fluorescence spectra were performed on a Varian Cary Eclipse spectrofluorometer. The HRMS spectra were measured on an electrospray ionization mass spectrometer (microTOF, Bruker Daltonics).

2.4 Synthesis of Glc-DHP

2.4.1 Preparation of 2-deoxy-2-[*p*-methoxybenzylidene(amino)]-D-glucopyranose 20.
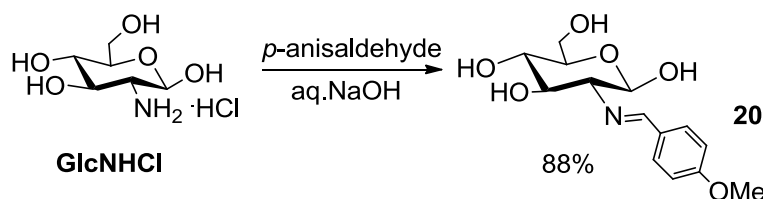
To a prepared aqueous solution of 1 M NaOH 120 mL of D-glucosamine hydrochloride (25.0 g, 116 mmol) was added *p*-anisaldehyde (17 mL, 1.2 eq.) under stirring. After a short time crystallization began, the mixture was refrigerated 2 h. Then the precipitated product was filtered off and washed with cold water, and followed by a mixture of 1:1 EtOH–Et$_2$O to give 2-deoxy-2-[*p*-methoxybenzylidene(amino)]-D-glucopyranose **1** (30.4 g, 88%) as white precipitate. ^{1}H NMR (400 Hz, DMSO-d$_6$) δ 8.11 (s, 1H, C*H*=N), 7.68 (d, J = 8.4 Hz, 2H, Ar-*H*), 6.98 (d, J = 8.4 Hz, 2H, Ar-*H*), 6.54 (d, J = 6.8 Hz, 1H, *H*-1), 3.47 (dd, J = 11.8, 5.8 Hz, 1H, *H*-3), 3.31 (dd, 1H, *H*-4), 3.22-3.18 (m, 1H, *H*-6), 3.15-3.09 (m, 1H, *H*-5), 2.78 (t, J = 8.3 Hz, 1H, *H*-2). The data given was proved to be consistent with that of reported literature [55].

2.4.2 Preparation of 1,3,4,6-tetra-*O*-acetyl-2-deoxy-2-[*p*-methoxybenzylidene (amino)]-β-D-glucopyranose 21.
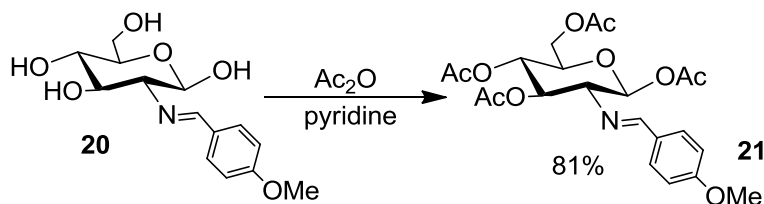
The intermediate product **1** (30.0 g, 101 mmol) was added successively to a cooled (icewater) mixture of Ac$_2$O (75 mL, 8 eq.) and pyridine 200 mL. The mixture was stirred in ice-bath 1 h and then at room temperature overnight. The yellow solution was poured into 600 mL of ice-water. The precipitate white product was filtered, washed with cold water and dried. The obtained white powder product was identified as 1,3,4,6-tetra-*O*-acetyl-2-deoxy-2-[*p*-methoxybenzylidene(amino)]-β-D-glucopyranose **2** (38.1 g, 81%). ^{1}H NMR (400 Hz, CDCl$_3$) δ 8.15 (s, 1H, C*H*=N), 7.65 (d, J = 8.6 Hz, 2H, Ar-*H*), 6.91 (d, J = 8.8 Hz, 2H, Ar-*H*), 5.94 (d, J = 8.3 Hz, 1H, *H*-1), 5.43 (t, J = 9.6 Hz, 1H, *H*-3), 5.14 (t, J = 9.8 Hz, 1H, *H*-4), 4.38 (dd, J = 12.2, 4.4 Hz, 1H, *H*-6'), 4.13 (d, J = 12.2 Hz, 1H, *H*-6), 3.94-3.89 (m, 1H, *H*-5), 3.84 (s, 3H, Ar-O-C*H*$_3$), 3.41 (t, 1H, *H*-2), 2.10 (s, 3H, Ac), 1.98 (s, 3H, Ac), 1.97 (s, 3H, Ac), 1.78 (s, 3H, Ac). The data given above was proved to be consistent with that of reported literature [55].

2.4.3 Preparation of 1,3,4,6-tetra-*O*-acetyl-β-D-glucosamine hydrochloride 22.
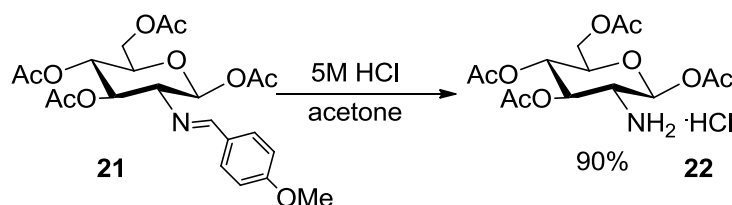
Into a warm acetone solvent (300 mL) of the imine compound **2** (38.0 g, 81 mmol), was added 5 M HCl (20 mL, 1.2 eq.) with immediate formation of a white precipitate. After the mixture was cooled down to room temperature, Et$_2$O 300 mL was added, and the mixture was stirred for 2 h before refrigerated overnight. The white precipitate was filtered, washed with Et$_2$O and dried to give 1,3,4,6-tetra-*O*-acetyl-β-D-glucosamine hydrochloride **3** (27.9 g, 90%) as white powder. ^{1}H NMR

(400 Hz, MD$_3$OD) δ 5.81 (d, J = 8.3 Hz, 1H, *H*-1), 5.34 (t, J = 9.6 Hz, 1H, *H*-3), 5.27 (t, J = 9.8 Hz, 1H, *H*-4), 4.26 (dd, J = 12.6, 4.5 Hz, 1H, *H*-6'), 4.07 (dd, J = 12.5, 2.1 Hz, 1H, *H*-6), 3.98-3.94 (m, 1H, *H*-5), 3.59 (dd, J = 10.5, 8.8 Hz, 1H, *H*-2), 2.18 (s, 3H, Ac), 2.11 (s, 3H, Ac), 2.05 (s, 3H, Ac), 1.94 (s, 3H, Ac). The data given above was proved to be consistent with that of reported literature [55].

2.4.4 Preparation of 1,3,4,6-tetra-*O*-acetyl-β-D-glucosamine 23.
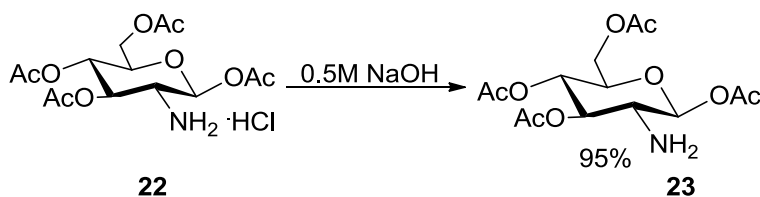
The solution of glucosamine salt **3** (2.5 g, 6.5 mmol) in CH$_2$Cl$_2$ 25 mL was neutralized by adding 0.5 M NaOH 13 mL and the reaction mixture was stirred at room temperature. After 1 h. the solution was quenched with distilled deionized water (3x25 mL) and the mixture was extracted with CH$_2$Cl$_2$ 25 mL. The organic phase was washed with deionized water (3x25 mL), dried over MgSO$_4$, and evaporated under reduced pressure to give 1,3,4,6-tetra-*O*-acetyl-β-D-glucosamine **4** (2.2 g, 95%) as white powder. ^{1}H NMR (400 Hz, MD$_3$OD) δ 5.45 (d, J = 8.5 Hz, 1H, *H*-1), 5.03-4.87 (m, 2H, *H*-3 and *H*-4), 4.31 (dd, J = 12.4, 4.5 Hz, 1H, *H*-6'), 4.07 (d, J = 12.4 Hz, 1H, *H*-6), 3.81 (m, 1H, *H*-5), 3.59 (t, J = 9.0 Hz, 1H, *H*-2), 2.17 (s, 3H, Ac), 2.12 (s, 3H, Ac), 2.06 (s, 3H, Ac), 2.03 (s, 3H, Ac). The data given was proved to be consistent with that of reported literature [55].

2.4.5 Preparation of ethyl β-amino acrylate 24.
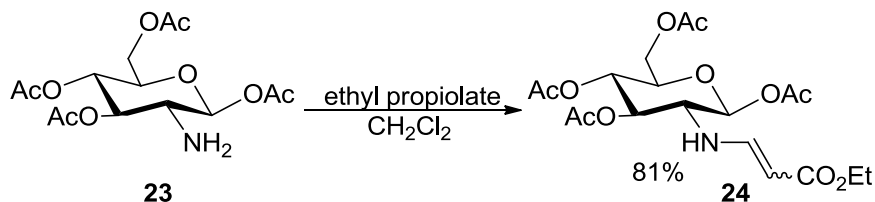
To the solution of primary amine **4** (2.0 g, 5.75 mmol) in CH$_2$Cl$_2$ 25 mL, ethyl propiolate (2.3 mL, 5 eq.) was slowly added, and the reaction mixture was stirred under refluxing temperature for 3 days. The mixture was evaporated in *vacuo*, and condensed residue was purified by column chromatography (EtOAc/Hexane=3/7) to

provide the ethyl β-amino acrylate **5** (2.1 g, 81%) as a pale yellow oil. ^{1}H NMR (400 Hz, CDCl$_3$) δ 7.62 (t, J = 10.8 Hz, 1H, N*H*), 6.47 (dd, J = 12.2, 8.3 Hz,1H, =C*H*N), 5.56 (d, J = 9.2 Hz, 1H, *H*-1), 5.27 (dd, 1H, *H*-3), 5.05 (dd, 1H, *H*-4), 4.46 (dd, J = 8.3 Hz,1H, C*H*=CHN), 4.30 (dd, 1H, *H*-6), 4.21(dd, 1H, *H*-6'), 4.08 (q, 2H, OC*H*$_2$CH$_3$), 3.81-3.76 (m, 1H, *H*-5), 3.21 (q, 1H, *H*-2), 2.12 (s, 3H, Ac), 2.08 (s, 3H, Ac), 2.05 (s, 3H, Ac), 1.89 (s, 3H, Ac), 1.18 (t, J = 9.9 Hz, 3H, OCH$_2$C*H*$_3$). ^{13}C NMR (100 MHz, CDCl3) δ 170.7, 170.2, 170.1, 169.1, 168.9, 150.3, 93.1, 85.9, 72.9, 72.6, 68.1, 62.1, 61.7, 59.2, 20.9, 20.8, 20.7, 20.6, 14.5. HRMS (ESI): M+Na$^+$, found 468.1446. C$_{19}$H$_{27}$NNaO$_{11}^+$ requires 468.1446.

2.4.6 Preparation of 1,3,4,6-tetra-*O*-acetyl-β-D-glucosaminyl-1,4-dihydropiridine (Glc-DHP 1).
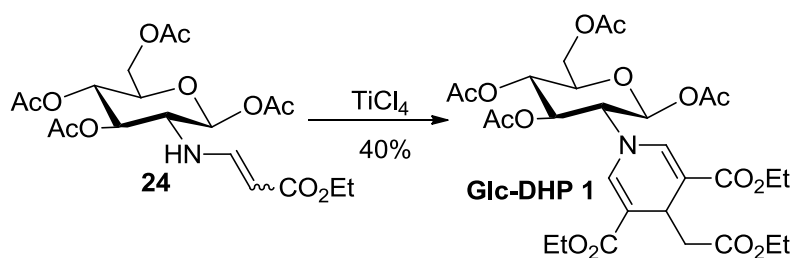
To the solution of ethyl β-amino acrylate **5** (2.0 g, 4.5 mmol) in dry CH$_2$Cl$_2$ 25 mL in an ice bath, TiCl$_4$ (0.15 mL, 0.3 eq.) was added rapidly and the reaction mixture was stirred overnight at room temperature under nitrogen atmosphere. After that the solution was quenched with distilled deionized water 25 mL, and the mixture was extracted with CH$_2$Cl$_2$ (3x25 mL). The organic portions were combined and neutralized by addition of 10% w/v NaHCO$_3$ solution. The organic phase was washed with deionized water (3x25 mL), dried over MgSO$_4$, and evaporated under reduced pressure. The crude product was purified by column chromatography (EtOAc/Hexane=2/8) to provide the 1,3,4,6-tetra-*O*-acetyl-β-D-glucosaminyl-1,4-dihydropiridine (Glc-DHP **1**) (0.38 g, 40%) as a pale yellow oil. ^{1}H NMR (400 Hz, CDCl$_3$) δ 7.13 (d, J = 8.7 Hz, 2H, C*H*=C), 5.80 (d, J= 8.9 Hz, 1H, *H*-1), 5.40 (t, J= 9.5 Hz, 1H, *H*-3), 5.11 (t, J= 9.5 Hz, 1H, *H*-4), 4.30 (1H, *H*-6), 4.23-4.06 (m, 5H, DHP-CO$_2$C*H*$_2$CH$_3$ and C*H*CH$_2$CO$_2$Et), 3.87-3.83 (m, 1H, *H*-6'), 3.81-3.77 (m, 1H, *H*-5), 3.74 (q, 2H, CH$_2$CO$_2$C*H*$_2$CH$_3$), 3.51 (t, J = 9.7 Hz, 1H, *H*-2), 2.48 (d, 2H, C*H*$_2$CO$_2$Et), 2.17 (s, 3H, Ac), 2.11 (s, 3H, Ac), 2.07 (s, 3H, Ac), 1.91 (s, 3H, Ac), 1.28 (dd, J =

13.4, 7.2 Hz, 6H, DHP-CO$_2$CH$_2$CH_3), 1.18 (t, J = 7.0 Hz, 3H, CH$_2$CO$_2$CH$_2$CH_3). ^{13}C NMR (100 MHz, CDCl3) δ 171.5, 170.7, 169.8, 169.6, 168.9, 166.5, 166.4, 107.8, 107.6, 100.0, 72.8, 70.4, 68.5, 65.8, 61.6, 60.5, 60.0, 39.8, 29.6, 20.9, 20.8, 20.7, 20.6, 14.5, 14.3, 1.2. HRMS (ESI): M+Na$^+$, found 664.2206. C$_{29}$H$_{38}$NNaO$_{15}^+$ requires 664.2206.

2.5 Photophysical property study

The stock solutions of 0.29 mM Glc-DHP **1** (5% acetonitrile) diluted to 100 μM with milliQ water, 50 mM phosphate buffer (PB) pH 8.0 and phosphate buffer saline (PBS) pH 7.4 were prepared, respectively. The photophysical properties of those stock solutions were achieved by using UV-visible spectrophotometer and fluorescence spectrophotometer.

2.5.1 UV-Visible spectroscopy

The UV-Visible absorption spectra of the stock solutions of Glc-DHP **1** fluorophore were recorded in a range from 200 nm to 700 nm at ambient temperature.

2.5.2 Fluorescence spectroscopy

The stock solution of Glc-DHP **1** fluorophore was diluted to 1 μM by adding respective solvents; milliQ water, PB solution pH 8 and PBS solution pH 7.4. The emission spectra of the fluorophore were recorded from 370 nm to 600 nm at ambient temperature using an excitation wavelength at 360 nm.

2.5.3 Fluorescence quantum yields

The fluorescence quantum yield of Glc-DHP **1** fluorophore was performed in PB 50 mM pH 8.0 by using quinine sulfate (Φ_F = 0.54) in 0.1 M H$_2$SO$_4$ as a reference [53]. The UV-Visible absorption spectra of five analytical samples and five reference samples at varied concentrations were recorded. The maximum absorbance of all samples should never exceed 0.1. The fluorescence emission spectra of the same solution using appropriate excitation wavelengths selected were recorded based on the absorption maximum wavelength (λ_{max} = 360 nm) of Glc-DHP **1**. Graphs of integrated fluorescence intensity were plotted against the absorbance at the respective

excitation wavelengths. Each plot should be a straight line with one interception and gradient *m* [54].

In addition, the fluorescence quantum yield (Φ_F) was obtained from plotting of integrated fluorescence intensity *vs* absorbance represented into the following equation:

$$\Phi_X = \Phi_{ST} \left(\frac{Grad_X}{Grad_{ST}} \right) \left(\frac{\eta_X^2}{\eta_{ST}^2} \right)$$

The subscripts Φ_{ST} denote the fluorescence quantum yield of a standard reference which used quinine sulfate in 0.1 M H_2SO_4 ($\Phi = 0.54$) and Φ_X is the fluorescence quantum yield of sample and η is the refractive index of the solvent.

2.5.4 Molar extinction coefficient (ε)

Molar extinction coefficient (ε) of Glc-DHP **1** was calculated from the UV-Visible absorption spectra in milliQ water of analytical samples at various concentrations. The absorption maximum wavelength (λ_{max}) of each compound was plotted against the concentrations at the respective excitation wavelength. Each plot should be a straight line goes through origin. Molar extinction coefficient (ε) can also be calculated from plotting absorption maximum (A) vs concentration (C) represented into the following equation:

$$A = \varepsilon bC$$

2.6 Fluorescent sensor study

The preparation of the stock solution was undertaken in the same manner to that of 2.4.

2.6.1 Nitroaromatic explosive sensor

Solutions of Glc-DHP **1** and nitroaromatic explosives were prepared in milliQ water. Concentrations of Glc-DHP **1** stock solution and all stock nitroaromatic explosive solutions were adjusted to 0.10 mM and 0.5 mM, respectively.

a) Selectivity study

To attain the fluorescence quenching profile, the Glc-DHP **1** solution was adjusted to 1 µM and mixed with nitroaromatic explosive solutions 100 µM at the ratio 1:100. The response was collected from 370 nm to 600 nm at ambient temperature by fluorescence spectrophotometer. In order to achieve the visible fluorescence response and photograph under black light, the stock solution of Glc-DHP **1** was diluted to 2 µM and mixed with nitroaromatic explosives in a concentration of 200 µM.

b) Fluorescence titration

In order to obtain the fluorescence titration spectra, the mixtures of Glc-DHP **1**/TNP were prepared with the ratio of 1/0-100 at room temperature. The spectra were recorded as described previously.

c) Stability study of Glc-DHP 1 after quenching

The kinetic response of the Glc-DHP **1** to TNP was investigated by checking the fluorescence intensity of the Glc-DHP **1** solution after incubation with TNP for a different period of time in a long period of time at least 4.5 h. The Glc-DHP **1** solution was adjusted to 1 µM and mixed with TNP solution 40 µM in the ratio 1:40. The response was collected from 370 to 600 nm at ambient temperature by fluorescence spectrophotometer.

d) Interference study

The mixture of Glc-DHP **1**/TNP/other nitroaromatic explosives in concentration of 1/10/50 µM with ratio 1/10/50 were used to investigate the competitive quenching from nitroaromatic explosives in the Glc-DHP **1** fluorophore-TNP system. The response was collected from 370 nm to 600 nm at ambient temperature by fluorescence spectrophotometer.

e) Detection of TNP in real samples

Water was collected from difference sources; seawater from the gulf of Thailand, Pattaya and industrial water from Ban Khai industrial estate, Rayong, Thailand. Water samples were used after filtrated through 0.45 μm filters. The water sample (900-990 μL) in a 1.5 mL quartz cuvette (1 cm light path) spiked with TNP solution (0-45 μM) was added to the Glc-DHP **1** stock solution (100 μM, 10 μL). The final solutions thus contained 1 μM Glc-DHP **1** and 0-45 μM TNP. The spectra were recorded as described previously in the **d**. The quenching efficiencies of TNP to the fluorescence emission of Glc-DHP **1** in milliQ water, seawater and industrial water were compared by using their Stern-Volmer plots.

f) Preparation of Glc-DHP 1 fluorescent paper sensor

A piece of filter paper was immerged in the fluorescent Glc-DHP **1** solution (1 mM in ethanol) for 60 sec. The filter paper was then removed from the solution and dried at room temperature for one day. Under the irradiation of a UV lamp, this filter paper emitted strong blue fluorescence. To demonstrate its application as a fluorescence paper sensor for TNP detection, the handwriting with of TNP solution as ink was pressed on the filter paper. Thereafter, the photograph of the paper with TNP solution handwriting was taken after the irradiation with a UV lamp by a digital camera.

g) Detection limit

Detection limit is the lowest amount of analyte in a sample that can be detected. But not necessarily quantitated as an exact value. The detection limit may be expressed as:

$$\text{Detection limit} = [I_0/(I-3\zeta) - 1] / K$$

Where; ζ is the standard deviation of the response deriving from intensity of Glc-DHP fluorophore at 1 μM of 9 samples.

K is the slope of calibration curve obtained from fluorescence titration spectra.

2.6.2 Protein sensor

The excitation wavelength was 360 nm and the emission was recorded from 370 nm to 600 nm. Solution of Glc-DHP **1** fluorophore was prepared in 10 mM PBS pH 7.4 using a sonication bath. Concentration of the fluorophore was adjusted to 100 μM and used as a stock solution. All protein stock solutions were prepared by dilution with PBS. The protein/Glc-DHP **1** fluorophore mixtures were prepared by mixing protein and diluted PBS to afford the final concentration of fluorophore equal to 1 μM, the protein concentration of 0-25 μM for hemoglobin, 0-50 μM for cytochrome c and myoglobin and 50 μM for other proteins.

2.6.3 Metal ion sensor

The excitation wavelength was 360 nm and the emission was recorded from 370 nm to 600 nm. Solution of Glc-DHP **1** was prepared in 50 mM PB pH 8.0 using a sonication bath. Concentration of Glc-DHP **1** was adjusted to 0.10 mM. Metal chloride solutions were prepared in milliQ water except for $CdSO_4$ and $FeSO_4$. All stock solutions were adjusted to the concentrations of 0.1 mM and were added in an appropriate amount (0-1000 μL) into the fluorophore solution. The final volume of the mixtures was adjusted to 1 mL to afford the final concentration of 1 μM for the fluorophore and 10 μM for metal ions.

CHAPTER III

RESULTS AND DISCUSSION

3.1 Synthesis and characterization of glucopyranosyl-1,4-dihydropyridine (Glc-DHP).

To enhance the water solubility of the Glc-DHP fluorophore, glucosamine moiety was attached to the 1,4-dihydropyridine core unit. GlcNHCl, prepared by HCl treatment of chitosan, was initially treated with *p*-anisaldehyde for the protection of NH_2 group, and then followed by the acetylation, removal of the *p*-methoxybenzylidene protecting group with HCl in acetone and neutralization by 0.5M NaOH to obtain primary amine in 58% yield over 4 steps [55]. Glucopyranosyl-1,4-Dihydropyridine (Glc-DHP **1**) was synthesized via cyclotrimerization of the β-amino acrylate **24**, obtained from the reaction between primary amine and ethyl propiolate, in the presence of $TiCl_4$ (**Figure 3.1**). All new compounds were characterized by ^1H NMR, ^{13}C spectroscopy, MALDI-TOF-MS and high resolution mass spectrometry (HRMS).
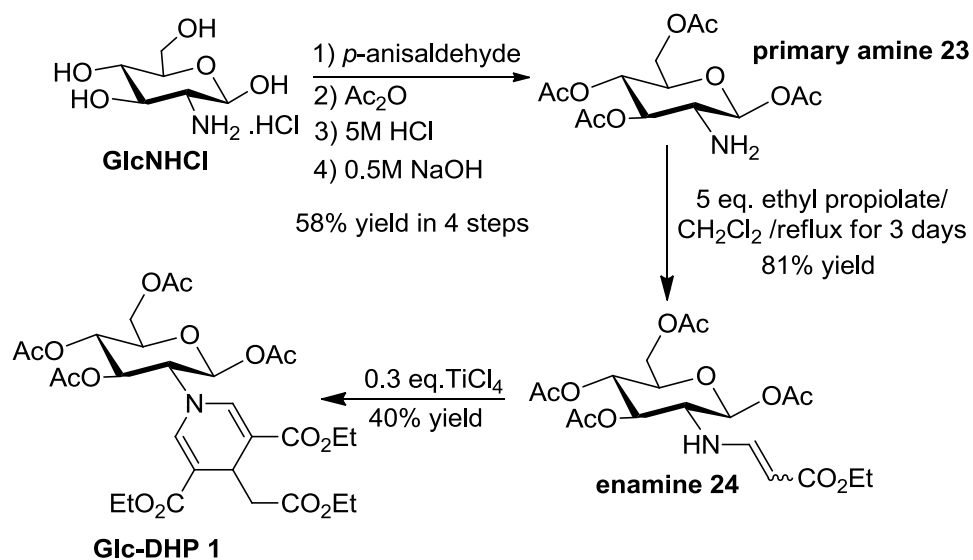
Figure 3.1 Synthesis of glucopyranosyl-1,4-dihydropyridine (Glc-DHP **1**).

N-Glucopyranosyl enamine **24** was obtained from the reaction between primary amine **23** and ethyl propiolate. Though such a coupling reaction is rapid, this addition of glucosamine to ethyl propiolate resulted in slow reaction, due to the bulkiness of glucosamine. Some reaction conditions were adjusted to solve this problem such as, increasing the reaction time, increasing the reaction temperature, using higher concentration of reagent (ethyl propiolate). Eventually, the temperature increased from room temperature to refluxing temperature, reaction time increased from overnight to 3 days and amount of ethyl propiolate increased from 1.2 eq. to 5 eq. have led to the formation of *N*-glucopyranosyl enamine **24** in high yield under the modified reaction condition (81% yield).

The formation of one DHP molecule requires three enamine molecules. Therefore, the product yield was calculated based on this consumption of the substrate; for instant, 100% yield of one mole enamine gives 1/3 mole of the product. In order to improve the product yield, the amount of catalytic TiCl$_4$ was varied. Moreover, the addition of ethyl propiolate was also expected to improve the product yield. Thus, several trials with various amount of TiCl$_4$ and ethyl propiolate were attempted (**Table 3.1**). As the results, there is no significant effect of the amount of ethyl propiolate added. Treatment of ethyl β-amino acrylate with 0.3 equivalents TiCl$_4$ in CH$_2$Cl$_2$ solution at room temperature for overnight provided Glc-DHP **1** in satisfactory yield (40% yield), which was the best yield occurred for the same reaction time.

Table 3.1 Optimization of the synthesis of Glc-DHP **1**

Entry	TiCl$_4$	Ethyl propiolate	%yield
1	1 eq.	-	trace
2	0.8 eq.	-	12
3	0.8 eq.	2 eq.	20
4	0.5 eq.	0.2 eq.	30
5	0.5 eq.	0.4 eq.	15
6	0.5 eq.	-	28
7	0.3 eq.	-	40
8	0.3 eq.	0.2 eq.	30

In order to obtain Glc-DHP **2** (deacetylated Glc-DHP **1**), several trials with various conditions of deacetylation were attempted (**Table 3.2**). As the results, reactions seemly cannot be completed probably due to bulkiness of glucopyranosyl unit and DHP moiety. Glc-DHP **2** final product was also very difficult to purify due to the by-products with similar polarity having different numbers of hydroxy groups.

Table 3.2 Various conditions of deacetylation

Entry	Conditions		Results
1		Na 1.5 eq., EtOH THF 10 mL under Ar rt, 1h	Could not purify
2		K$_2$CO$_3$ 4 eq., EtOH rt, 1h	Could not purify
3		KOH 4 eq., EtOH rt, overnight	N.A.
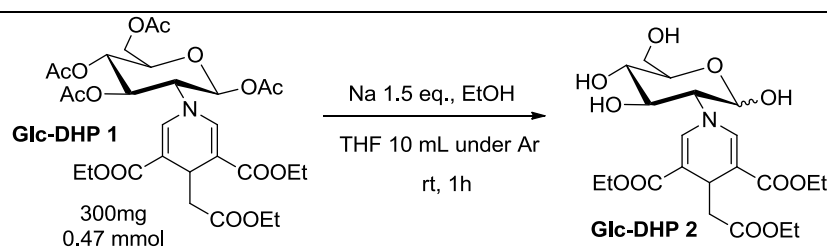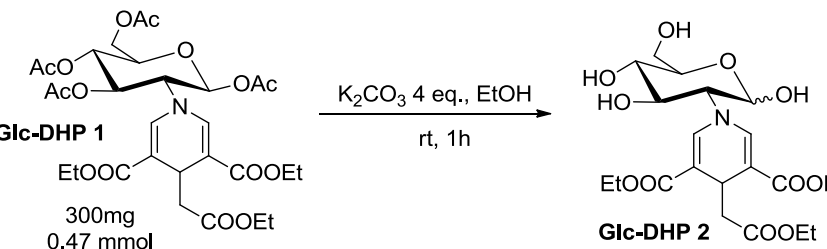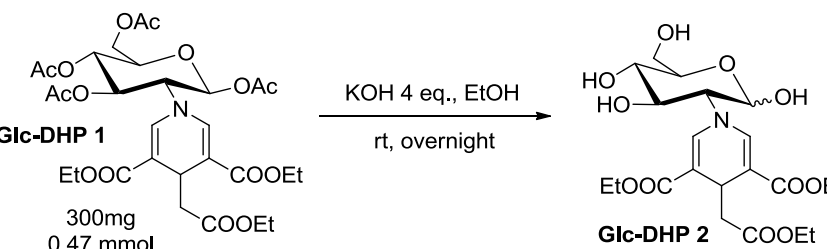
Several trials with various methods of purification of Glc-DHP **2** were attempted. Firstly, column chromatography was used but could not purify due to the high polarity of mixture of product and by products. Then, Sephadex column chromatography was also attempted, but could not purify too might be the similarity of size of product and by products. Lastly, re-crystallization method was also attempted, but could not purify probably became the mixture contained considerable amount of by-products.
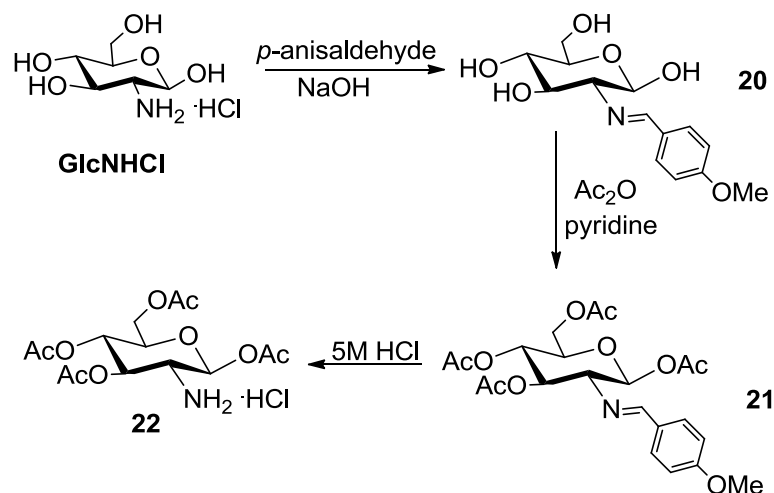
Figure 3.2 Synthesis of **20**, **21** and **22**

The ^{1}H NMR spectra of compound **20, 21** and **22** are shown in **Figure 3.3**. All signals were assigned to all protons in each corresponding structure. Initially, *p*-methoxybenzylidene **20** showed two doublet signals at 6.8 and 7.6 ppm corresponding to its aromatic protons, the alkene peaks represented as 'c' appeared at 8.2 ppm, four signals at around 4.5 - 5.0 ppm corresponding to hydroxy groups of glucopyranose and the singlet signal of methoxy at 3.7 ppm. In the case of tetraacetyl product **21** obtained from acetylation of **20**, the four signals of hydroxy groups of glucopyranose disappeared, while the new four singlet signals at around 1.8 – 2.2 ppm corresponding to their acetyl groups of glucopyranose appeared. And removal of the *p*-methoxybenzylidene protecting group gave glucosamine hydrochloride **22**, which has two doublet signals of aromatic protons, one singlet alkene peak and one singlet signals corresponding to the *p*-methoxybenzylidene group disappeared.
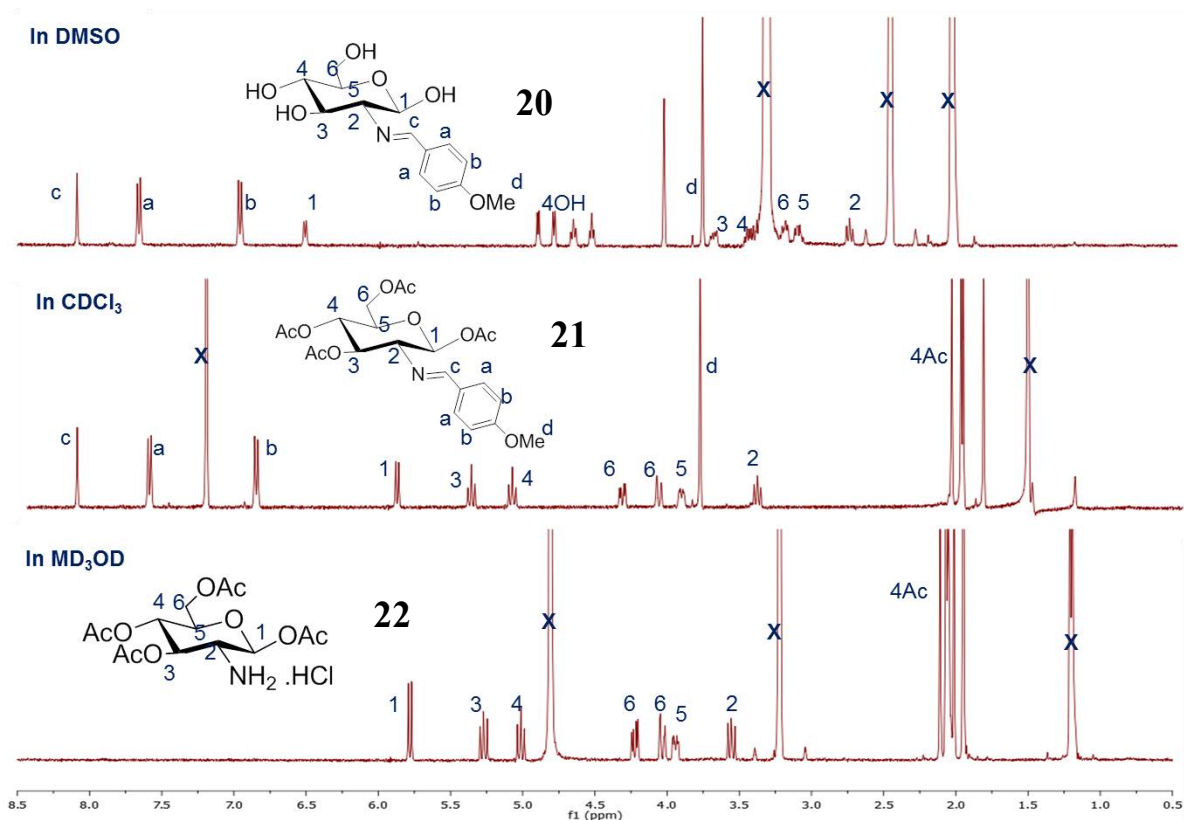
Figure 3.3 ^{1}H-NMR (400 MHz) of **20, 21** and **22.**
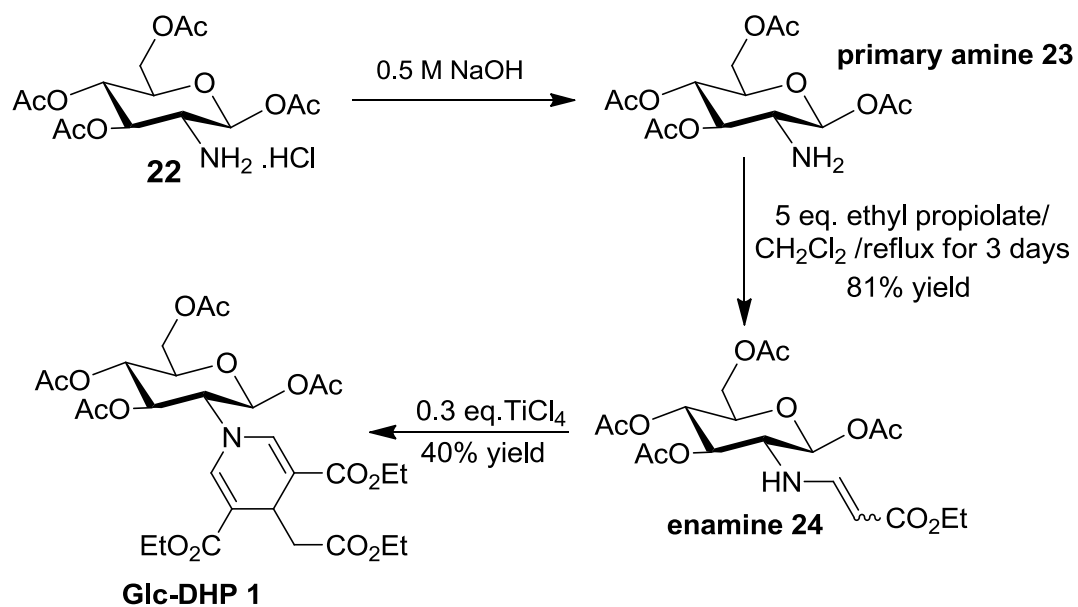
Figure 3.4 Synthesis of **23**, enamine **24** and Glc-DHP **1**

The ^{1}H NMR spectra of compound **23,** enamine **24** and Glc-DHP **1** are shown in staged manner in **Figure 3.5** for the comparison. All signals can be assigned to all protons in each corresponding structure. Glucosamine **23** showed four singlet signals at around 1.8 and 2.2 ppm corresponding to its acetyl group protons and the proton signals of glucopyranose was found at around 3.0 – 5.5 ppm. After, primary amine **23** was coupled with ethyl propiolate to produce glucopyranosyl-β-amino-acrylate **24**, the signals of this newly added unit appeared. A bunch of small signals appeared closely to the baseline in ^{1}H-NMR spectrum of the enamine, are signal of *trans*-isomer enamine substrate that can be easily isomerized from major *cis*-isomer. New ethyl ester product showed new signals for ester group; a quartet of the methylene (-C*H$_2$*) group at 4.0 ppm and a triplet signal of methyl (-C*H$_3$*) group at 1.1 ppm. The new triplet peak of secondary amine at 7.6 ppm and alkene signals of enamine at 4.5 and 6.5 ppm, were observed as characteristic signals for enamine unit. The cyclotrimerization of the β-amino-acrylate **24** produced Glc-DHP **1**, The spectrum of Glc-DHP **1** showed that the singlet signal of the alkene protons at 4.5 and 6.5 ppm totally disappeared upon the cyclotrimerization, while the doublet-like signal two of protons on the DHP ring was found at 7.15 ppm. Probably, the bulkiness of glucopyranose moiety might prevent the DHP ring from rotating. Moreover, two sets of ethyl ester groups showed the signal of the methylene (-C*H$_2$*-) of ester protons as a quartet at 3.8 and 4.2 ppm and a triplet signal at 1.1 and 1.2 ppm of methyl (-C*H$_3$*) of ester protons. The new doublet signal around 2.5 ppm was detected only in the Glc-DHP **1** product spectra corresponding to aliphatic proton(s) 'v'. (In COSY spectrum), this aliphatic proton(s) reveals the relation with the multiplet signal 'u' at 4.2 ppm (overlapping with methylene proton signals of ethyl ester). Acetyl group protons and the signals of glucopyranose protons still remain.
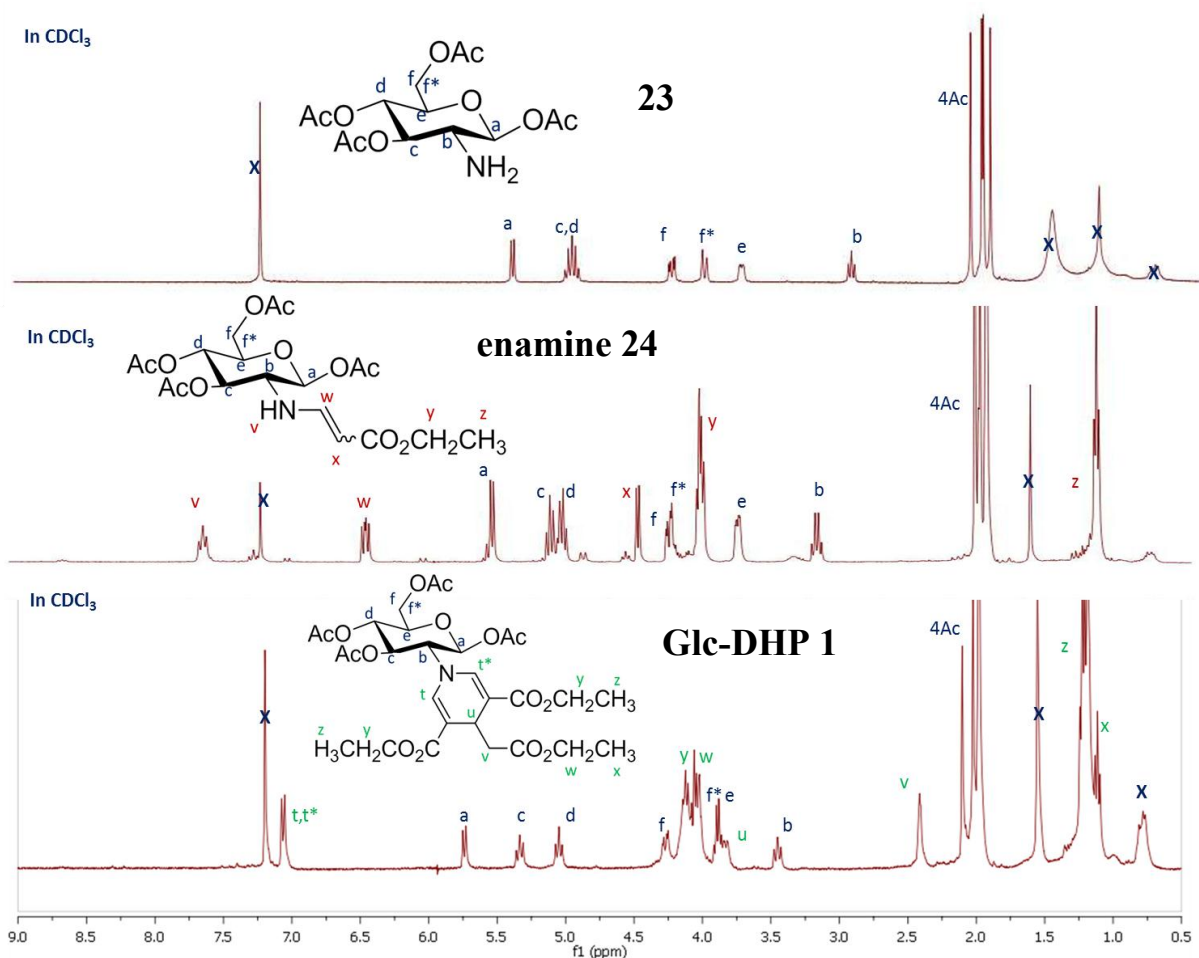
Figure 3.5 ^{1}H-NMR (400 MHz) of **23,** enamine **24** and Glc-DHP **1.**

The structural characterizations of the fluorophore was also confirmed by MALDI-TOF-MS in [M][+] mode showing the molecular ion peaks corresponding or directly related to their molecular weights (**Figure 3.6**). HRMS was achieved only in the case of novel (β-amino acrylate **24** and Glc-DHP **1**) for their complete characterization.
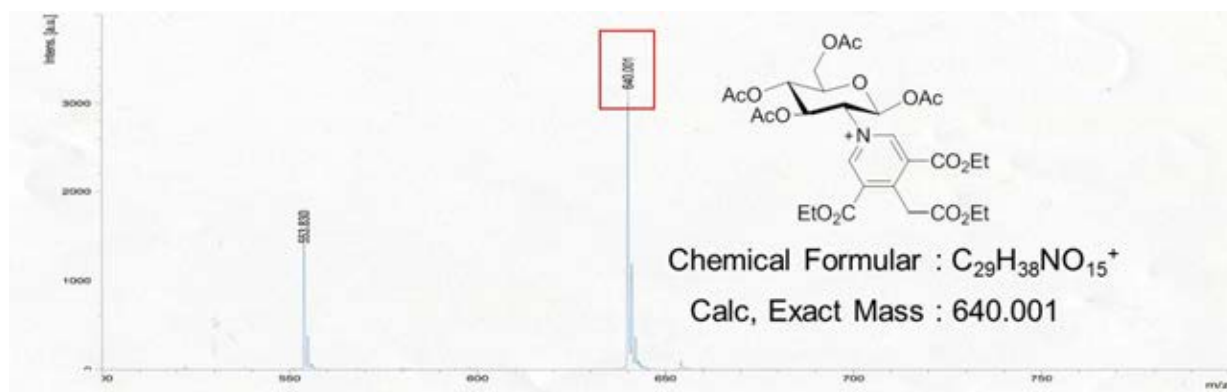
Figure 3.6 MALDI-TOF-MS of Glc-DHP **1**
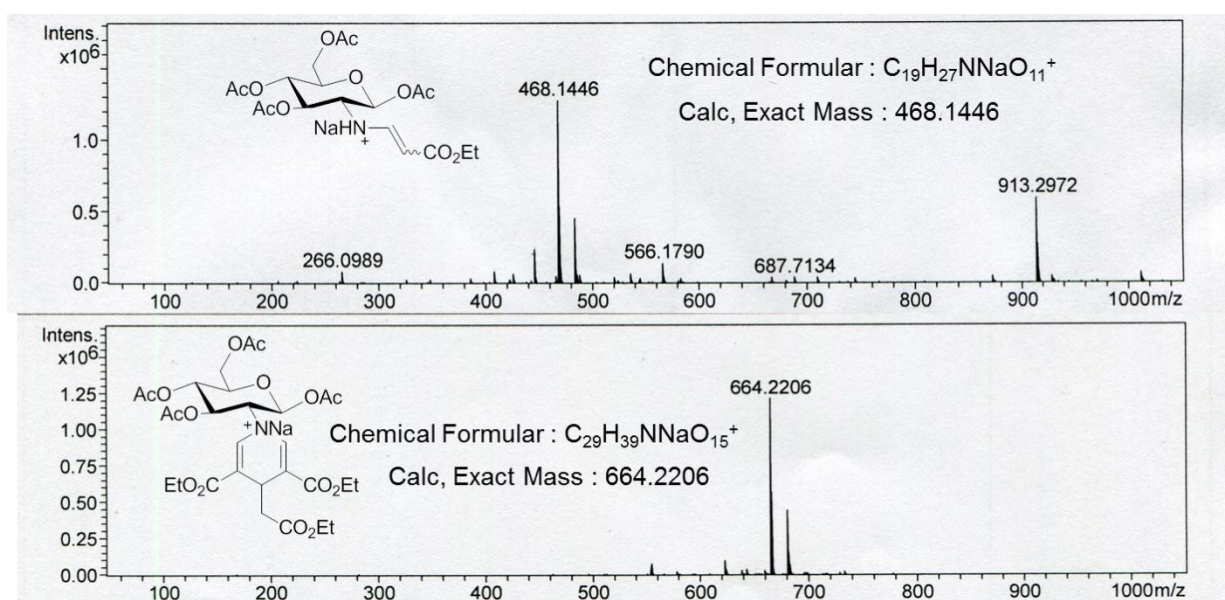
Figure 3.7 HRMS of enamine **24** and Glc-DHP **1**

3.2 Photophysical property study

The behavior of Glc-DHP **1** fluorophore was investigated by the fluorescence measurement in milliQ water (1μM) upon excitation at 360 nm (**Table 3.3** and **Figure 3.8**). The molar absorption coefficient of this DHP was determined as 6,900 M^{-1} cm^{-1}. This Glc-DHP **1** exhibited an emission peak at 450 nm with fluorescent quantum efficiency (Φ_f) of 0.29.

Table 3.3 Photophysical property of Glc-DHP **1** in aqueous solution.

Absorption		Emission		Appearance
λ_{max} (nm)	ε (M^{-1} cm^{-1})	λ_{max} nm	Φ_f	(2µM) under black light
360	6,900	450	0.29	

Quinine sulfate in 0.1 M H$_2$SO$_4$ (Φ_F = 0.54 %) was used as the reference.
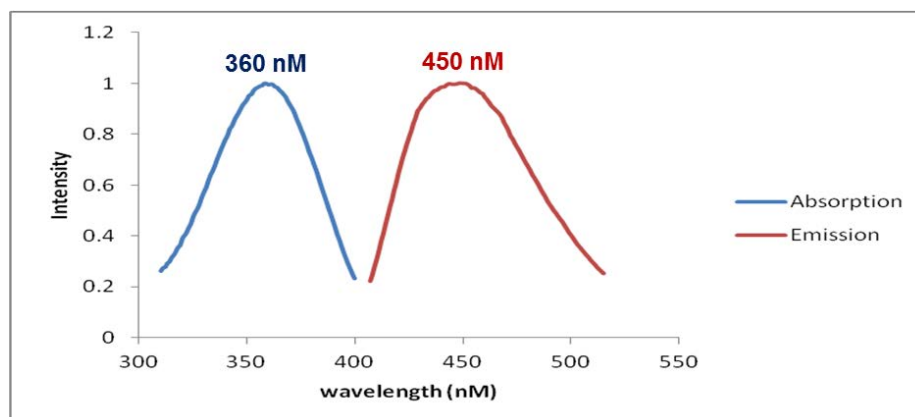
Figure 3.8 Normalized absorption and emission spectra of Glc-DHP **1** fluorophore (10 µM) in milliQ water

3.3 Nitroaromatic explosive sensor

Selective and sensitive sensor for the detection of nitroaromatic explosives, in particular 2,4,6-trinitrotoluene (TNT), 2,4-dinitrotoluene (DNT) and 2,4,6-trinitrophenol (TNP), are of great current interest in both national security and environmental protection. The importance of the detection of such nitroaromatics is that they are not only explosives but also recognized as toxic pollutants [56-57]. Although many procedures have been successfully developed for the detection of TNT, it is not easy to differentiate the influence from TNP due to the extremely similar structure of TNT and TNP. Also, few methods for the selective detection of

TNP were reported [58]. Furthermore, among various techniques used for detection of nitroaromatics, fluorescence-based detection offers several advantages; high sensitivity, specificity, and real-time monitoring with short response time.
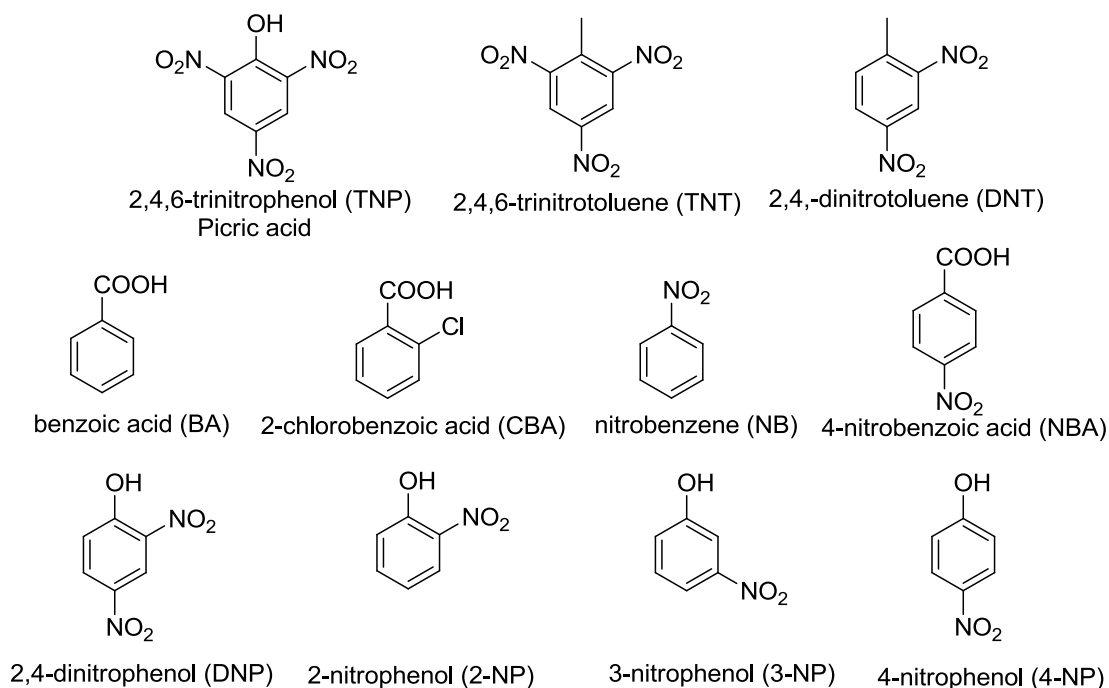
Figure 3.9 Structures of all nitroaromatic explosive compounds used in the study

3.3.1 Selectivity study

The strong emission of Glc-DHP **1** was used as chemosensor for the detection of nitroaromatics such as TNT, DNT, TNP, etc. The fluorescent responses of Glc-DHP **1** (1μM) towards nitroaromatic compounds (TNP, TNT, DNT, NB, BA, NBA and CBA) (**Figure 3.9**) were evaluated in milliQ water. In details, upon the addition of the nitroaromatic compound (100 equiv) into a solution of Glc-DHP **1**, only TNP caused a significant fluorescence quenching effect (**Figure 3.10**).
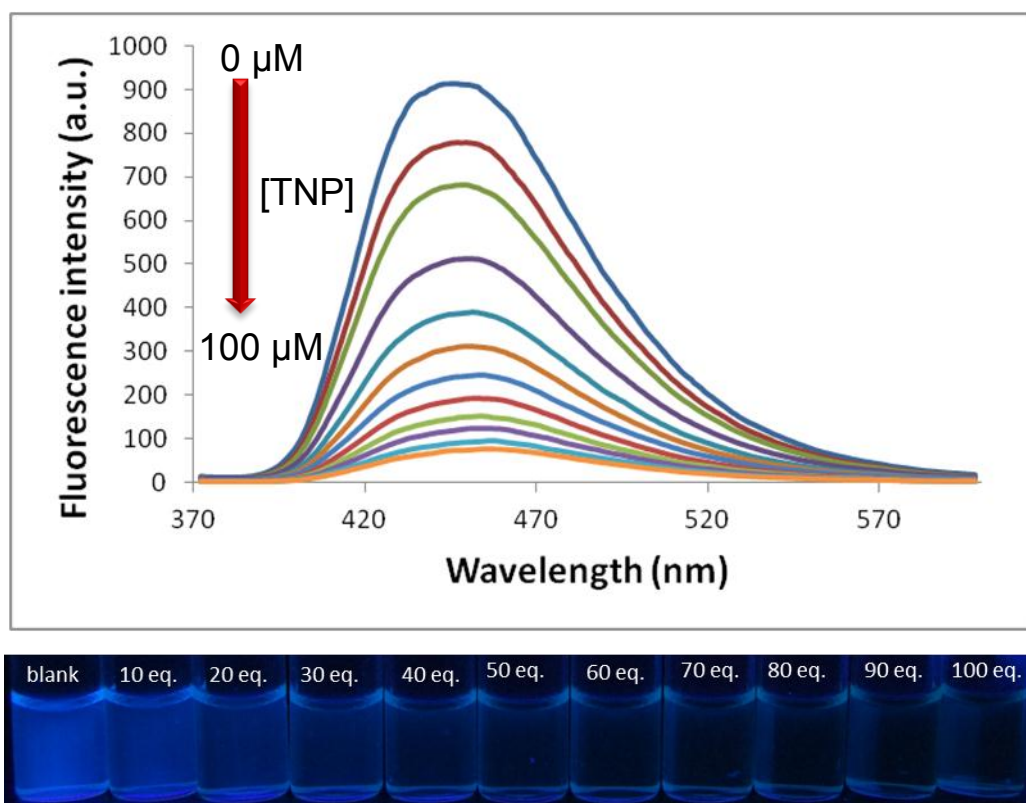
Figure 3.11 Fluorescence change of Glc-DHP **1** (1μM) with the addition of TNP (0 to 100 equiv) in milliQ water (λ_{ex} = 360nm). The photograph below shows the fluorescence appearance under black light of Glc-DHP **1** (2 μM) upon addition of TNP (0 to 100 equiv).

3.3.3 Stability study of Glc-DHP 1 after quenching monitoring

In addition, the kinetic response of Glc-DHP **1** to TNP was investigated by monitoring the fluorescence intensity of the Glc-DHP **1** solution after incubation with TNP for 4 hours. As shown in **Figure 3.12**, the fluorescence intensity of Glc-DHP **1** decreased dramatically and instantly by adding TNP (40 μM) within half a minute. Meanwhile, when the incubation time was prolonged to 4 h, the fluorescence intensity unchanged. This phenomenon demonstrated that the fluorescence quenching rate was very fast and the fluorescence was stable in a long period of time (at least 4 h). Suggesting this newly developed fluorescence sensor can be used as portable device for on-site detection of nitroaromatic explosives.
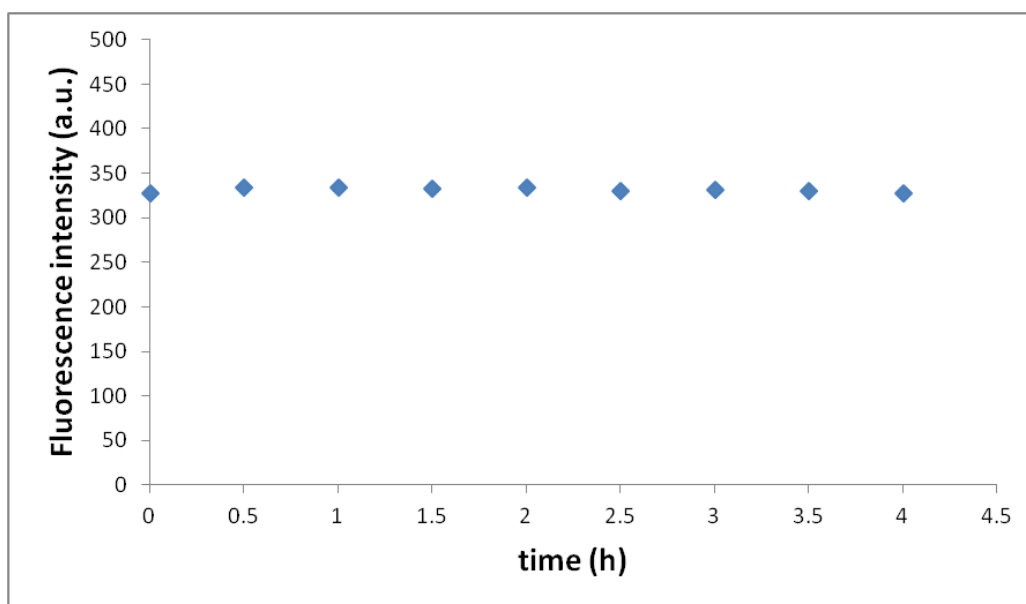
Figure 3.12 Influence of incubation time on the fluorescence quenching reaction between Glc-DHP **1** (1 µM) and TNP (40 µM) solution.

3.3.4 Detection limit

The emission response to TNP was studied by using Stern-Volmer relationship **(Figure 3.13)**. The fluorescence quenching profile can also be evaluated with the Stern-Volmer equation;

$$I_0/I - 1 = K_{sv}[\text{analyte}]$$

Where; K_{sv} is the Stern-Volmer quenching constant (K_{sv} = 44,700 M^{-1}).

Linear plot (inset **Figure 3.13**) were achieved with a Stern-Volmer constant of 44,700 M^{-1} was found when the concentration of TNP below 45 µM.

The limit of detection (LOD = 3ζ/K) of TNP is determined as 0.94 µM, ζ refers to the standard deviation of the blank measurement (n = 6), and K is the slope of calibration curve.
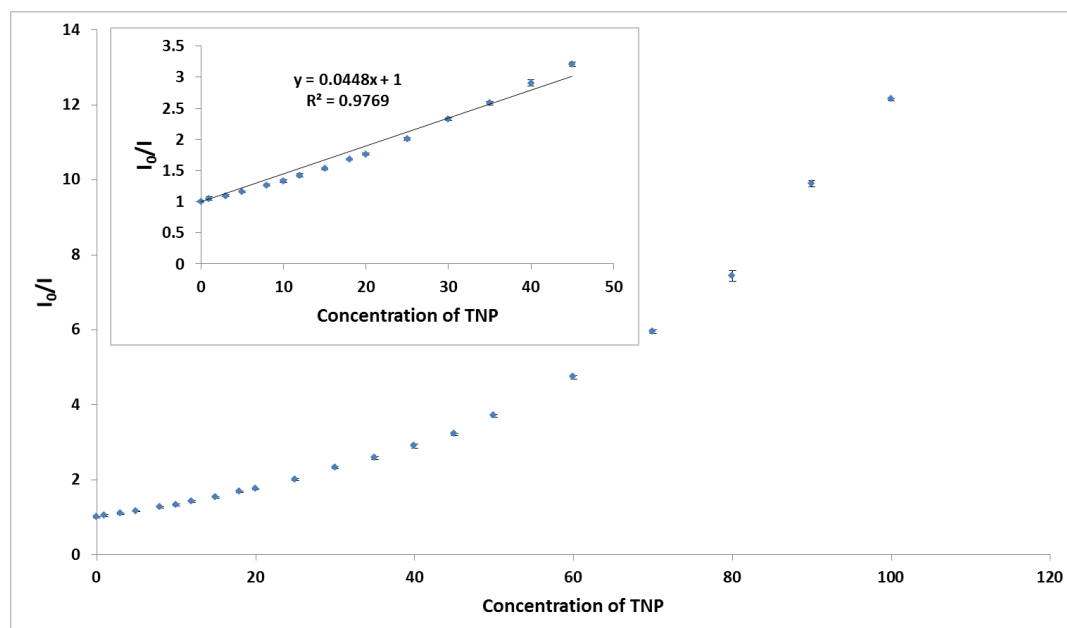
Figure 3.13 Stern-Volmer plot in response to TNP. Inset: Stern-Volmer plot obtained at lower concentration of TNP.

3.3.5 Interference study

To further check the selectivity and applicability, the Glc-DHP **1** fluorescent sensor has been applied to the analysis of TNP in water samples mixed with other nitroaromatics by using the developed fluorescence quantitation method [41]. In order to evaluate the developed method, recovery study was carried out on the standard TNP solution (10 µM) spiked with various concentrations of coexisting explosives (50 µM), including TNT, DNT, NB, NBA, BA and CBA. TNP levels in the mixed-water samples could be estimated from the standard curve and the recovery measurement. As shown in **Table 3.4**, the obtained recoveries of the samples varied from 93% to 106%, suggesting that the newly developed method is highly applicable to the selective fluorescence assay of trace amount of TNP in real samples.

Table 3.4 Detection of trace TNP in water samples mixed with other nitroaromatics

Sample	Concentration (µM)		Recovery (%)
	taken	Found (means, n=9)	
TNP	10	10.03 ± 0.42	100.29
TNP/TNT	10/50	10.32 ± 0.22	103.16
TNP/DNT	10/50	10.68 ± 0.25	106.76
TNP/NB	10/50	10.31 ± 0.33	103.11
TNP/ BA	10/50	9.32 ± 0.16	93.24
TNP/NBA	10/50	9.74 ± 0.42	97.38
TNP/CBA	10/50	9.39 ± 0.28	93.93

3.3.6 Detection of TNP in real samples

TNP is used as primary constituent of many unexploded landmines worldwide and widely used in the manufacture of rocket fuel, firework and matches. Sensing of TNP in groundwater and seawater is greatly demanded for locating underwater mines and for control the environmental pollution. In this work, were also compared the quenching efficiencies of TNP to the fluorescence emission of Glc-DHP **1** in pure water, industrial water and seawater. Interestingly, the three Stern-Volmer plots are nearly overlapped (**Figure 3.14**). In other words, this Glc-DHP **1** can be a good candidate for developing into a TNP sensor for its detection in seawater and industrial water.
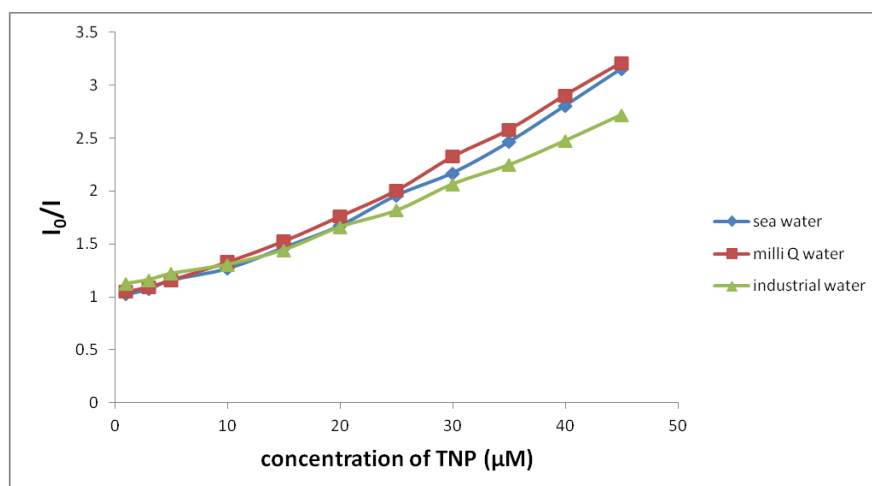
Figure 3.14 Stern-Volmer plots of Glc-DHP **1** against the concentrations of TNP in milliQ water, industrial water and seawater.

3.3.7 Glc-DHP fluorescent paper sensor

The Glc-DHP **1** fluorescent paper sensor was prepared by simply dipping a filter paper into a Glc-DHP **1** solution (1mM in ethanol). After solvent evaporation, a highly fluorescent emissive test paper was obtained. The detection process is fast and the assay procedure is simple. When a TNP solution (40 µM) is handwritten or dropped onto paper sensor, the fluorescence was immediately quenched and the dark pattern appeared on the paper, which is vividly discernible even by the naked eye (**Figure 3.15**). Therefore, we have successfully developed a rapid and simple fluorescent paper sensor for TNP-selective detection. This result encourages us to develop ultrasensitive and ultrafast chemosensor devices with portability for on-site detections of explosive vapors and particulates.

Figure 3.15 Glc-DHP **1** fluorescent paper sensor for TNP visual detection by handwriting on the paper using TNP solution (40 µM) as ink. The digital image was taken under a UV lamp (365-nm irradiation).

3.3.8 Quenching mechanism

As previously discovered, tricarboxyl DHP **11** can be utilized as a fluorescent sensor for Hg^{2+} [35]. The quenching process involves an oxidation of the DHP into a pyridinium ring specifically induced by Hg^{2+} (chemodosimeter), and confirmed by ^1H NMR data. Thus, in this work, the ^1H NMR experiment was also demonstrated. As the result, there was no significant change in the ^1H NMR spectrum, while fluorescence signal was significant disappeared. Moreover, according to in literature

reviews concerning to the TNP detection, main quenching mechanism for TNP was believed to be the energy transfer by presence of a spectral overlap between absorption spectrum of TNP and emission spectrum of fluorophore. And also based on results reported herein, we believe that the fluorescence quenching is probably due to the energy transfer from the excited state of Glc-DHP **1** to the ground state of TNP via the spectra overlap of the absorption of TNP and emission of the Glc-DHP **1** in the wavelength region of 400-480 nm (**Figure 3.16**). However, no spectral overlap between absorption of other nitroaromatic explosives and the emission of Glc-DHP **1** was observed. According to the Förster theory, the efficiency of FRET between donor and acceptor depends mainly on the following factors: (i) the donor can produce fluorescence light; (ii) fluorescence emission spectrum of the donor and UV–vis absorbance spectrum of the acceptor have significant spectral overlap; and (iii) the distance between the donor and the acceptor approach and is lower than 8 nm [59]. Here the donor and acceptor are Glc-DHP **1** and TNP, respectively.
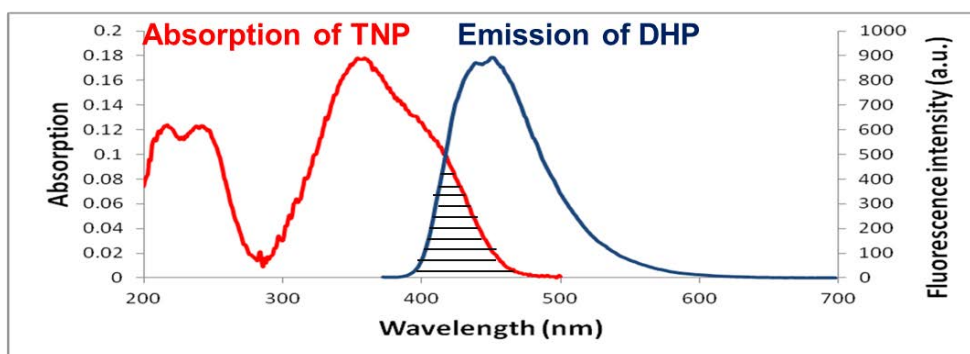
Figure 3.16 Spectral overlap of absorption spectrum of TNP and fluorescence spectrum of Glc-DHP **1**.

To confirm this hypothesis, the quenching efficiencies of other nitroaromatic phenols to the fluorescence emission of Glc-DHP **1** were investigated. As the result, the fluorescence emission of Glc-DHP **1** was also quenched by other nitro aromatic phenols such as 2,4-DNP, 4-NP, 2-NP and 3-NP (**Figure 3.17**). The fluorescence quenching degree of Glc-DHP **1** against TNP was about 2 times, 8 times, 12 times and 15 times, higher than those of 2,4-DNP, 4-NP, 2-NP and 3-NP, respectively. Probably the longer resonance system of TNP ring with less energy gap possess the

shorter maximum absorption (λ_{max}) resulting in more significant spectral overlap between UV–vis absorbance spectrum of the TNP and fluorescence emission spectrum of the Glc-DHP **1** than those of other nitroaromatic phenols.
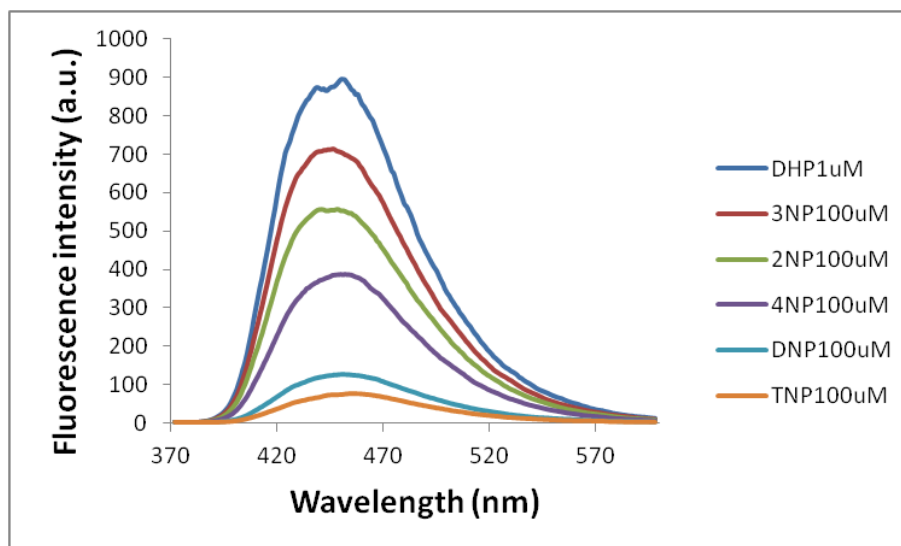
Figure 3.17 Fluorescence change of Glc-DHP **1** (1 μM) with the addition of nitroaromatic phenol derivatives (100 μM) in milliQ water (λ_{ex} = 360 nm).

In this section, we have reported a new fluorescent 1,4-dihydropyridine (Glc-DHP **1**), which can be used as a selective and sensitive detection of TNP in aqueous solution, independent of interference of other nitroaromatic explosives. The decrease of fluorescence signal was proportional to TNP concentration with high quenching efficiency (K_{sv} = 44,700) providing a detection limit of 0.94 μM. In addition, the fluorescent paper sensor was fabricated for portable, sensitive and selective on-site detection of trace amount of TNP.

3.4 Protein sensor

For the last 2-3 decades, heme proteins, metalloproteins containing the heme prosthetic group, either covalently or non-covalently bound to the protein, have been extensively studied, due to their capacities to undergo reduction and oxidation at the iron heme [60-61]. Some of these proteins are electron carriers (cytochrome c, catalase), others are involved in catalysis (e.g. peroxidase, cytochrome coxidase) and in active membrane transport or in oxygen transport (e.g. hemoglobin, myoglobin,

cytoglobin). Hemoglobin is a protein in red blood cells that transports oxygen throughout the body. The most common hemoglobin, tetramer consisting of four subunits non-covalently bound (see **Figure 3.17** for heme chemical structure), is normally tested for the diagnosis of the diseases such as anemia, leukemia [62-63]. Myoglobin is a monomeric single heme protein, relatively small (Mw=16,700) found mainly in muscle tissue where it serves as an intracellular storage site for oxygen and facilitates oxygen diffusion in rapidly contracting muscle tissue [64]. Among the current methods for protein detection, fluorescence-based biosensors have received considerable attention due to their sensitivity and detection simplicity.
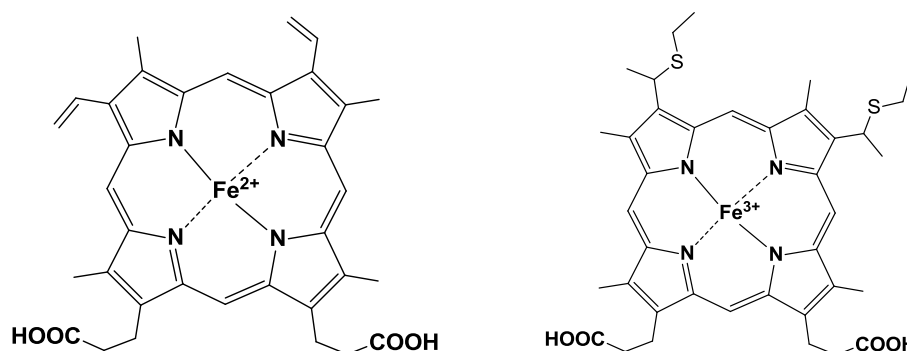
Figure 3.18 Structures of heme proteins in hemoglobin, myoglobin (left) and heme protein in cytochrome c (right).

By possessing excellent fluorescence property, this Glc-DHP **1** was used as fluorescent biosensor for the detection of proteins; e.g. bovine serum albumin (BSA), papain, hemoglobin. The solution of Glc-DHP **1** fluorophore (1 µM) in PBS pH 7.4 was tested with 12 protein solutions (50 µM). The selected proteins included metalloproteins such as myoglobin (Myo, 17.0 kDa), cytochrome c (Cyt C, 12.3 kDa), hemoglobin (HHb, 68 kDa) and carbonic anhydrase (CA, 29.0 kDa) and also nonmetalloproteins such as bovine serum albumin (BSA, 66.3 kDa), histone (His, 21.5 kDa), lysozyme (Lys, 14.4 kDa), and papain (Pap, 23.0 kDa), α-lactalbumin, β-lactalbumin, α-cesein, and concanavalin A. In details, upon the addition of the proteins (50 eq.) into a solution of Glc-DHP **1**, only HHb, Cyt C and Myo caused a significant fluorescence quenching effect (**Figure 3.18**).
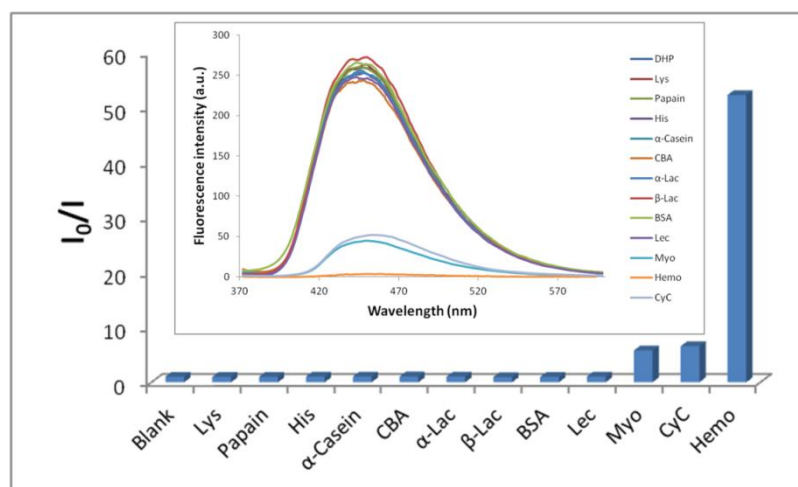
Figure 3.19 Fluorescence quenching profile of Glc-DHP **1** (1 µM), after addition of each protein (50 µM) (only hemoglobin 25 µM) in PBS (λ_{ex} = 360 nm).

The protein sensing properties of the Glc-DHP **1** were characterized by monitoring the fluorescence quenching behaviors of Cyt C, HHb, and Myo as a function of their concentration. The fluorescence intensity decreased proportionally and rapidly as HHb concentration increased (**Figure 3.19A**). Upon addition of incremental amount of 1 µM of HHb to the solution of Glc-DHP **1** in aqueous solution, the quenching in fluorescence emission was observed at the concentration as low as 25 equiv. As shown in the spectra, along with the increase of HHb concentration from 0 to 5 µM, the fluorescent signal was rapidly decreased. However, at a higher concentration of HHb (from 6 to 25 µM), the fluorescence signal was gradually dropped and was completely quenched at 25 µM. Similar behaviors were also observed in Cyt C and Myo cases (**Figure 3.19B** and **3.19C**), but their intensity decreasing rates were slightly slower than that of HHb. Several papers proposed that, the metalloproteins containing Fe^{3+} *i.e.* HHb, Cyt C and Myo quench most of the fluorescence signals, perhaps by either the electron or energy transfer process [65-66, 67]. Therefore, it might be possible in our case also that the efficient quenching effects of the metalloproteins, HHb, Cyt C and Myo, are primarily due to the energy transfer of the Glc-DHP **1** with the protein as Cyt C, Myo and HHb contain metallo-heme portions within the protein. Some of the quenching effects for proteins can be attributed to electron transfer between metalporphyrin moiety of proteins and the Glc-DHP **1**.
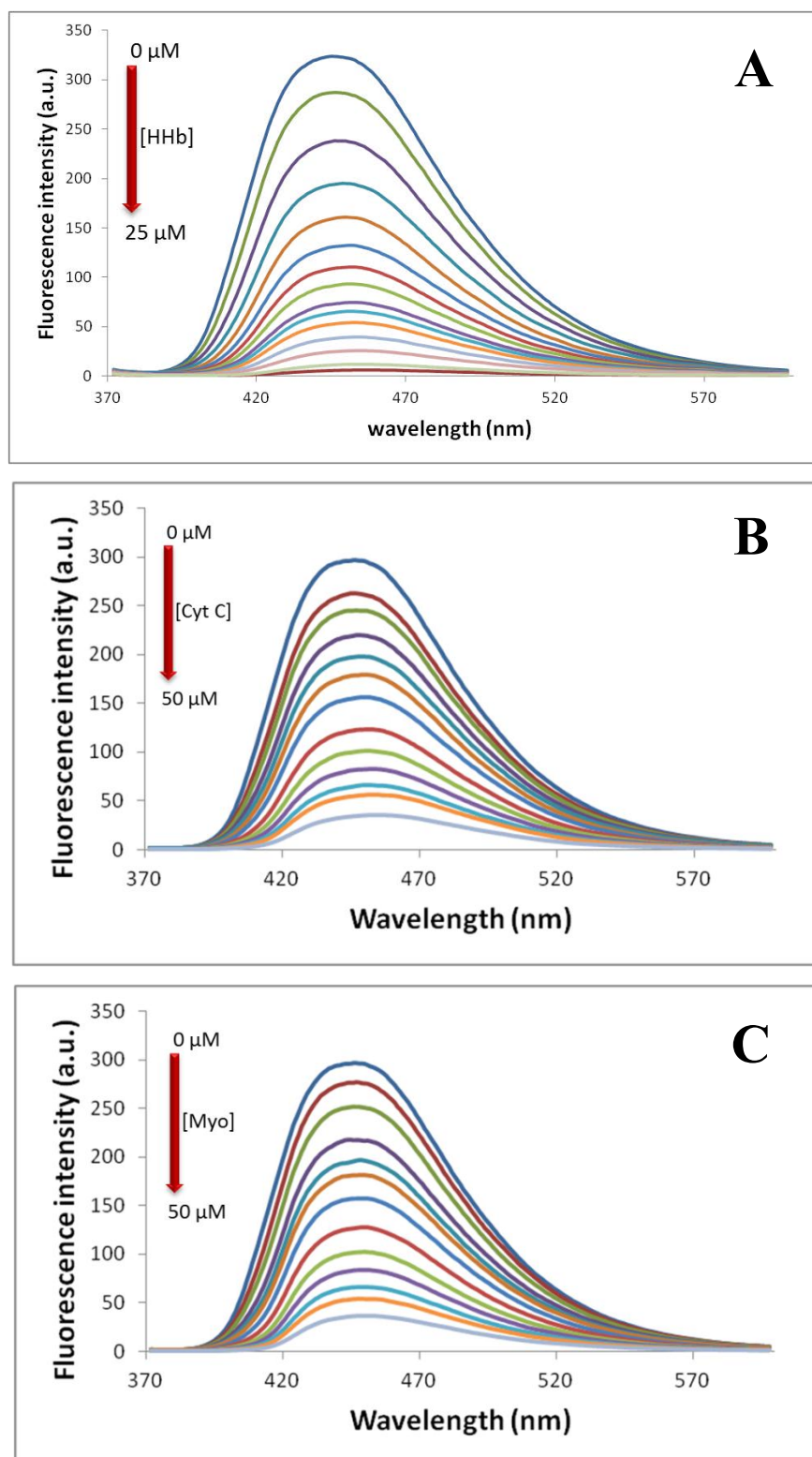
Figure 3.20 Fluorescence emission spectra of the Glc-DHP **1** in response to varied concentrations of (A) HHb (0 to 25 equiv), (B) Cyt C, and (C) Myo ($\lambda_{ex}/\lambda_{em} = 360/450$ nm.) in PBS.

Since HHb sensing gave the best quenching efficiency; the emission response to hemoglobin was also investigated by using Stern-Volmer relationship. Linear plot (inset **Figure 3.20**) was also run from the concentration of 0 µM to 7 µM and Stern-Volmer constant of 424,000 M^{-1} at the concentration of hemoglobin was below 7 µM. The limit of detection (LOD = 3ζ/K) of HHb is about 0.1 µM. ζ refers to the standard deviation of the blank measurement (n = 6), and K is the slope of calibration curve.
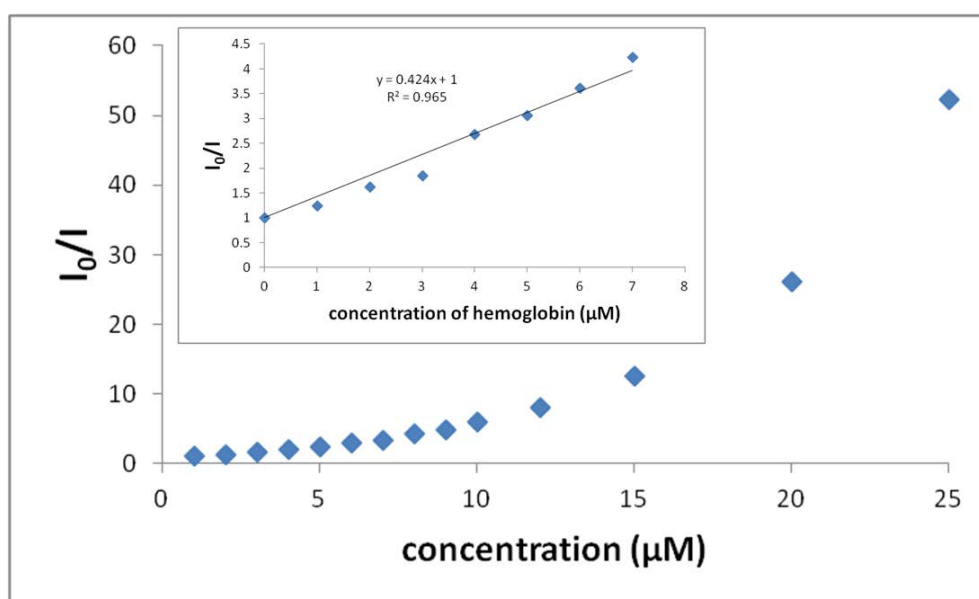
Figure 3.21 Stern-Volmer plot in response to hemoglobin. Inset: Stern-Volmer plot obtained at lower concentration of hemoglobin (7 µM).

Glc-DHP **1** evidently exhibited selective fluorescence quenching by metalloproteins containing porphyrin unit; HHb, Cyt C and Myo. In order to evaluate the quenching efficiency of the three proteins, Stern-Volmer plots were constructed by varying the protein concentration and monitoring the fluorescent signal of the Glc-DHP **1** fluorophore (**Figure 3.21**). A linear relationship between quencher concentration and I_0/I was obtained. The K_{SV}, sensitivity of Glc-DHP **1**, was found to be 4.24×10^6, 5.22×10^5 and 5.34×10^5 M^{-1} for HHb, Cyt C and Myo, respectively.
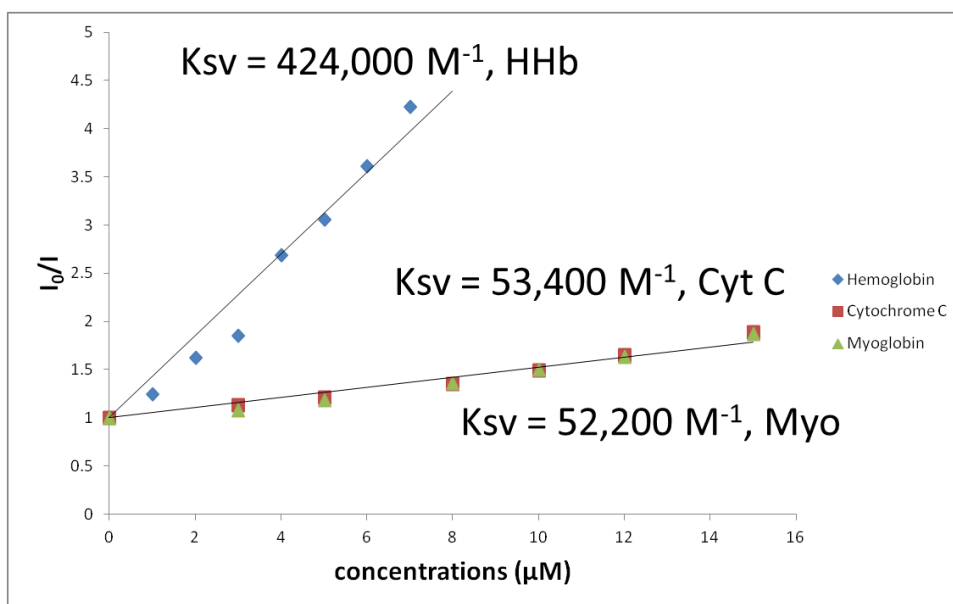
Figure 3.22 Stern-Volmer plots in various concentrations of HHb, Cyt C and Myo

The quenching efficiency analysis of the Glc-DHP **1** sensor for HHb, Cyt C and Myo is shown in **Figure 3.22** and **Figure 3.23**. At concentrations ranged between 0 μM and 25 μM, a relationship between I_0/I and quencher concentration and a relationship between quenching efficiency and quencher concentration were obtained. While HHb showed strong quenching signal, Cyt C and Myo tested under the same experimental conditions demonstrated merely a small quenching.
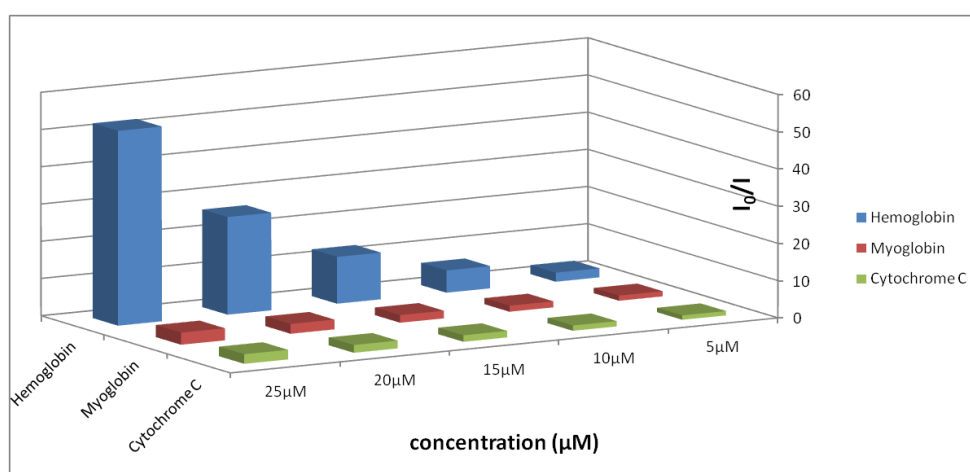
Figure 3.23 A relationship between I_0/I and concentrations of HHb, Cyt C and Myo
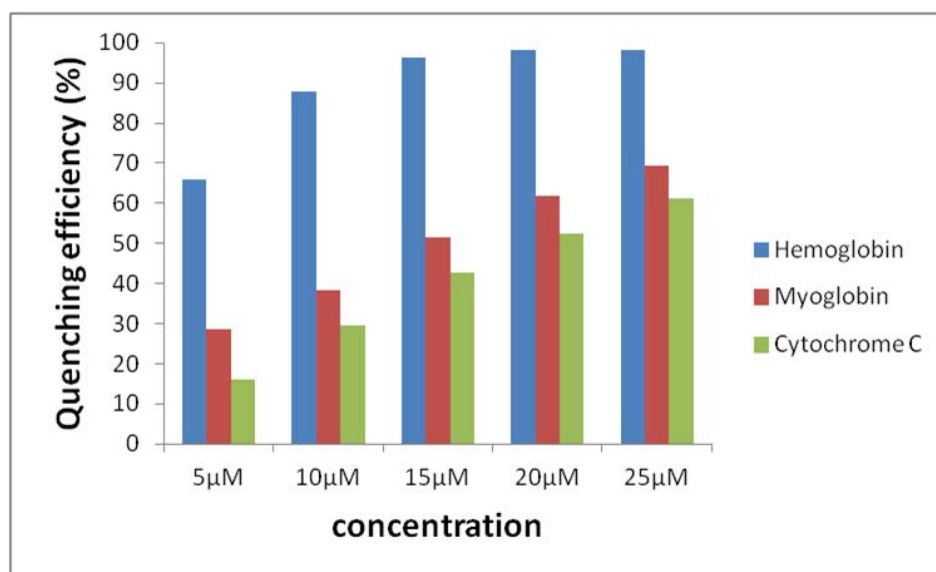
Figure 3.24 A relationship between quenching efficiency and concentrations of HHb, Cyt C and Myo

The fact that HHb, Cyt C and Myo exhibited fluorescence quenching suggested that these responses might cause by the electron transfer process between metalporphyrin moiety in the proteins and the Glc-DHP **1** fluorophore.

3.5 Metal ion sensor.

As previously discovered, tricarboxyl DHP **11** can be utilized as a fluorescent sensor for Hg^{2+} [35]. Metal ion scanning experiment, thus, was attempted with Glc-DHP **1**. Fluorescence quenching profile towards 15 metal ions (Na^+, Ca^{2+}, Zn^{2+}, Hg^{2+}, Co^{2+}, Ni^{2+}, Cu^{2+}, Ag^+, Fe^{2+}, Fe^{3+}, Cd^{2+}, Al^{3+}, Au^{3+}, Mn^{2+} and Pb^{2+}) were evaluated in aqueous PB solutions pH 8. Upon the addition of the metal ion (50 eq.) into a solution of Glc-DHP **1**, fluorescence spectra showed no significant decreasing.
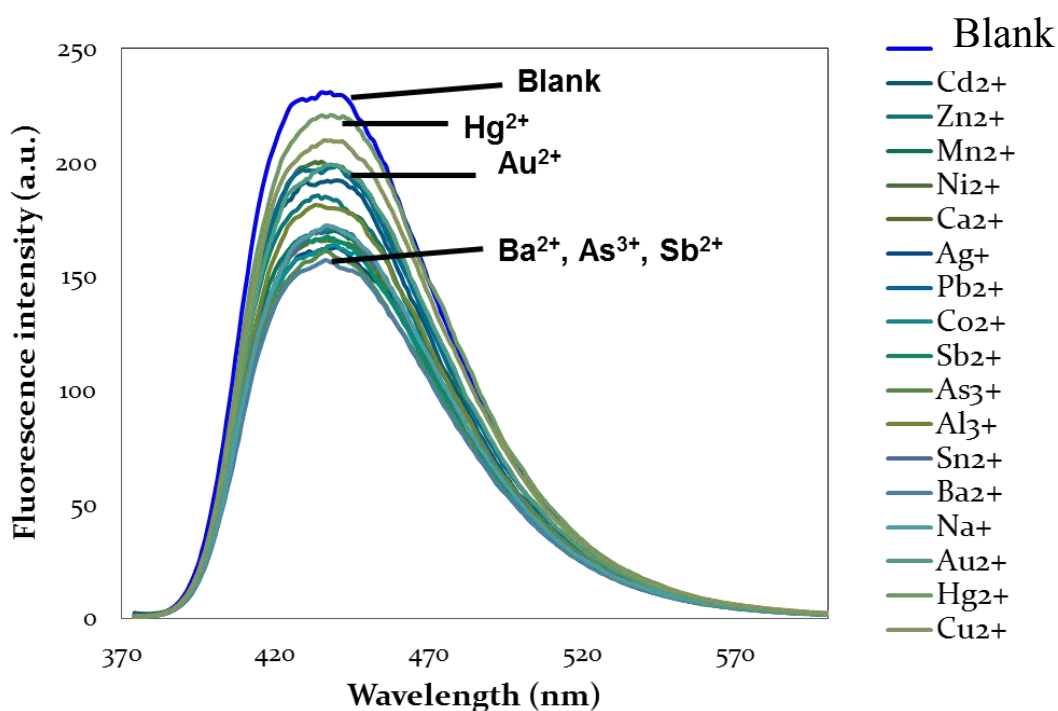
Figure 3.25 Fluorescence profile of Glc-DHP **1** (1 μM)**,** addition of each metal ion (50 μM) in PB solution pH 8.0 (λ_{ex} = 360 nm). Acetate salts were used except for $CdSO_4$, $FeSO_4$ and $FeCl_3$.

CHAPTER IV

CONCLUSION

4.1 Conclusion

In conclusion, glucopyranosyl-1,4-dihydropyridine (Glc-DHP **1**) was successfully synthesized and developed as a new fluorescent sensor. Primary amine **4** was obtained from D-glucosamine hydrochloride (GlcNHCl) as the starting material by using the reported synthetic procedure. Subsequent addition reaction of the primary amine **4** and ethyl propiolate in CH_2Cl_2 under refluxing temperature for 3 days was carried out to produce β-amino acrylate **5**. Because β-amino acrylate **5** has both nucleophilic and electrophilic sites, the cyclotrimerization (3 eq.) of the β-amino acrylate to Glc-DHP **1** was observed smoothly in the presence of $TiCl_4$. This DHP derivative was proved to be useful for sensing applications in aqueous media due to their water solubility and selective fluorogenic responses. The photophysical properties of Glc-DHP **1** fluorophore was demonstrated in milliQ water. The molar absorption coefficient of this DHP was determined as 6,900 M^{-1} cm^{-1}. This Glc-DHP **1** exhibited an emission peak at 450 nm with fluorescent quantum efficiency (Φ_f) of 0.29. By possessing fluorescence property, this Glc-DHP **1** was used as fluorescent sensor for the detection of nitroaromatic explosives; e.g. TNP, TNT, DNT, etc. Glc-DHP **1** showed specific fluorescent quenching only with TNP. The decrease of fluorescence signal was proportional to TNP concentration with high quenching efficiency (K_{sv} = 44,700 M^{-1}) providing a detection limit of 0.94 µM. The fluorescence quenching is probably due to the energy transfer from the excited state of Glc-DHP **1** to the ground state of TNP via the spectra overlap of the absorption of TNP and emission of the Glc-DHP **1** in the wavelength region of 400-480 nm. Moreover, Glc-DHP **1** was demonstrated in protein sensing study. Upon the addition of the proteins (50 eq.) into a solution of Glc-DHP **1**, only HHb, Cyt C and Myo caused a significant fluorescence quenching effect. While HHb showed strong quenching signal, Cyt C and Myo tested under the same experimental conditions demonstrated a small quenching. Since HHb sensing gave the best quenching efficiency; the emission response to hemoglobin was also investigated by using Stern-Volmer relationship with K_{sv} = 424,000 M^{-1} providing a detection limit of 0.1 µM. HHb, Cyt C and Myo exhibited fluorescence quenching suggested that these responses might cause by the electron transfer process between metalporphyrin moiety in the proteins and the Glc-DHP **1** fluorophore. Additionally, metal ion scanning experiment was

attempted with Glc-DHP **1**. Upon the addition of the metal ion (50 eq.) into a solution of Glc-DHP **1**, fluorescence spectra showed no significant decreasing.

4.2   Suggestion for future work

To obtain the Glc-DHP derivative with tetrahydroxy groups to be used as water soluble moiety, linker (spacer) should be installed between DHP unit and glucopyranose moiety, as Glc-DHP 1 with only one single bond linkage faced some problems during the acetylation process. According to our hypothesis, the bulkiness of both glucopyranosyl and DHP unit might be the reason of this difficulty. Therefore, the insertion of longer linker into the new target molecule may be use alternative way to the solution.
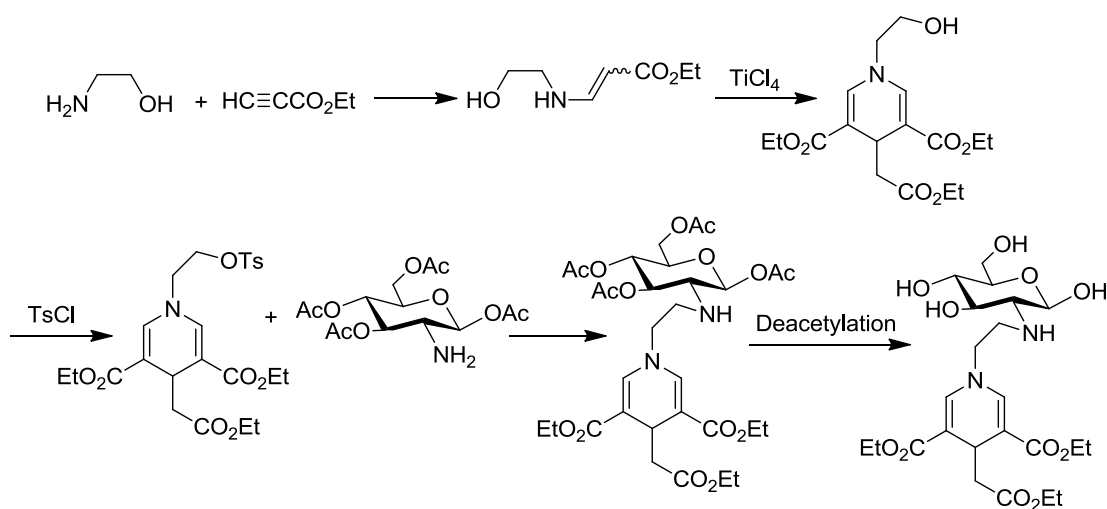
Scheme 4.1 Synthesis of new target molecule

REFERENCES

[1]   Muzzarelli R. A. A., Ed. Natural chelating polymers. New York: *Pergamon Press*, (1973).

[2]   Zikakis J. P., Ed. Chitin, chitosan and enzymes. Orlando: *Academic Press*, (1984).

[3]   Pillai, C. K. S.; Paul, W.; Sharma, C. Chitin and chitosan polymers: Chemistry, solubility and fiber formation. *Prog. Polym. Sci.* 34 (2009): 641–678.

[4]   Rinaudo, M. Chitin and chitosan: Properties and applications. *Prog. Polym. Sci.* 31 (2006): 603‑632.

[5]   Siwilai, R.; Meksud, L.; Pawason, P. Biological and ecological factors study of shrimp farm. *Center of Excellence for Environmental and Hazardous Waste Management* 10 (2011): 1-9.

[6]   Gandhi, N.; Laidler, J. K. Preparation of glucosamine hydrochloride. *U.S. patent* 6 (2002): 307 B1.

[7]   Ajavakom, A.; Supsvetson, S.; Somboot, A.; Sukwattanasinitt, M. Products from microwave and ultrasonic wave assisted acid hydrolysis of chitin. *Carbohydrate Polymers* 90 (2012): 73– 77.

[8]   Hantzsch, A. Uber die synthese pyridinartiger verbindungen aus acetessigather und aldehyammoniak. *Ann. Chem.* 215 (1882): 1–82.

[9]   Fukuzumi, S.; Koumitsu, S.; Hironaka, K.; Tanaka, T. Energetic comparison between photoinduced electron-transfer reactions from NADH model compounds to organic and inorganic oxidants and hydride-transfer reactions from NADH model compounds to *p*-benzoquinone derivatives. *J. Am. Chem. Soc.* 109 (1987): 305-316.

[10] Mochizuki, A.; Fukuoka, T.; Kanada, M.; Kinjou, N.; Yamamoto, T. Development of photosensitive porous polyimide with low dielectric constant. *J. Photopolym. Sci. Technol.* 15 (2002): 159-165.

[11] Yamamoto, T.; Ohno, S.; Niwa, S.; Tokumasu, M.; Hagihara, M.; Koganei, H.; Fujita, S.; Takeda, T.; Saitou, Y.; Iwayama, S.; Takahara, A.; Iwata, S.; Shoji, M., Asymmetric synthesis and biological evaluations of (+)- and (-)-6-dimethoxymethyl-1,4-dihydropyridine-3-carboxylic acid derivatives blocking N-type calcium channels. *Bioorg. Med. Chem. Lett.* 21 (2011): 3317-3319.

[12] Briede, J.; Daija, D.; Bisenieks, E.; Makarova, N.; Uldrikis, J.; Poikans, J.; Duburs, G. Effects of some 1,4-dihydropyridine Ca antagonists on the blast transformation of rat spleen lymphocytes. *Cell Biochem. Funct.* 17 (1999): 97-105.

[13] Janis, R. A.; Triggle, D. J. New developments in Ca^{2+} channel antagonists. *J. Med. Chem.* 25 (1983): 775–785.

[14] Manhold, R.; Jablonka, B.; Voigdt, W.; Schoenfinger, K.F.; Schravan, K. Calcium- and calmodulin-antagonism of elnadipine derivatives: comparative SAR. *Eur. J. Med. Chem.* 27 (1992): 229–235.

[15] Striessnig, J.; Grabner, M.; Mitterdorfer, J.; Hering, S.; Sinnegger, M. J.; Glossmann, H. Structural basis of drug binding to L Ca^{2+} channels. *Trends Pharmacol. Sci.* 19 (1998): 108–115.

[16] Kikuchi, S.; Iwai, M.; Murayama, H.; Fukuzawa, S. i. Catalytic synthesis of 1,4-dihydropyridine derivatives using scandium(III) triflate**.** *Tetrahedron Lett.* 49 (2008): 114-116.

[17] Vohra, K. R.; Bruneau, C.; Renaud, J. Lewis acid catalyzed sequential transformations: straight forward preparation of functional dihydropyridines. *Adv. Synth. Catal.* 348 (2006): 2571-2574.

[18] Sirijindalert, T.; Hansuthirakul, K.; Rashatasakhon, P.; Sukwattanasinitt, M., Ajavakom, A. Novel synthetic route to 1,4-dihydropyridines from β-amino acrylates by using titanium(IV) chloride under facile conditions. *Tetrahedron* 66 (2010): 5161-5167.

[19] Sueki, S.; Takei, R.; Abe, J.; Shimizu, I. Ytterbium-catalyzed synthesis of dihydropyridines. *Tetrahedron Lett.* 52 (2011): 4473-4477.

[20] Fasani, E.; Fagnoni, M.; Dondi, D.; Albini, A. Intramolecular electron transfer in the photochemistry of some nitrophenyldihydropyridines. *J. Org. Chem.* 71 (2006): 2037-2045.

[21] Jimenez, A. J.; Fagnoni, M.; Mella, M.; Albini, A. Photoinduced Electron and Energy Transfer in Aryldihydropyridines. *Org. Chem. 74* (2009): 6615–6622.

[22] Fasani, E.; Dondi, D.; Ricci, A.; Albini, A. Photochemistry of 4-(2-nitrophenyl)-1,4-dihydropyridines. Evidence for electron transfer and formation of an intermediate. *Photochem. Photobiol.* 82 (2006): 225-230.

[23] Pavez, P.; Encinas, M. V. Photophysics and photochemical studies of.1,4-dihydropyridine derivatives. *Photochem. Photobiol.* 83 (2007): 722-729.

[24] Yamaoka, T.; Yokoyama, S.; Omote, T.; Naitoh, K.; Yoshida, K. Photochemical behavior of nifedipine derivatives and application to photosensitive polyimide. *Polymeric Materials for Microelectronic Applications: Science and Technology* 579 (1994): 253-270.

[25] Chen, B.; Peng, M. L.; Wu, L. Z.; Zhang, L. P.; Tung, C. H. Switch between charge transfer and local excited states in 4-aminophenyl-substituted Hantzsch 1,4-dihydropyridine induced by pH change and transition metal ions. *Photochem. Photobiol. Sci.* 5 (2006): 943-947.

[26] Lohani, C. R.; Lee, K. H. The effect of absorbance of Fe^{3+} on the detection of Fe^{3+} by fluorescent chemical sensors *Sens. Actuator B-Chem.* 143 (2010): 649–654.

[27] Lakowicz, J. R. Principles of Fluorescence Spectroscopy; 3rd ed.; John Wiley & Sons Inc., Kluwer, 2006.

[28] Wu, J.; Liu, W.; Ge, J.; Zhang, H.; Wang, P. New sensing mechanisms for design of fluorescent chemosensors emerging in recent years. *Chem. Soc. Rev.* 40 (2011): 3483–3495.

[29] W. M. Keck Center for cellular imaging. Fluorescence Resonance Energy Transfer spectroscopy [online]. (2010). Available from: http://www.kccivirginia.edu/FRET/index.php.

[30] Xu, Z. C.; Baek, K. H.; Kim, H. N.; Cui, J. N.; Qian, X. H.; Spring, D. R.; Shin, I.; Yoon, J. Zn^{2+}-triggered amide tautomerization produces a highly Zn^{2+}-selective, cell-permeable, and ratiometric fluorescent sensor. *Am. Chem. Soc.* 132 (2010): 601-610.

[31] Sparano, B. A.; Koide, K. A Strategy for the development of small-molecule-based sensors that strongly fluorescenece when bound to a specific RNA. *J. Am. Chem. Soc.* 127 (2005): 14954-14955.

[32] Mitra, A.; Ramanujam, B.; Rao, C. P. 1-(D-Glucopyranosyl-20-deoxy-20-iminomethyl)-2-hydroxynaphthalene as chemosensor for Fe^{3+} in aqueous HEPES buffer based on colour changes observable with the naked eye. *Tetrahedron Lett.* 50 (2009): 776-780.

[33] Sirilaksanapong, S.; Sukwattanasinittin, M.; Rashatasakhona, P. 1,3,5-Triphentlbenzene fluorophore as a selective Cu2+ sensor in aqueous media. *Chem. Commun.* 48 (2012) 293-295.

[34] Niamnont, N.; Siripornnoppakhun, W.; Rashatasakhona, P.; Sukwattanasinittin, M. A polyanionic dendritic fluorophore for

selective detection of Hg^{2+} in Triton X-100 aqueous media. *Oganic Letters* 11 (2009) 2768-2771.

[35] Homraruen, D.; Sirijindalert, T.; Dubas, L.; Mongkol, S.; Ajavakom, A. Selective fluorescent sensor for mercury ions in aqueous media. *Tetrahedron* 69 (2013): 1617-1621.

[36] Singh, S. Sensors-an effective approach for the detection of explosives. *Journal of Hazardous Materials* 144 (2007): 15–28.

[37] Lee, Y. H.; Liu, H.; Lee, J. Y.; Kim, S. H.; Kim, S. K.; Sessler, J. L.; Kim, Y.; Kim, J. S. Dipyrenylcalix[4]arene - a fluorescence-based chemosensor for trinitroaromatic explosives. *Chem. Eur. J.* 20 (2010): 5895 - 5901.

[38] Toal, J. S.; Trogler C. W. Polymer sensors for nitroaromatic explosives detection. *J. Mater. Chem.* 16 (2006): 2871–2883.

[39] Shanmugaraju, S.; Joshi, S. A.; Mukherjee, P. S. Fluorescence and visual sensing of nitroaromatic explosives using electron rich discrete fluorophores. *J. Mater. Chem.* 21 (2011): 9130–9138.

[40] Germain, M. E.; Knapp, M. Optical explosives detection: from color changes to fluorescence turn-on. *J. Chem. Soc. Rev.* 38 (2009): 2543-2555.

[41] Ma, Y.; Li, H.; Peng, S.; Kim, W. L. Highly selective and sensitive fluorescent paper sensor for nitroaromatic explosive detection. *Anal. Chem.* 84 (2012): 8415−8421.

[42] Bhalla, V.; Gupta, A.; Kumar, M. Fluorescent nanoaggregates of pentacenequinone derivative for selective sensing of picric acid in aqueous media. *Org. Lett.* 14 (2012): 3112-3115.

[43] Liu, T.; Zhao, K.; Liu, K.; Ding, L.; Yin, S.; Fang Y. Synthesis, optical properties and explosive sensing performances of a series of novel π-

conjugated aromatic end-capped oligothiophenes. *Journal of Hazardous Materials* 246 (2013): 52–60.

[44] Zhao, Z.; Liu, J.; Lam, J.W. Y.; Chan, K.; Qiu, H.; Tang, Z. Luminescent aggregates of a starburst silole-triphenylamine adduct for sensitive explosive detection. *Dyes and Pigments* 91 (2011): 258-263.

[45] He, G.; Yan, N.; Yang, J.; Wang, H.; Ding, L.; Yin, S.; Fang, Y. Pyrene-containing conjugated polymer-based fluorescent films for highly sensitive and selective sensing of TNT in aqueous medium. *Macromolecules* 44 (2011): 4759–4766.

[46] Roy, B.; Bar, A.; Gole, B.; Mukherjee, P. Fluorescent tris-imidazolium sensors for picric acid explosive. *J. Org. Chem.* 78 (2013): 1306−1310.

[47] Daniels, M.; Wang, Y.; Lee, M.; Venkitaraman, A. Abnormal cytokinesis in cells deficient in the breast cancer susceptibility protein BRCA2. *Science* 306 (2004): 876–879.

[48] Nelson, M.; Lehninger C. Principles of Biochemistry, fifth ed., W.H. Freeman, USA, (2008).

[49] Earmrattana, N.; Sukwattanasinitt, M.; Rashatasakhon, P. Water-soluble anionic fluorophores from truxene. *Dyes and Pigments* 93 (2012): 1428-1433.

[50] Niamnont, N.; Mungkarndee, R.; Techakriengkrai, I.; Rashatasakhon, P.; Sukwattanasinitt, M. Protein discrimination by fluorescent sensor array constituted of variously charged dendritic phenylene–ethynylene fluorophores. *Biosensors and Bioelectronics* 26 (2010): 863–867.

[51] Chen, T.; Zhu, S.; Cao, H.; Shang, Y.; Wang, M.; Jiang, G.; Shi, Y.; Lu, T. Studies on the interaction of salvianolic acid B with human hemoglobin by multi-spectroscopic techniques. *Spectrochimica Acta Part A* 78 (2011): 1295–1301.

[52] Fang, C.; Peng, M.; Li, G.; Tian, J.; Yin, D. New functions of glucosamine as a scavenger of the lipid peroxidation product malondialdehyde. *Chem. Res. Toxicol.* 20 (2007): 947-953.

[53] Du, H.; Fuh, R. A.; Li, J.; Corkan, A.; and Lindsey, J. S. Photochem CAD: A computer-aided design and research tool in photochemistry. *Photochem Photobiol.* 68 (1998): 141-142.

[54] Fery-Forgues, S.; and Lavabe, D. Are fluorescence quantum yields so tricky to measure a demonstration using familiar stationery products. *J. Chem. Educ.* 76 (1999): 1260-1264.

[55] Myszka, H.; Bednarczyk, D.; Najder, M.; Kaca W. Synthesis and induction of apoptosis in B cell chronic leukemia by diosgenyl 2-amino-2-deoxy-_-D-glucopyranoside hydrochloride and its derivatives. *Carbohydrate Research* 338 (2003): 133–141.

[56] Sohn, H.; Calhoun, R. M.; Sailor, M. J.; Trogler, W. C. Detection of TNT and picric acid on surfaces and in seawater by using photoluminescent polysiloles. *Angew. Chem., Int. Ed.* 40 (2001): 2104–2105.

[57] Albert, K. J.; Lewis, N. S.; Schauer, C. L.; Sotzing, G. A.; Stitzel, S. E.; Vaid, T. P.; Walt, D. R. Cross-reactive chemical sensor arrays. *Chem. Rev.* 100 (2000): 2595–2626.

[58] Nagarkar, S.; Joarder, B.; Chaudhari, K.; Mukherjee, S.; Ghosh, K. Highly selective detection of nitro explosives by a luminescent metal–organic. *Angew. Chem., Int. Ed.* 52 (2013): 2881-2885.

[59] Jiang Y, Wang Y, Hua J, Tang J, Li B, Qian S, et al. Multibranched triarylamine end-capped triazines with aggregation-induced emission and large two photon absorption cross-sections. *Chem. Commun.* 46 (2010): 4689-4691.

[60] Wu, Y.; Hu, S. Biosensors based on direct electron transfer in redox proteins. *Microchim. Acta* 159 (2007): 1–17.

[61] Gorton, L.; Lindgren, A.; Larsson, T.; Munteanu, F.; Ruzgas, T.; Gazarian, I. Direct electron transfer between heme-containing enzymes and electrodes as basis for third generation biosensors. *Anal. Chim. Acta* 400 (1999) 91–108.

[62] Chen, T.; Zhu, S.; Shang, Y.; Ge, C.; Jiang, G. Binding of dihydromyricetin to human hemoglobin: Fluorescence and circular dichroism studies. *Spectrochimica Acta Part A* 93 (2012): 125– 130.

[63] Ding, F.; Sun, Y.; Diao, J.; Li, X.; Yang, X.; Sun, Y.; Zhang L. Features of the complex of food additive hesperidin to hemoglobin. *Journal of Photochemistry and Photobiology B: Biology* 106 (2012): 53‑60.

[64] Barsan, M.; Pinto, E.; Brett, C. Interaction between myoglobin and hyaluronic acid in layer-by-layer structures-An electrochemical study. *Electrochimica Acta* 55 (2010): 6358–6366.

[65] Kim, I. B.; Dunkhorst, A.; and Bunz, U. H. F. Nonspecific interactions of a carboxylate-substituted PPE with proteins. a cautionary tale for biosensor applications. *Langmuir* 21 (2005): 7985–7989.

[66] Tolosa, J.; and Bunz, U. H. F. Water soluble cruciforms: effect of surfactants on fluorescence. *Chem. Asian J.* 4 (2009): 270–276.

[67] Jiwpanich, S.; Sandanaraj, B. S.; and Thayumanavan, S. Fluorophore-cored dendrimers for patterns in metalloprotein sensing. *Chem. Commun.* 43 (2009): 806–808.
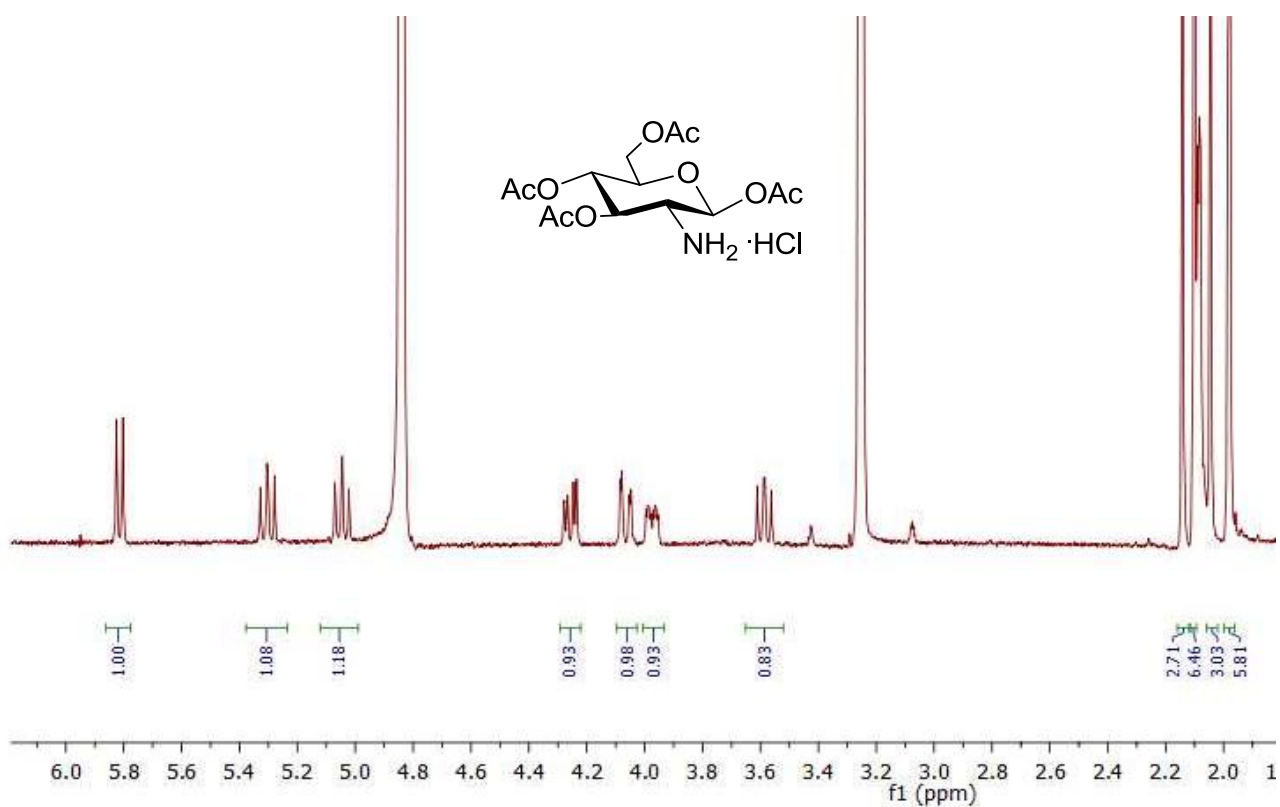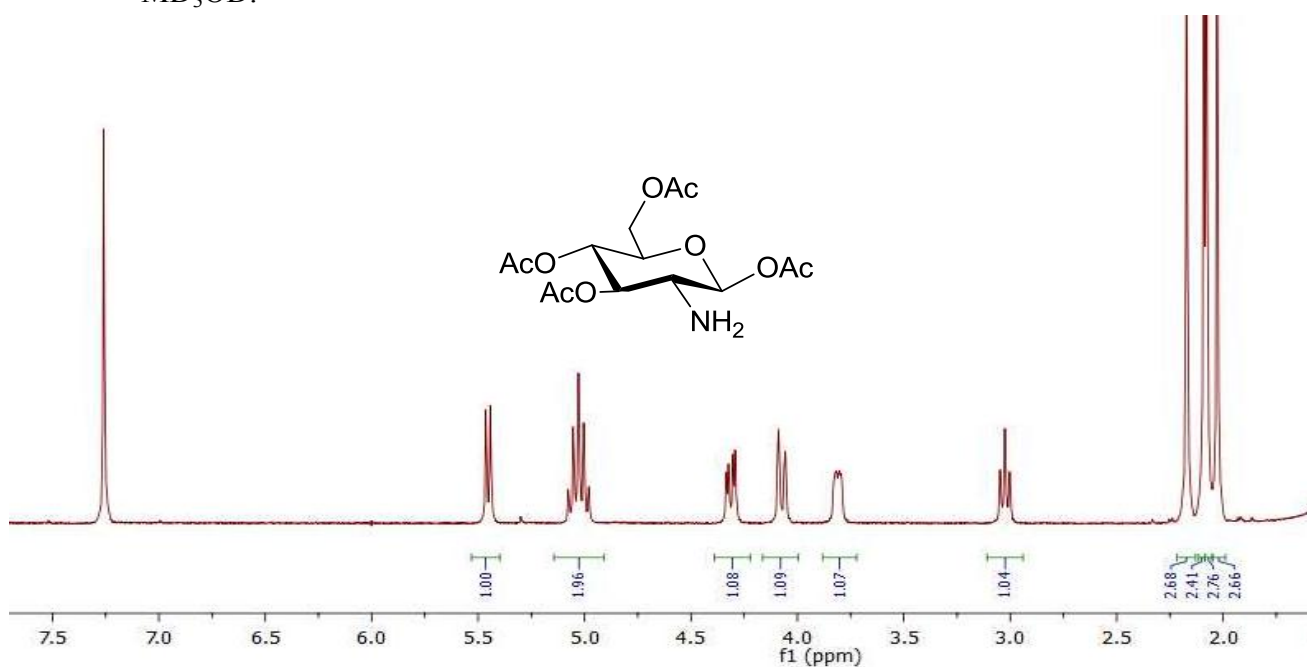
APPENDIX
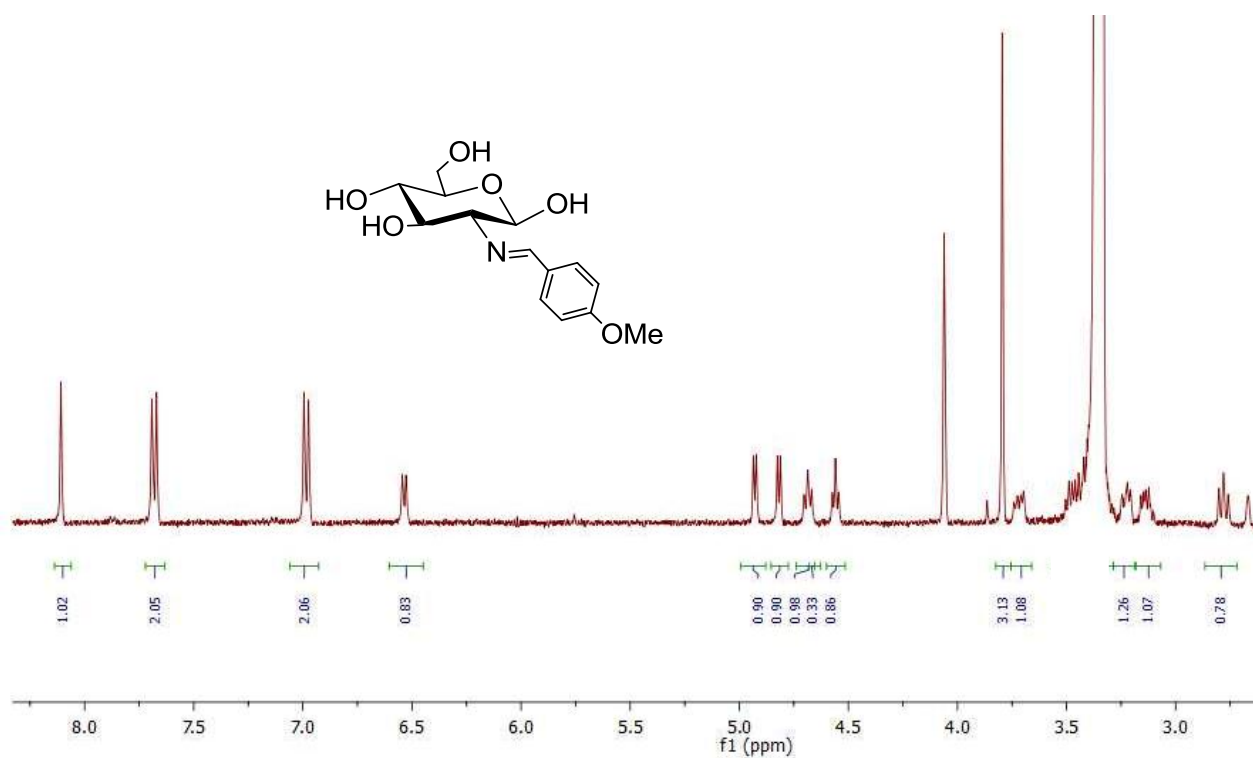
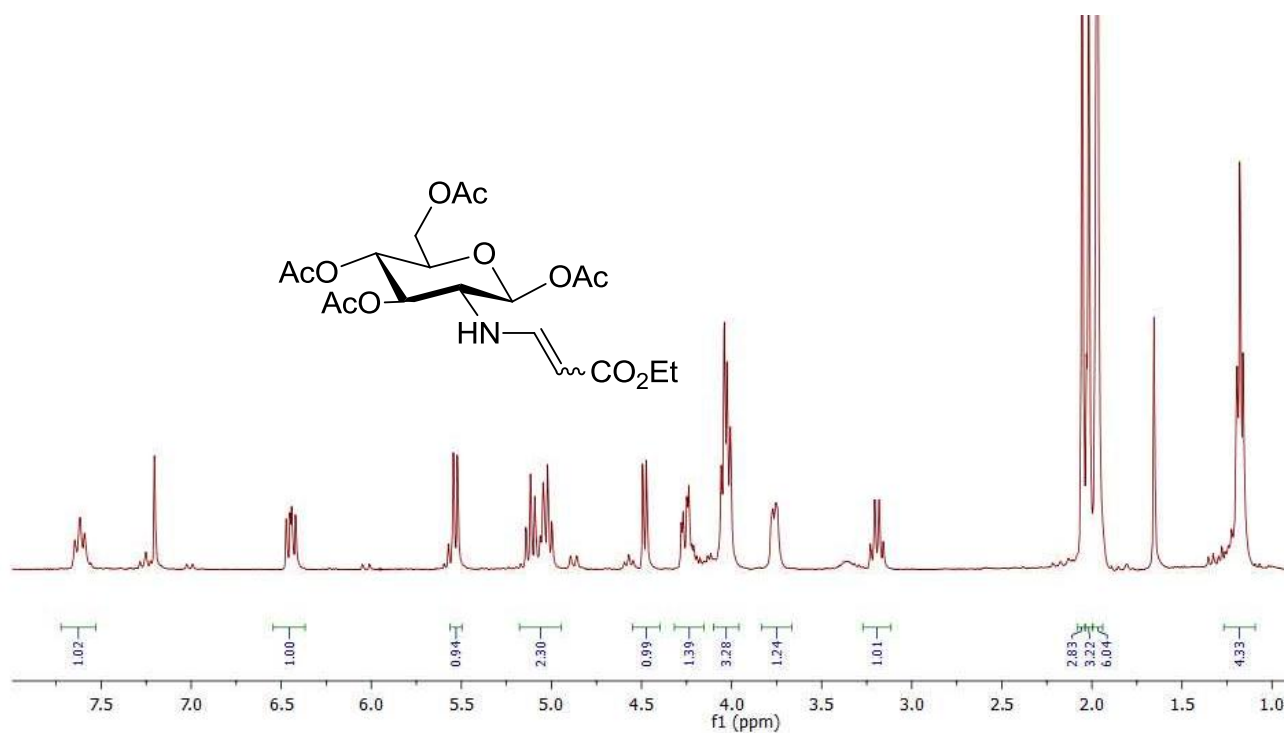**Figure A.1** The ^{1}H NMR of 2-deoxy-2-[*p*-methoxybenzylidene(amino)]-D-glucopyranose in DMSO-d_6.
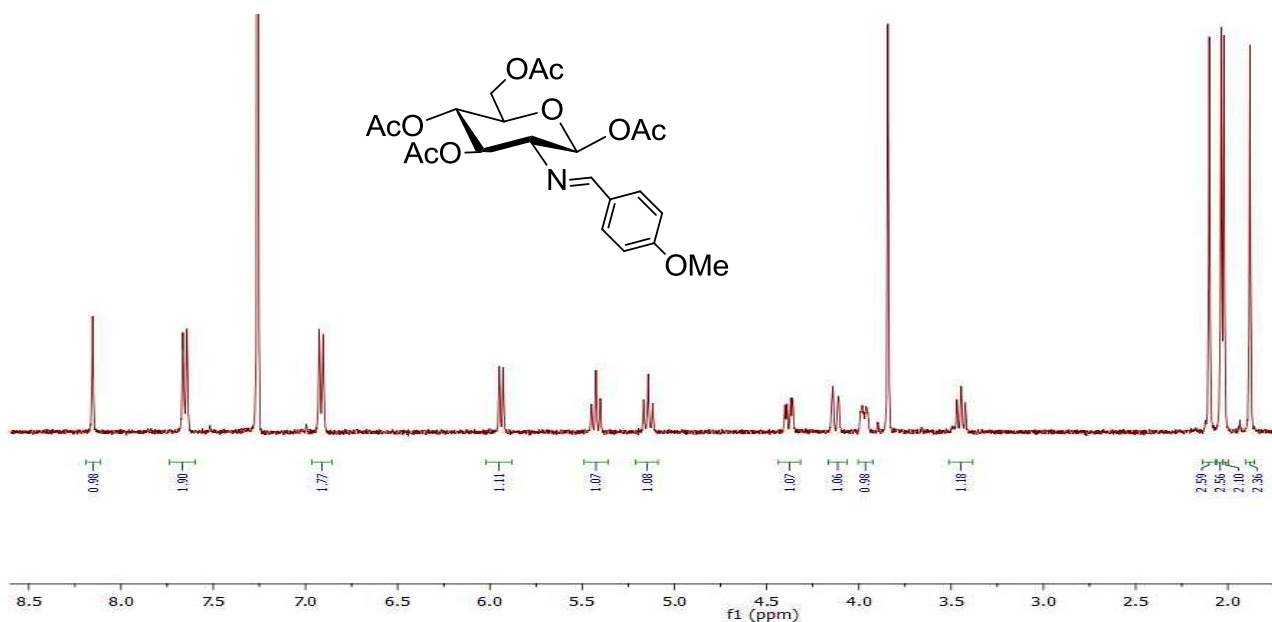
Figure A.2 The ^{1}H NMR of 1,3,4,6-tetra-*O*-acetyl-2-deoxy-2-[p-methoxybenzylidene(amino)]-β-D-glucopyranose in CDCl$_3$.

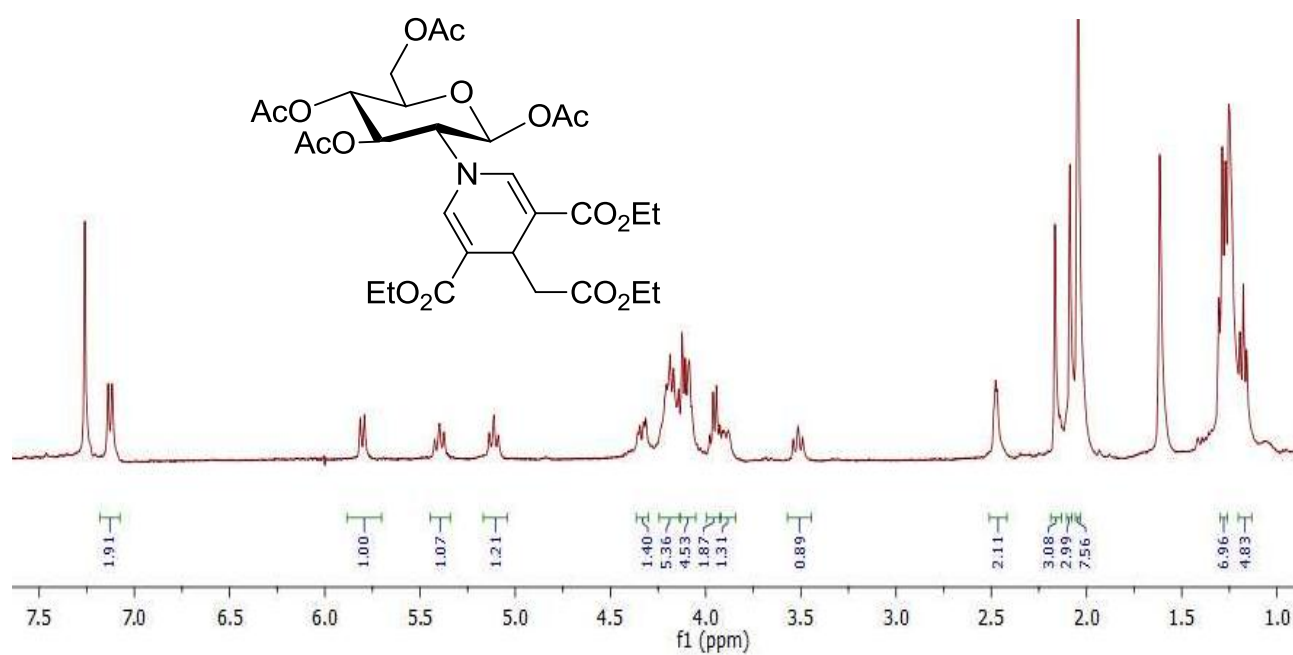**Figure A.3** The ^{1}H NMR of 1,3,4,6-tetra-*O*-acetyl-β-D-glucosamine hydrochloride in MD$_3$OD.

Figure A.4 The ^{1}H NMR of 1,3,4,6-tetra-*O*-acetyl-β-D-glucosamine in CDCl$_3$.

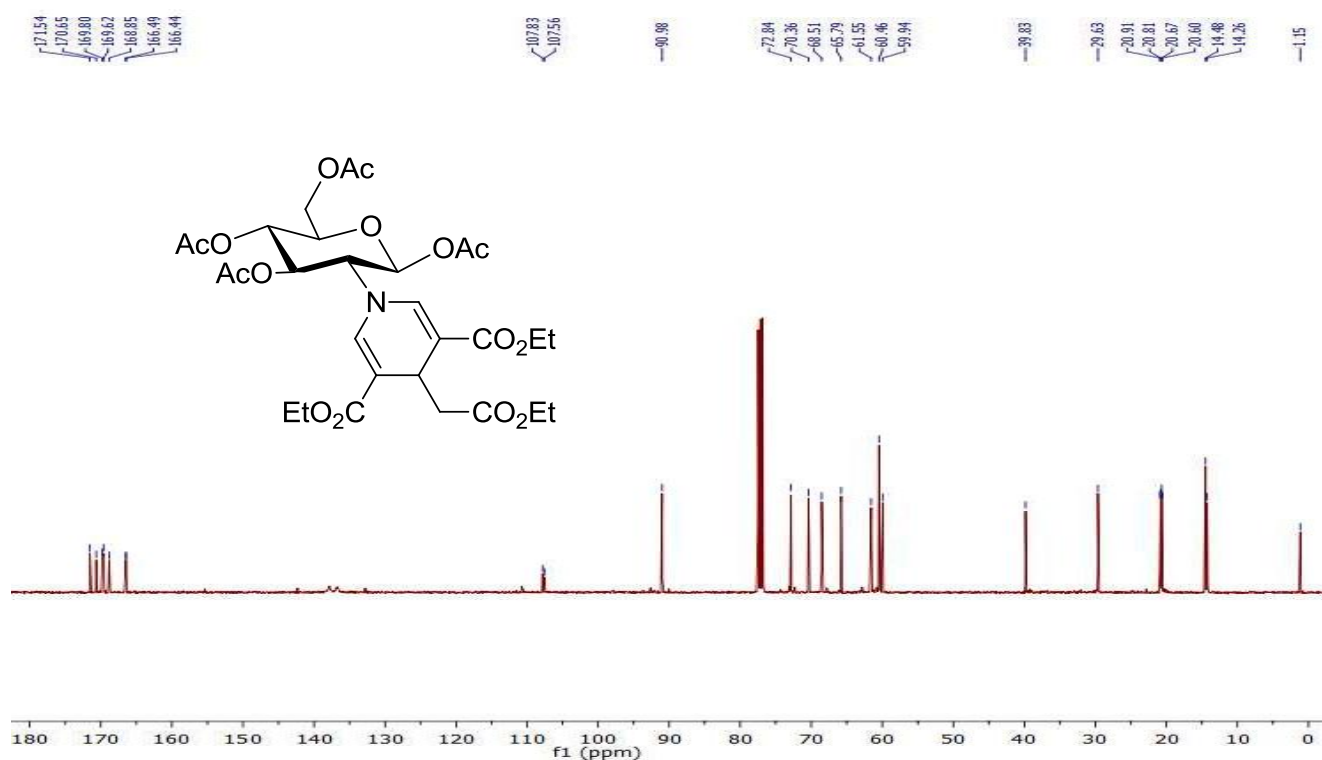**Figure A.5** The ¹H NMR of ethyl β-amino acrylate in CDCl₃.

Figure A.6 The ¹H NMR of 1,3,4,6-tetra-*O*-acetyl-β-D-glucosaminyl-1,4-dihydropiridine (Glc-DHP **1**) in CDCl₃.
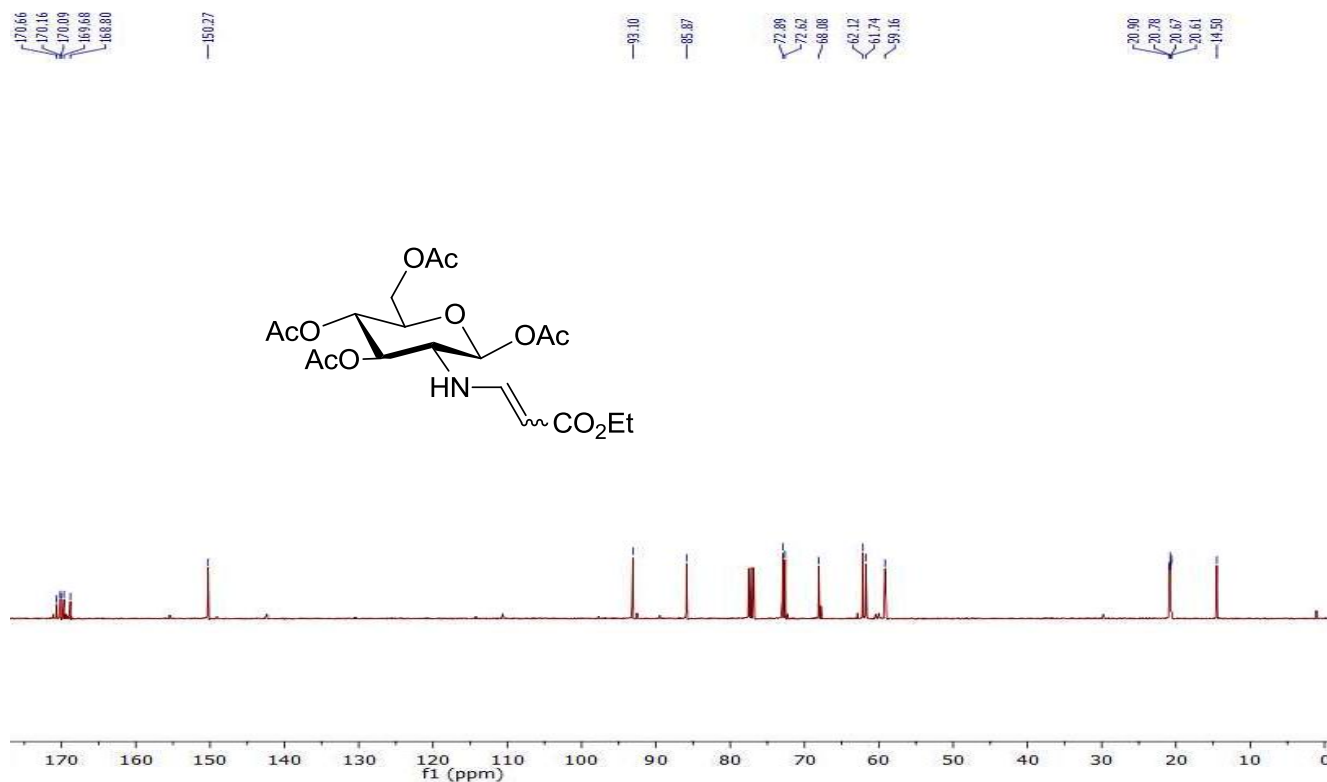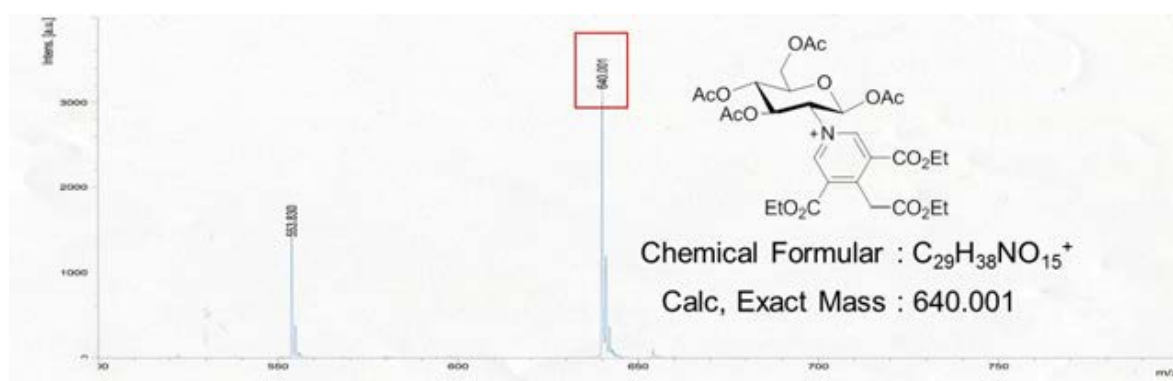
Figure A.7 The ^{13}C NMR ethyl β-amino acrylate in CDCl$_3$.
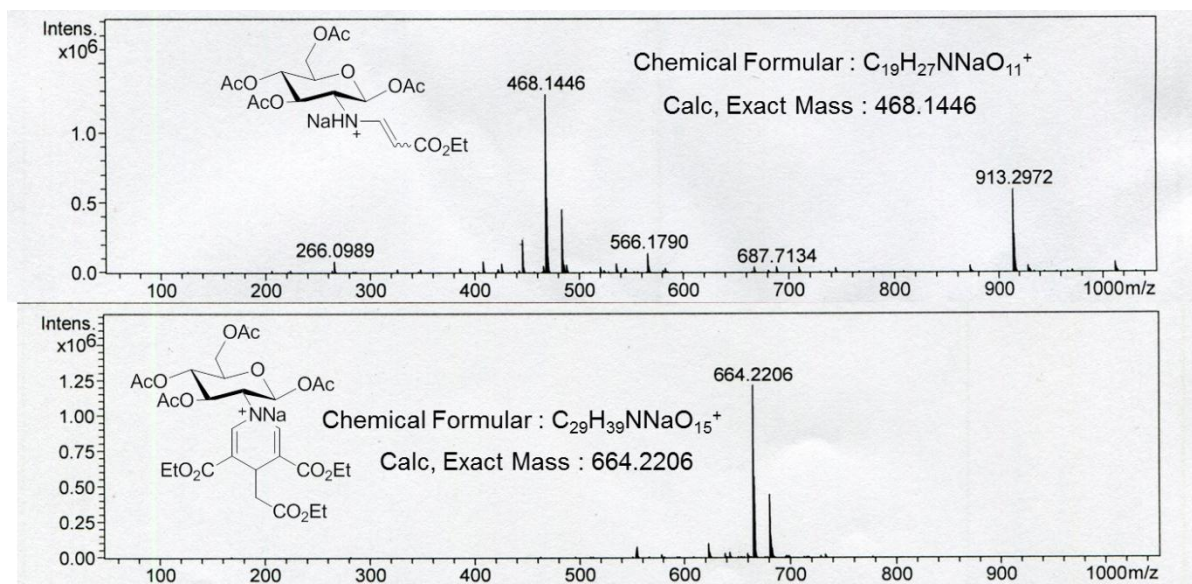
Figure A.8 The HRMS of ethyl β-amino acrylate and 1,3,4,6-tetra-*O*-acetyl-β-D-glucosaminyl-1,4-dihydropiridine (Glc-DHP **1**).

Figure A.9 The ¹³C NMR of 1,3,4,6-tetra-*O*-acetyl-β-D-glucosaminyl-1,4-dihydropiridine (Glc-DHP **1**) in CDCl₃.

Figure A.10 The MALDI-TOF of 1,3,4,6-tetra-*O*-acetyl-β-D-glucosaminyl-1,4-dihydropiridine (Glc-DHP **1**).

VITAE

Mr. Oran Pinrat was born on September 24th, 1987 in Uttaradit, Thailand. He graduated with Bachelor Degree of Science, majoring in Chemistry from King Mongkut Institute Technology Ladkrabang in 2010. In the same year, he became a master degree student received a Master's Degree in Petrochemistry and Polymer Science program at Chulalongkorn University. He had presented his research in Pure and Applied Chemistry International Conference (PACCON 2013).

His present address is 158/6, Charuenbandid Road, Tha-it, Mueng, Uttaradit, Thailand 53000.